Recent Change—North Sea

3

John Huthnance, Ralf Weisse, Thomas Wahl, Helmuth Thomas, Julie Pietrzak, Alejandro Jose Souza, Sytze van Heteren, Natalija Schmelzer, Justus van Beusekom, Franciscus Colijn, Ivan Haigh, Solfrid Hjøllo, Jürgen Holfort, Elizabeth C. Kent, Wilfried Kühn, Peter Loewe, Ina Lorkowski, Kjell Arne Mork, Johannes Pätsch, Markus Quante, Lesley Salt, John Siddorn, Tim Smyth, Andreas Sterl and Philip Woodworth

Electronic supplementary material Supplementary material is available in the online version of this chapter at 10.1007/978-3-319-39745-0_3.

J. Huthnance (✉) · A.J. Souza · P. Woodworth
National Oceanography Centre, Liverpool, UK
e-mail: jmh@noc.ac.uk

A.J. Souza
e-mail: ajso@noc.ac.uk

P. Woodworth
e-mail: plw@noc.ac.uk

R. Weisse (✉) · J. van Beusekom · F. Colijn · M. Quante
Institute of Coastal Research, Helmholtz-Zentrum Geesthacht, Geesthacht, Germany
e-mail: ralf.weisse@hzg.de

J. van Beusekom
e-mail: Justus.Beusekom@hzg.de

F. Colijn
e-mail: franciscus.colijn@hzg.de

M. Quante
e-mail: markus.quante@hzg.de

T. Wahl
College of Marine Science, University of South Florida, St. Petersburg, USA

T. Wahl
University of Southampton, Southampton, UK
e-mail: t.wahl@soton.ac.uk

H. Thomas
Department of Oceanography, Dalhousie University, Halifax, Canada
e-mail: helmuth.thomas@posteo.org

J. Pietrzak
Environmental Fluid Mechanics Section, Delft University of Technology, Delft, The Netherlands
e-mail: J.D.Pietrzak@tudelft.nl

S. van Heteren
Department of Geomodeling, TNO-Geological Survey of the Netherlands, Utrecht, The Netherlands
e-mail: sytze.vanheteren@tno.nl

N. Schmelzer · J. Holfort
Federal Maritime and Hydrographic Agency (BSH), Rostock, Germany
e-mail: natalija.schmelzer@bsh.de

J. Holfort
e-mail: juergen.holfort@bsh.de

I. Haigh
Ocean and Earth Science, University of Southampton, Southampton, UK
e-mail: I.D.Haigh@soton.ac.uk

S. Hjøllo · K.A. Mork
Institute of Marine Research (IMR), Bergen, Norway
e-mail: solfrid.hjollo@imr.no

K.A. Mork
e-mail: kjell.arne.mork@imr.no

E.C. Kent
National Oceanography Centre, Southampton, UK
e-mail: eck@noc.ac.uk

W. Kühn · J. Pätsch
Institute of Oceanography, CEN, University of Hamburg, Hamburg, Germany
e-mail: wilfried.kuehn@uni-hamburg.de

J. Pätsch
e-mail: johannes.paetsch@uni-hamburg.de

P. Loewe · I. Lorkowski
Federal Maritime and Hydrographic Agency (BSH), Hamburg, Germany
e-mail: peter.loewe@bsh.de

I. Lorkowski
e-mail: ina.lorkowski@bsh.de

L. Salt
Royal Netherlands Institute for Sea Research, Texel, The Netherlands
e-mail: lesleyannesalt@gmail.com

M. Quante and F. Colijn (eds.), *North Sea Region Climate Change Assessment*, Regional Climate Studies, DOI 10.1007/978-3-319-39745-0_3

Abstract

This chapter discusses past and ongoing change in the following physical variables within the North Sea: temperature, salinity and stratification; currents and circulation; mean sea level; and extreme sea levels. Also considered are carbon dioxide; pH and nutrients; oxygen; suspended particulate matter and turbidity; coastal erosion, sedimentation and morphology; and sea ice. The distinctive character of the Wadden Sea is addressed, with a particular focus on nutrients and sediments. This chapter covers the past 200 years and focuses on the historical development of evidence (measurements, process understanding and models), the form, duration and accuracy of the evidence available, and what the evidence shows in terms of the state and trends in the respective variables. Much work has focused on detecting long-term change in the North Sea region, either from measurements or with models. Attempts to attribute such changes to, for example, anthropogenic forcing are still missing for the North Sea. Studies are urgently needed to assess consistency between observed changes and current expectations, in order to increase the level of confidence in projections of expected future conditions.

3.1 Introduction

John Huthnance, Ralf Weisse

Physical variables, most obviously sea temperature, relate closely to climate change and strongly affect other properties and life in the sea. This chapter discusses past and ongoing change in the following physical variables within the North Sea: temperature, salinity and stratification (Sect. 3.2), currents and circulation (Sect. 3.3), mean sea level (Sect. 3.4) and extreme sea levels, i.e. contributions from wind-generated waves and storm surges (Sect. 3.5). Also considered are carbon dioxide (CO_2), pH, and nutrients (Sect. 3.6), oxygen (Sect. 3.7), suspended particulate matter and turbidity (Sect. 3.8), coastal erosion, sedimentation and morphology (Sect. 3.9) and sea ice (Sect. 3.10). The distinctive character of the Wadden Sea is addressed in Sect. 3.11, with a particular focus on sediments and nutrients. The chapter covers the past 200 years. Chapter 1 described the North Sea context and physical process understanding, so the focus of the present chapter is on the historical development of evidence (measurements, process understanding and models), the form, duration and accuracy of the evidence available (further detailed in Electronic (E-) Supplement S3) and what the evidence shows in terms of the state and trends in the respective variables.

J. Siddorn
Met Office, Exeter, UK
e-mail: john.siddorn@metoffice.gov.uk

T. Smyth
Plymouth Marine Laboratory, Plymouth, UK
e-mail: tjsm@pml.ac.uk

A. Sterl
Royal Netherlands Meteorological Institute (KNMI), De Bilt, The Netherlands
e-mail: sterl@knmi.nl

3.2 Temperature, Salinity and Stratification

John Huthnance, Elizabeth C. Kent, Tim Smyth, Kjell Arne Mork, Solfrid Hjøllo, Peter Loewe

3.2.1 Historical Perspective

Observations of sea-surface temperature (SST) have been made in the North Sea since 1823, but were sparse initially. The typical number of observations per month (from ships, and moored and drifting buoys) increased from a few hundred in the 19th century to more than 10,000 in recent decades, despite the Voluntary Observing Ship (VOS) fleet declining from a peak of about 7700 ships worldwide in 1984/85 to about 4000 in 2009 (www.vos.noaa.gov/vos_scheme.shtml). Early SST observations used buckets (Kent et al. 2010); adjustments of up to ~0.3 °C in the annual mean, and 0.6 °C in winter, may be needed for these early data owing to sample heat loss or gain (Folland and Parker 1995; Smith and Reynolds 2002; Kennedy et al. 2011a, b). The adjustments depend on large-scale forcing and assumptions about measurement methods—local variations add uncertainty. Cooling water intake temperatures have been measured on ships since the 1920s but data quality is variable, sometimes poor (Kent et al. 1993). Temperature sensors on ships' hulls became more numerous in recent decades (Kent et al. 2010). About 70 % of in situ observations in 2006 came from moored and drifting buoys

(Kennedy et al. 2011b). Other modern shipboard methods include radiation thermometers, expendable bathythermographs (XBTs) and towed thermistors (Woodruff et al. 2011). Satellite estimates of SST are regularly available using Advanced Very High Resolution Radiometers (AVHRR; from 1981) and passive microwave radiometers (with little cloud attenuation; from 1997).

Below the sea surface, temperature was measured by reversing (mercury) thermometers until the 1960s. Since then, electronic instruments lowered from ships (conductivity-temperature-depth profilers; CTDs) enable near-continuous measurements. Since about 2005, multi-decadal model runs have become increasingly available and now provide useful information on temperature distribution to complement the observational evidence (see E-Supplement Sect. S3.1).

Early salinity estimates used titration-based chemical analysis of recovered water samples (from buckets and water intakes) and from lowered sample bottles. Titration estimates usually depended on assuming a constant relation between chlorinity and total dissolved salts (a subject of discussion since 1900), with typical error O(0.01 ‰). Since the 1960s–1970s lowered CTD conductivity cells enable near-continuous measurements, calibrated by comparing the conductivity of water samples against standardised sea water; typical error O(0.001 ‰). Consistent definition of salinity has continued to be a research topic (Pawlowicz et al. 2012).

Thermistors and conductivity cells as on CTDs now record temperature and salinity of (near-surface) intake water on ships. Since the late 1990s, CTDs on profiling 'Argo' floats have greatly increased available temperature and salinity data for the upper 2000 m of the open ocean (www.argo.ucsd.edu). Although not available for the North Sea, these data greatly improve estimates of open-ocean temperature and salinity and thereby North Sea model estimates by better specifying open-ocean boundary conditions.

The history of stratification estimates, based on profiles of temperature and salinity (or at least near-surface and near-bottom values), corresponds with that of subsurface temperature and salinity.

Detail on time-series evidence for coastal and offshore temperature and salinity variations is given in E-Supplement S3.1 and S3.2.

3.2.2 Temperature Variability and Trends

3.2.2.1 Northeast Atlantic

Most water entering the North Sea comes from the adjacent North Atlantic via Rockall Trough and around Scotland. The North Atlantic has had relatively cool periods (1900–1925, 1970–1990) and warm periods (1930–1960, since 1990; Holliday et al. 2011; Dye et al. 2013a; Ivchenko et al. 2010 using 1999–2008 Argo float data). Adjacent to the north-west European shelf, however, different Atlantic water sources make varying contributions (Holliday 2003). For Rockall Trough surface waters, the period 1948–1965 was about 0.8 °C warmer on average than the period 1876–1915 (Ellett and Martin 1973). Subsequently, temperatures of upper water (0–800 m) in Rockall Trough and Atlantic water on the West Shetland slope (Fig. 3.1) oscillated with little trend until around 1994. Temperatures then rose,

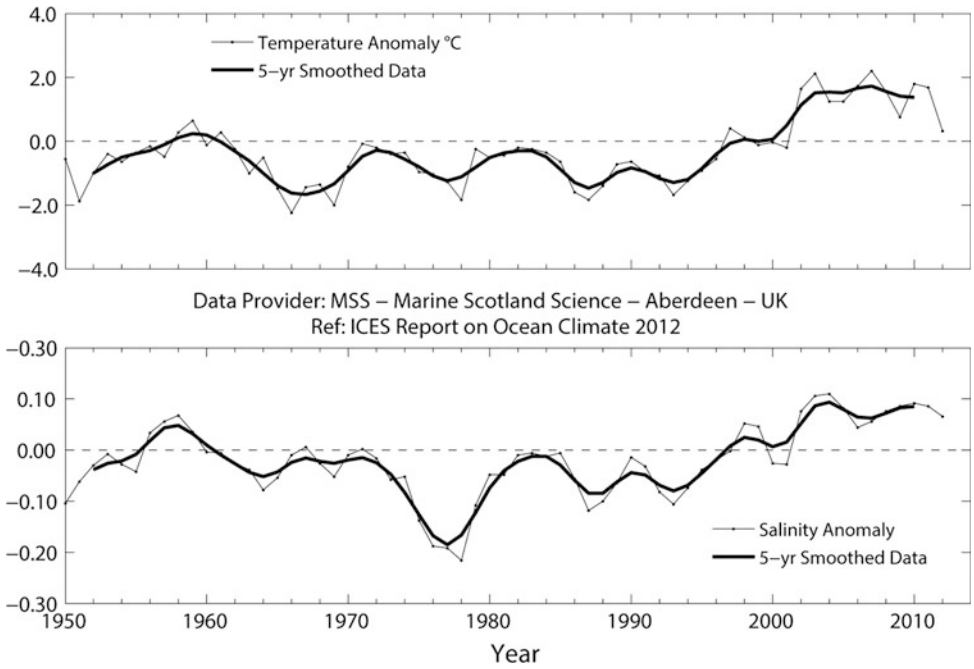

Fig. 3.1 Atlantic Water in the Faroe–Shetland Channel slope current. Temperature (*upper*) and salinity (*lower*) anomalies relative to the 1981–2010 average (Beszczynska-Möller and Dye 2013)

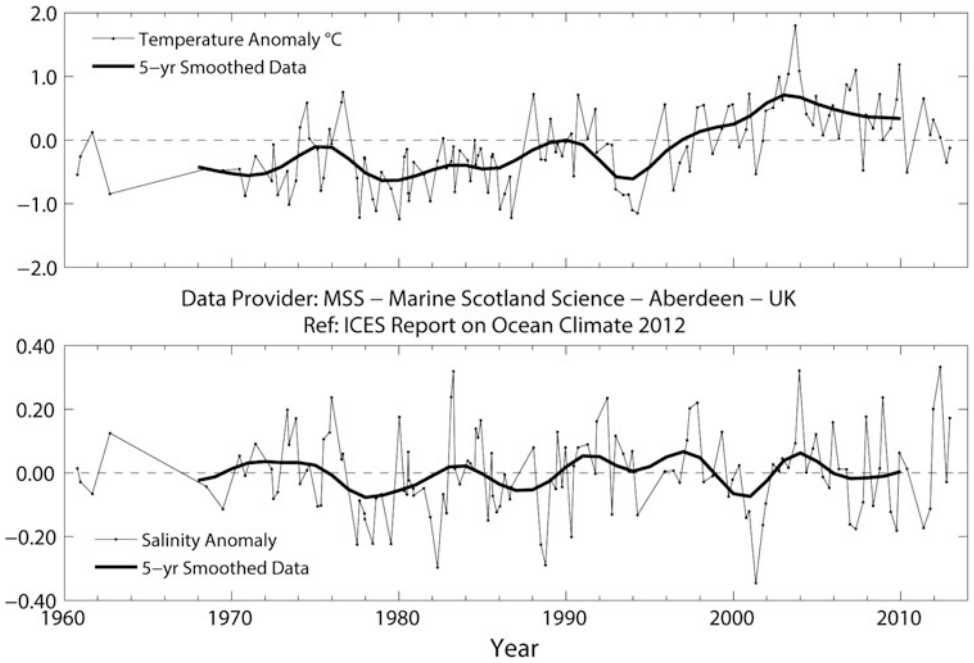

Fig. 3.2 Fair Isle Current entering the northern North Sea from the west and north of Scotland. Annual upper water temperature (*upper*) and salinity (*lower*) anomalies relative to the 1981–2010 average (Beszczynska-Möller and Dye 2013)

peaked in 2006, and subsequently cooled to early 2000s values (Berx et al. 2013; Beszczynska-Möller and Dye 2013; Holliday and Cunningham 2013).

West and north of Britain, the HadISST data set shows an SST trend of 0.2–0.3 °C decade^{-1} over the period 1983–2012, which is higher than the global average (Rayner et al. 2003; see Dye et al. 2013a among several references). Thus positive temperature anomalies exceeding one standard deviation (based on the period 1981–2010) were widespread in adjacent Atlantic Water and the northern North Sea during 2003–2012 (Beszczynska-Möller and Dye 2013). In fact, several authors suggest an inverse relation between Subpolar Gyre strength and the extent of warm saline water (e.g. Hátún et al. 2005; Johnson and Gruber 2007; Haekkinen et al. 2011).

3.2.2.2 North Sea

In Atlantic Water inflow to the North Sea at the western side of the Norwegian Trench (Utsira section, 59.3°N), 'core' temperature has risen by about 0.8 °C since the 1970s and about 1 °C near the seabed in the north-western part of the section (estimated from Holliday et al. 2009). Figure 3.2 shows long-term temperature variability in the Fair Isle Current flowing into the North Sea on the shelf.

For the North Sea as a whole, annual average SST derived from six gridded data sets (Fig. 3.3) shows relatively cool SST from 1870, especially in the early 1900s, 'plateaux' in the periods 1932–1939 and 1943–1950, and then overall decline to a minimum around 1988 (anomaly about −0.8 °C). This was followed by a rise to a peak in 2008 (anomaly about 1 °C) and subsequent fall. SST trends

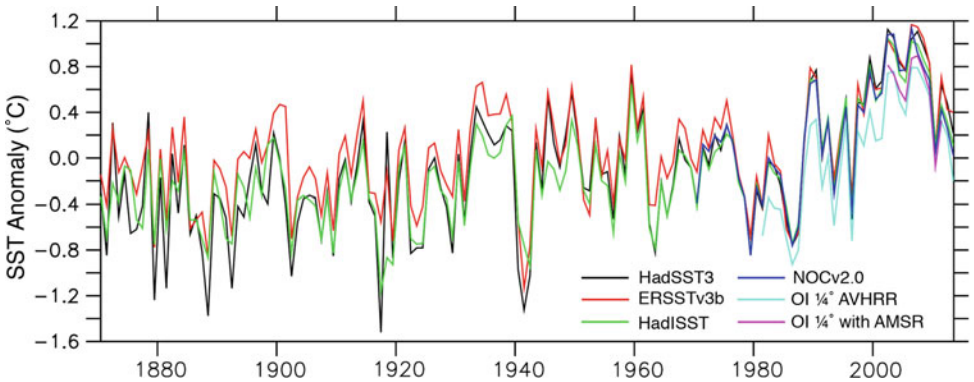

Fig. 3.3 North Sea region annual sea-surface temperature (SST) anomalies relative to the 1971–2000 average, for the datasets in E-Supplement Table S3.1 (figure by Elizabeth Kent, UK National Oceanography Centre)

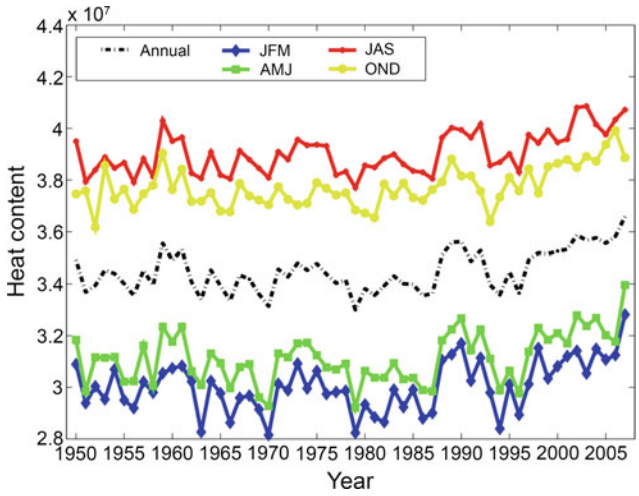

Fig. 3.4 Annual and seasonal mean North Sea heat content (10^7 J m^{-3}) (reprinted from Meyer et al. 2011)

generally show also in heat content (Hjøllo et al. 2009; Meyer et al. 2011) and in all seasons (Fig. 3.4), despite winter-spring variability exceeding summer-autumn variability. The increase in North Sea heat content between 1985 and 2007 was about 0.8×10^{20} J, much less than the seasonal range (about 5×10^{20} J) and comparable with interannual variability (Hjøllo et al. 2009).

Despite an inherent anomaly adjustment time-scale of just a few months (Fig. 3.5 and Meyer et al. 2011), the longer-term decline in SST from the 1940s to 1980s and subsequent marked rise to the early 2000s are widely reported. The basis is in observations, for example those shown by McQuatters-Gollop et al. (2007 using HADISST v1.1; see Fig. 3.6 and E-Supplement Table S3.1), Kirby et al. (2007), Holt et al. (2012, including satellite SST data, Fig. 3.7) and multi-decadal hindcasts, such as those of Meyer et al. (2011) and Holt et al. (2012). Particular features noted

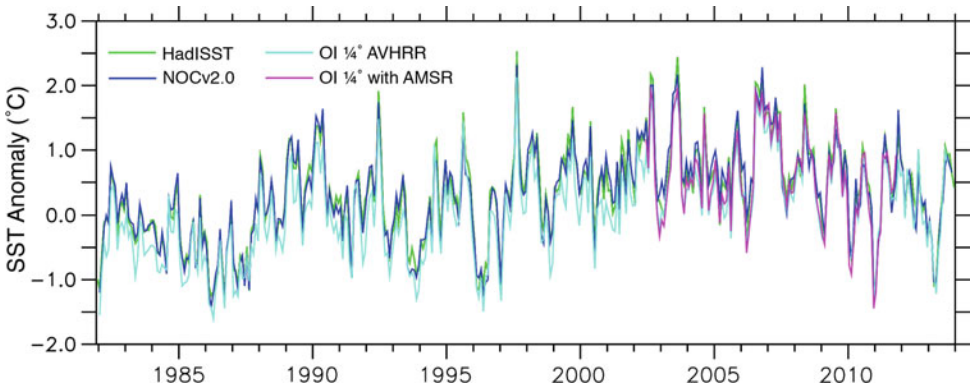

Fig. 3.5 North Sea region monthly sea-surface temperature (SST) anomalies relative to 1971–2000 monthly averages, for the gridded datasets in E-Supplement Table S3.1 with resolution of 1° or finer. Sharp month-to-month variability indicates an inherent anomaly 'adjustment' time of just a few months (figure by Elizabeth Kent, UK National Oceanography Centre)

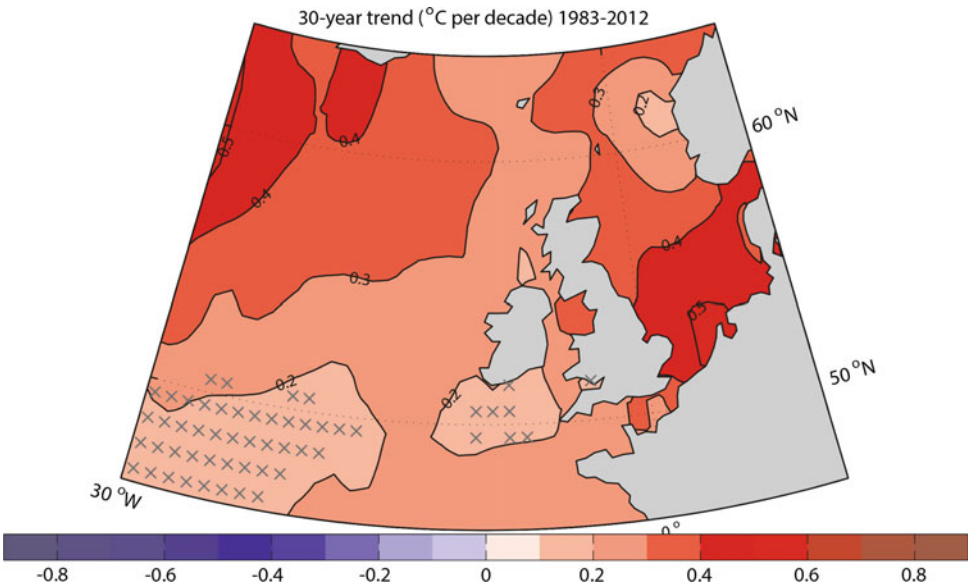

Fig. 3.6 Linear sea-surface temperature trends (°C $decade^{-1}$) in annual values for the period 1983–2012. From the HadISST1 dataset (Rayner et al. 2003). Hatched areas: trend not significantly different from zero at 95 % confidence level (Dye et al. 2013a, see Acknowledgement)

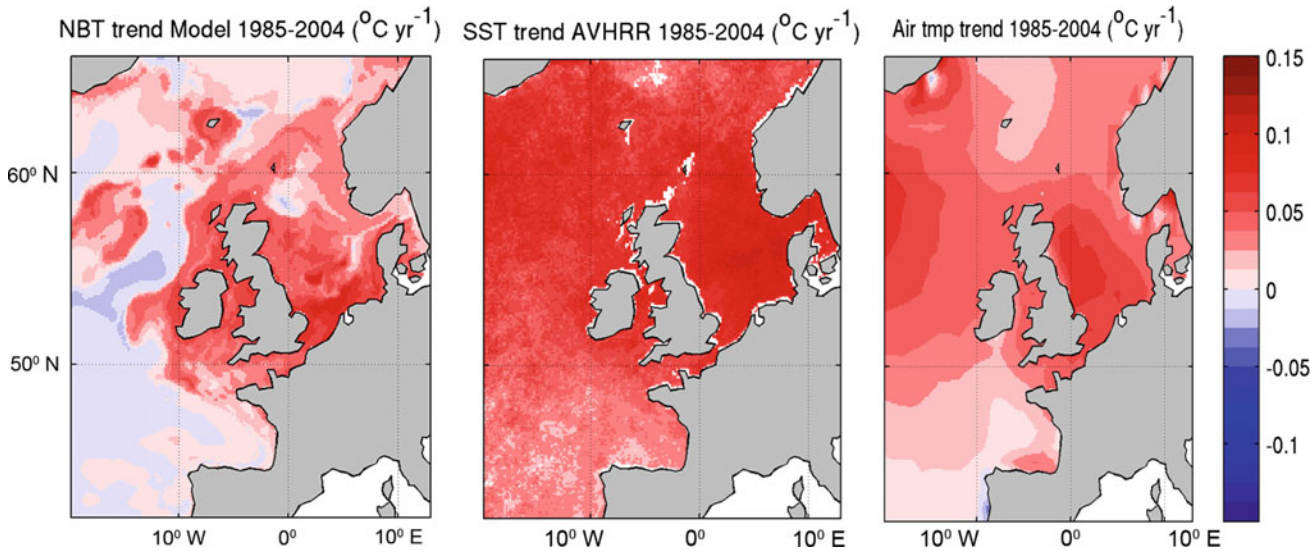

Fig. 3.7 Linear trends for the period 1985–2004 in model near-bed temperature (*left*), satellite sea-surface temperature (SST; *middle*) and 2-m ERA40 air temperature (*right*) (Holt et al. 2012)

are rapid cooling in the period 1960–1963, rapid warming in the late 1980s, followed by cooling again in the early 1990s and then resumed warming to about 2006. The warming trends of the 1980s to 2000s are widely reported to be significant (e.g. Holt et al. 2012) and are mainly but not entirely accounted for by trends in air temperature (see hindcasts of Meyer et al. 2011; Holt et al. 2012). Observed North Sea winter bottom temperature between 1983 and 2012 shows a typical trend of 0.2–0.5 °C decade^{-1} (Dye et al. 2013a) superimposed on by considerable interannual variability.

3.2.2.3 Regional Variations

The rise in North Sea SST since the 1980s increased from north (trend <0.2 °C decade^{-1}) to south (trend 0.8 °C decade^{-1}; Fig. 3.6; McQuatters-Gollop et al. 2007). Based on HadISST1 for the period 1987–2011, the EEA (2012) showed warming of 0.3 °C decade^{-1} in the Channel, 0.4 °C decade^{-1} off the Dutch coast, and less than 0.2 °C decade^{-1} at 60°N off Norway.

The German Bight shows the largest warming trend in recent decades (Fig. 3.6) with a rapid SST rise in the late 1980s (Wiltshire et al. 2008; Meyer et al. 2011). Variability is also large, between years O(1 °C) and longer term (Wiltshire et al. 2008; Meyer et al. 2011; Holt et al. 2012). At Helgoland Roads Station (54° 11′N, 7° 54′E) decadal SST trends since 1873 show the warming after the early 1980s was the strongest.

For southern North Sea SST, the 1971–2010 ferry data (Fig. 3.8) show a rise of O(2 °C) from 1985/6 to 1989; the five-year smoothing emphasises a late 1980s rise of about 1.5 °C followed by 5- to 10-year fluctuations superimposed on a slow decline from the early 1990s to about 1 °C above the 1971–1986 average (smoothed values). Model hindcast spatial averages between Dover Strait and 54.5°N (water column mostly well-mixed; Alheit et al. 2012 based on Meyer et al. 2011) also show cold winters for 1985 to 1987 but the 1990 winter as the warmest since 1948 (and winter 2007 as warmer again). Anomalies (observations and model results) became mainly positive from the late 1980s apart from a dip in the early 1990s. This all illustrates the late 1980s temperature rise.

The Dutch coastal zone shows a trend of rising SST since 1982 (van Aken 2010), despite a very cold winter in 1996 (January–March; about 4 °C below the 1969–2008 average; van Hal et al. 2010). Factors contributing to this rise are thermal inertia (seasonally), winds and cloudiness or bright sunshine (van Aken 2010). The 1956–2003 Marsdiep winter temperature (Tsimplis et al. 2006) and Wadden Sea winter and spring temperature (van Aken 2008) were significantly correlated with the winter North Atlantic Oscillation (NAO) index (see Annex 1). However, decadal to centennial temperature variations (a cooling of about 1.5 °C over the period 1860–1890 and a similar warming in the last 25 years) were not related to long-term changes in the NAO.

The western English Channel (50.03°N, 4.37°W) warmed in the 1920s and 1930s (Southward 1960); after a dip it warmed again in the 1950s, cooled in the 1960s and warmed over the full water column from the mid-1980s to the early 2000s (0.6 °C decade^{-1}, Smyth et al. 2010; see E-Supplement Fig. S3.2). The greatest (1990s) temperature rise coincided with a decrease in median wind speed (from 3.5 to 2.75 m s^{-1}) and an increase in surface solar irradiation (of about 20 %), both correlated with changes in the NAO (Smyth et al. 2010).

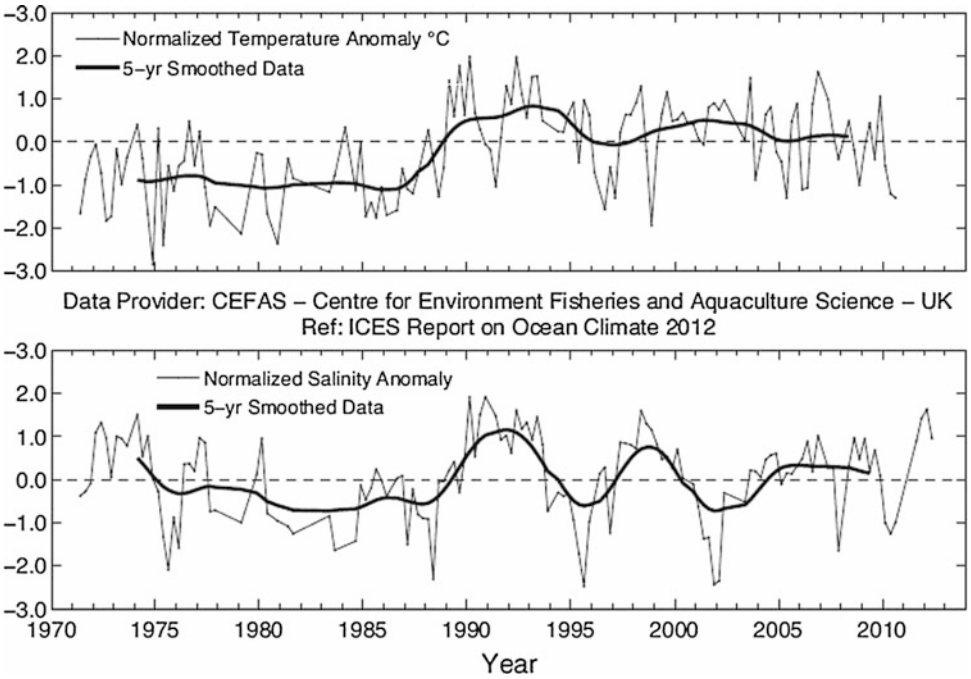

Fig. 3.8 Ferry-based sea-surface temperature (*upper*) and salinity (*lower*) anomalies relative to the 1981–2010 average, along 52°N at six standard stations. The graphic shows three-monthly averages (DJF, MAM, JJA, SON) (Beszczynska-Möller and Dye 2013)

Off northern Denmark and Norway, coastal waters in winter (JFM) were 0.8–1.3 °C warmer in the period 2000–2009 than the period 1961–1990 (Albretsen et al. 2012); the corresponding rise at 200 m depth was 0.55–0.8 °C. Winter–spring observed SST in the Kattegat and Danish Straits rose by about 1 °C between 1897–1901 and the 1980s, and again by about 1 °C to the 1990s–2006 period (Henriksen 2009). Summer–autumn trends were not as clear.

3.2.3 Salinity Variability and Trends

3.2.3.1 Northeast Atlantic

North Atlantic surface salinity shows pronounced interannual and multi-decadal variability. In the Subpolar Gyre salinity variations are correlated with SST such that high salinities usually coincide with anomalously warm water and vice versa (such as in Rockall Trough; Beszczynska-Möller and Dye 2013). On decadal time scales, upper-layer salinity is also positively correlated with the winter NAO, especially in the eastern part of the gyre (Holliday et al. 2011). Shelf-sea and oceanic surface waters to the north and west of the UK had a salinity maximum in the early 1960s and a relatively fresh period in the 1970s, associated with the so-called Great Salinity Anomaly (Dickson et al. 1988). In Rockall Trough the minimum occurred about 1975 (Dickson et al. 1988) and was followed by increasing salinities, interrupted by a mid-1990s minimum (Holliday et al. 2010; Hughes et al. 2012; Sherwin et al. 2012).

Correspondingly, the Fair Isle—Munken section (~2°W 59.5°N to 6°W 61°N across the Faroe-Shetland Channel) at 50–100 m depth showed an upward salinity trend of 0.075 decade^{-1} during the period 1994–2011 (Fig. 3.1; Berx et al. 2013). Likewise, the salinity of Atlantic water inflow to the Nordic Seas through Svinøy section (to the north-west off Norway through ~4°E 63°N) has increased by about 0.15 since the 1970s (Holliday et al. 2008; Beszczynska-Möller and Dye 2013), for example by 0.08 from 1992 to 2009 (Mork and Skagseth 2010).

3.2.3.2 North Sea

Salinity has shown a long-term (1958–2003) increase around northern Scotland (Leterme et al. 2008) and (1971–2012) in the northern North Sea (Fig. 3.9). This is confirmed by Hughes et al. (2012) who charted pentadal-mean upper-ocean salinity showing positive anomalies (relative to the 1971–2000 mean) since 1995 in the northern North Sea most influenced by the Atlantic. Linkage to more saline Atlantic inflow has been suggested (Corten and van de Kamp 1996).

On the western side of the Norwegian Trench and in the central northern North Sea (Utsira section, 59.3°N), influenced by Atlantic water, salinity has increased by about 0.05 since the late 1970s (when values were relatively stable after the Great Salinity Anomaly; Beszczynska-Möller and Dye 2013). On the other hand, salinity in the Fair Isle Current shows interannual variability and no clear long-term trend (Fig. 3.2), being influenced by the fresher waters of the Scottish Coastal Current from west of Scotland.

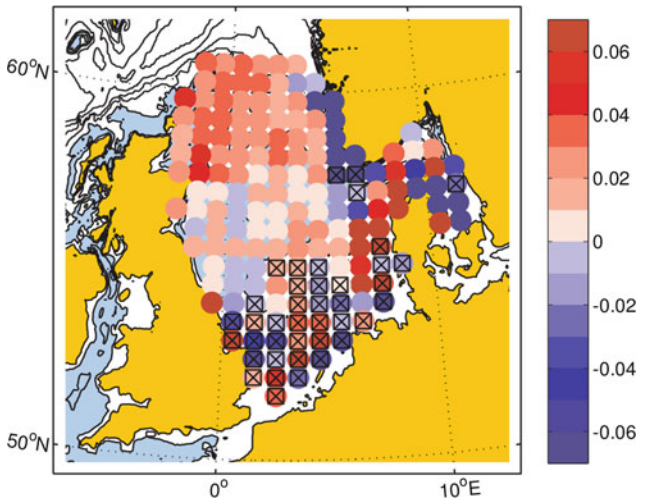

Fig. 3.9 Linear trend per decade in winter bottom salinity, from International Bottom Trawl Survey (IBTS) Quarter 1 data, 1971–2012. Values are calculated for ICES rectangles with more than 30 years of data (hatched areas: trend not significantly different from zero at 95 % confidence level, Dye et al. 2013b; see Acknowledgement, updated from UKMMAS 2010, courtesy of S. Hughes, Marine Scotland Science)

Coastal regions of the southern North Sea, notably the German Bight, are influenced by fluvial inputs (primarily from the rivers Rhine and Elbe) as well as Atlantic inflows (Heyen and Dippner 1998; Janssen 2002). Away from coastal waters, the influence of Atlantic inflow dominates. For the German Bight, Heyen and Dippner (1998) reported no substantial trends in sea-surface salinity (SSS) for the period 1908–1995, a result confirmed by earlier analysis of Helgoland Roads SSS for the period 1873–1993 (Becker et al. 1997) and the analyses of Janssen (2002). German Bight studies (e.g. Fig. 3.10) agree on a temporal minimum around 1982 and a maximum during the early 1990s with a difference of about 0.7 between the two. 1971–2010 ferry data (Fig. 3.8) show pentadal fluctuations with a temporal minimum and maximum also around 1982 and the early 1990s respectively.

The western English Channel (50.03°N, 4.37°W), away from the coast, is influenced by North Atlantic water, showing a similar increase in salinity in recent years (Holliday et al. 2010). Local weather effects (mixed vertically by tidal currents) add to interannual salinity variability which is much greater than in the open ocean. For example, station L4 off Plymouth experiences pulses of surface freshening after intense summer rain increases riverine input (Smyth et al. 2010). However, there is no clear trend over a century of measurements (see also E-Supplement Fig. S3.3, E-Supplement Sect. S3.2).

In the Kattegat and Skagerrak, salinities are affected by low-salinity Baltic Sea outflow. Skagerrak coastal waters in winter (January–March) were up to 0.5 more saline in the period 2000–2009 than the period 1961–1990, but further west and north around Norway their salinity decreased slightly (Albretsen et al. 2012). Shorter-term variability is larger. Salinity variability in the Kattegat and Skagerrak exceeds that in Atlantic water, owing to varying Baltic outflow (see Sect. 3.3) and net precipitation minus evaporation in catchments.

Salinity variability on all time scales to multi-decadal exceeds and obscures any potential long-term trend. For

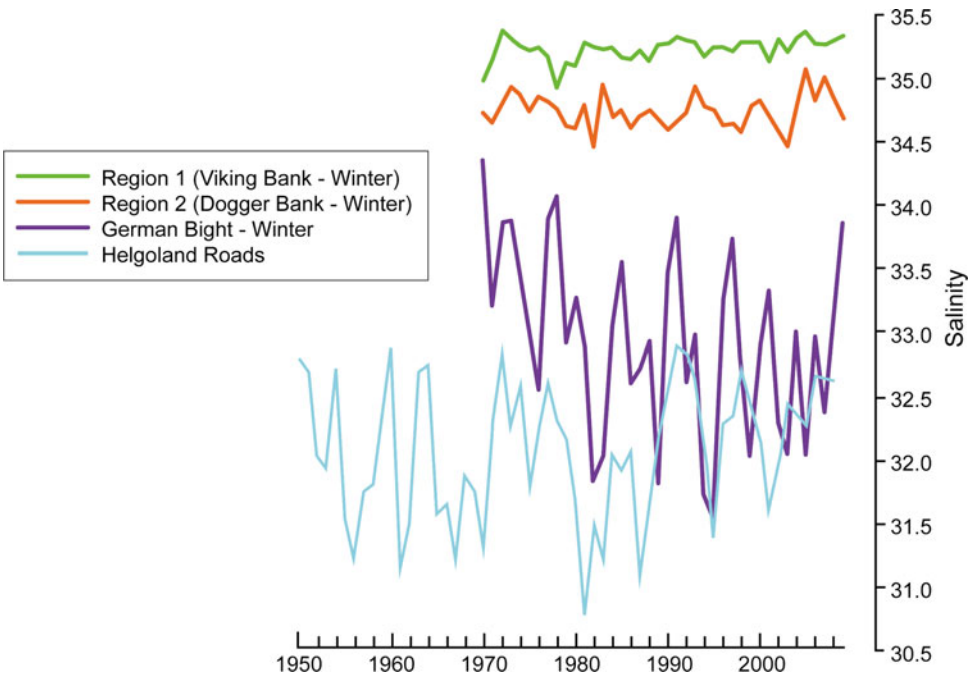

Fig. 3.10 Winter bottom salinity from the ICES International Bottom Trawl Survey (IBTS) dataset at Viking Bank, Dogger Bank and German Bight, together with annual mean salinity from Helgoland Roads (Holliday et al. 2010; see Acknowledgement)

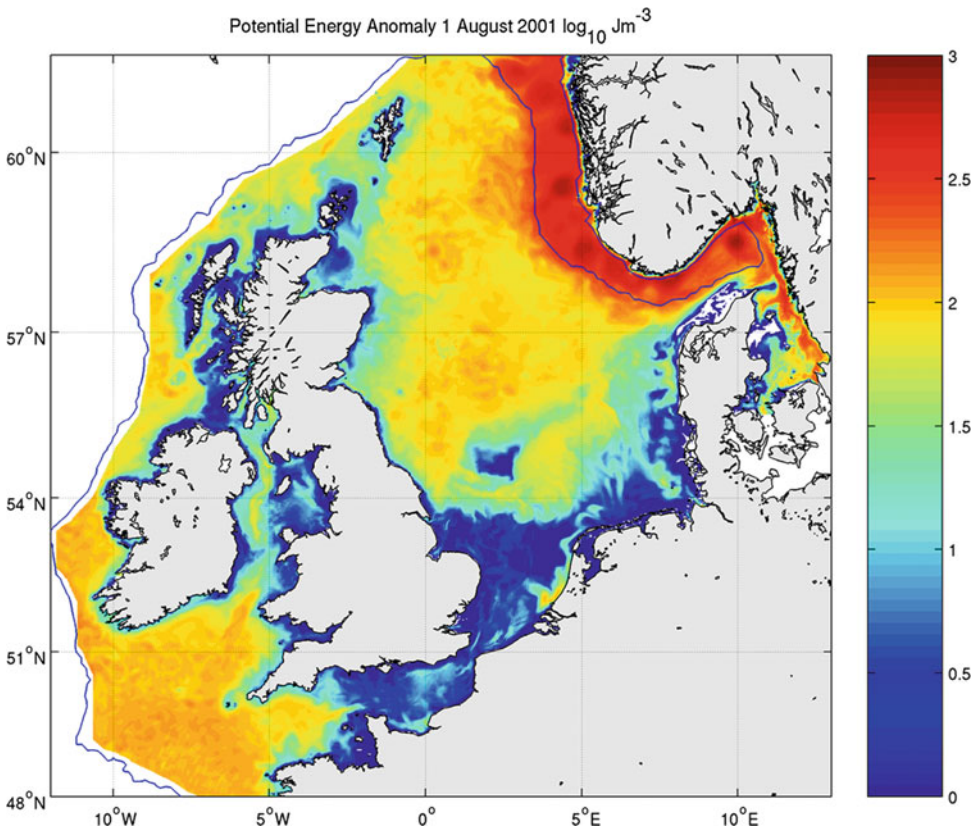

Fig. 3.11 Distribution of potential energy anomaly (energy required to completely mix the water column; log scale, 1 August 2001) (Holt and Proctor 2008)

example, in winter 2005, a series of storms drove much high-salinity Atlantic water across the north-west boundary into the North Sea as far south as Dogger Bank and bottom-water salinity exceeded 35 in 63 % of the North Sea area (Loewe 2009). Adjacent Atlantic waters in the period 2002–2010 (Hughes et al. 2011) show positive salinity anomalies of more than two (one) standard deviation in Rockall Trough (Faroe-Shetland Channel) while the North Sea has no comparably clear signal.

3.2.4 Stratification Variability and Trends

Stratification is a key control on shelf-sea marine ecosystems. Strong stratification inhibits vertical exchange of water. Spring–summer heating reduces near-surface density where tidal currents are too weak to mix through the water depth (Simpson and Hunter 1974), typically where depth is about 50 m or more. The configuration of summer-stratified regions controls much of the average flow in shelf seas (Hill et al. 2008). Mixed-layer data are available albeit only on a 2° grid.[1] The distribution of summer stratification (mainly thermal) is illustrated in Figs. 3.11 and 3.12.

Annual time series of ECOHAM4 simulated thermocline characteristics averaged over the North Sea were reported by Lorkowski et al. (2012). The maximum depth of the thermocline[2] is much more variable interannually than its mean depth. Thermocline intensity shows no trend and only moderate variability. The annual number of days with a mean thermocline greater than 0.2 °C m^{-1} ranged from 31 to 101. The warmest summer in the period simulated (2003) hardly shows in any thermocline characteristics (Lorkowski et al. 2012). In the north-western North Sea, the strength of thermal stratification varies interannually (with no clear trend but periodicity of about 7–8 years; Sharples et al. 2010). The multi-decadal hindcast by Meyer et al. (2011) for the North Sea confirmed that variability in stratification is mainly interannual. In seasonally stratified regions, Holt et al. (2012) modelling showed 1985–2004 warming trends to be greater at the surface than at depth (reflecting an increase in stratification), especially in the central North Sea, at frontal areas of Dogger Bank, in an area north-east of Scotland and in inflow to the Skagerrak. They also found this pattern in annual trends of ICES (International Council for the Exploration of the Sea) data, albeit limited by a lack of seasonal resolution.

[1] www.ifremer.fr/cerweb/deboyer/mld/home.php.

[2] Defined here as (existence of) the uppermost vertical temperature gradient $\Delta T/\Delta z \geq 0.1$; T(°C) is temperature, z (m) is depth.

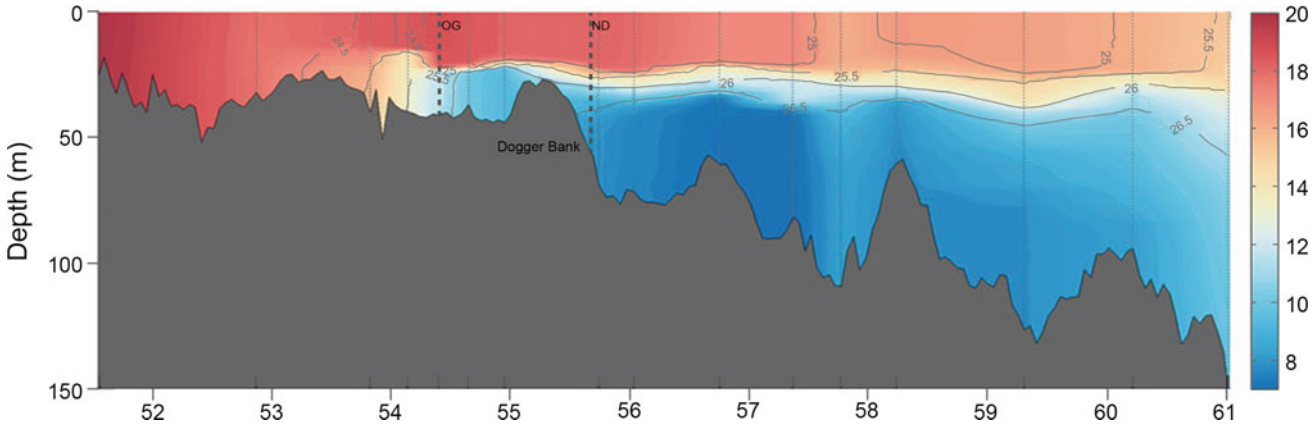

Fig. 3.12 South-north section of potential temperature (°C) near 2.5°E (but further east around Dogger Bank), August 2010 (Queste et al. 2013)

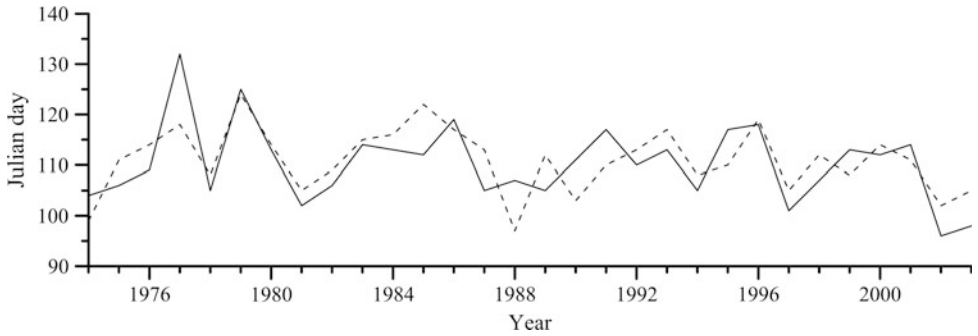

Fig. 3.13 Modelled timing (Julian day) of spring stratification (when the surface-bottom temperature difference first exceeds 0.5 °C for at least three days; *solid line*) and spring bloom (*dashed line*) between 1974 and 2003 in 60 m water depth near 1.4°W 56.2°N (reprinted from Fig. 5a of Sharples et al. 2006)

Lorkowski et al. (2012) found the time of initial thermocline development to vary between Julian days 54 and 107, with relatively large values (i.e. a late start) from 1970 to 1977. Other evidence also suggests a recent trend to earlier thermal stratification (Young and Holt 2007, albeit for the Irish Sea). The timing of spring stratification in the north-western North Sea was modelled for the period 1974–2003 and compared with observed variability by Sharples et al. (2006; Fig. 3.13). Persistent stratification typically begins (on 21 April ± three weeks range) as tidal currents decrease from springs to neaps. The main meteorological control is air temperature; since the mid-1990s its rise seems to have caused stratification to be an average of one day earlier per year with wind stress (linked to the NAO) having had some influence before the 1990s. Holt et al. (2012), modelling 1985–2004, found an extension to the stratified season in the central North Sea and north-east of Scotland.

In estuarine outflow regions, strong short-term and interannual variability in precipitation (hence fluvial inputs) and tidal mixing mask any longer-term trends in stratification (timing or strength).

3.3 Currents and Circulation

John Huthnance, John Siddorn, Ralf Weisse

3.3.1 Historical Perspective

The earliest evidence for circulation comes from hydrographic sections, for time scales longer than a day, and from drifters, observed by chance or deliberately deployed. Prior to satellite tracking (of floats or drogued buoys), typically only drifters' start and end points would be known; temporal and spatial resolution were lacking. Moored current meters record time series at one location; their use was rare until the 1960s. Within the area (5°W–13°E, 48°N–62°N) the international current meter inventory at the British Oceanographic Data Centre[3] records just 27 year-long records and 3025 month-long records to 2008; by decade from the

[3]https://www.bodc.ac.uk/data/information_and_inventories/current_meters/search.

1950s, the numbers of month-long records are 1, 32, 1306, 1201, 381, 124. Occasionally, submarine cables have monitored approximate transport across a section (notably for flow through Dover Strait; e.g. Robinson 1976; Prandle 1978a) and HF radar has given spatial coverage for surface currents within a limited range (Prandle and Player 1993).

Detail on evidence for currents, circulation and their variations is given in E-Supplement Sect. S3.3.

3.3.2 Circulation: Variability and Trends

The Atlantic Meridional Overturning Circulation (AMOC), and its warm north-eastern limb in the Subpolar Gyre, influence the flow and properties of Atlantic Water bordering and partly flowing onto the north-west European shelf and into the North Sea. The AMOC has much seasonal and some interannual variability: mean 18.5 Sv (SD ~ 3 Sv) for April 2004 to March 2009 (Sv is Sverdrup, 10^6 m^3 s^{-1}) (McCarthy et al. 2012). The AMOC probably also varies on decadal time scales (e.g. Latif et al. 2006). Longer-term trends are not yet determined (Cunningham et al. 2010) even though Smeed et al. (2014) found the mean for April 2008 to March 2012 to be significantly less than for the previous four years. The Subpolar Gyre extent correlates with the NAO (Lozier and Stewart 2008). It strengthened overall from the 1960s to the mid-1990s, then decreased (Hátún et al. 2005). While the Subpolar Gyre was relatively weak in the period 2000–2009, more warm, salty Mediterranean and Eastern North Atlantic waters flowed poleward around Britain (Lozier and Stewart 2008; Hughes et al. 2012). Negative NAO also correlates with more warm water in the Faroe-Shetland Channel (Chafik 2012). However, observations show no significant longer-term trend in Atlantic Water transport to the north-east past Scotland and Norway (Orvik and Skagseth 2005; Mork and Skagseth 2010; Berx et al. 2013).

Inflow of oceanic waters to the North Sea from the Atlantic Ocean, primarily in the north driven by prevailing south-westerly winds, has been modelled by Hjøllo et al. (2009; 1985–2007), Holt et al. (2009) and using NORWECOM/POM (3-D hydrodynamic model; Iversen et al. 2002; Leterme et al. 2008, for 1958–2003; Albretsen et al. 2012). Relative to the long-term mean, results show weaker northern inflow between 1958 and 1988; within this period, there were increases in the 1960s and early 1970s, a decrease from 1976 to 1980 and an increase in the early and mid-1980s. The northern inflow was greater than the long-term mean in 1988 to 1995 with a maximum in 1989 (McQuatters-Gollop et al. 2007) but smaller again in 1996 to 2003. This inflow is correlated positively with salinity, SST (less strongly) and the NAO (especially in winter), and negatively with discharges from the rivers Elbe and Rhine (less strongly). For the period 1985–2007, Hjøllo et al. (2009) found a weak trend of −0.005 Sv $year^{-1}$ in modelled Atlantic Water inflows (mean 1.7 Sv, SD 0.41 Sv, correlation with NAO ~0.9). Strong flows into the North Sea (and Nordic Seas) frequently correspond to high-salinity events (Sundby and Drinkwater 2007).

Dover Strait inflow, of the order 0.1 Sv (Prandle et al. 1996), was smaller than the long-term mean from 1958 to 1981 and then greater until 2003 (Leterme et al. 2008). Baltic Sea outflow variations (modelled freshwater relative to salinity 35.0) correlate with winds, resulting sea-surface elevation and NAO index; correlation coefficients with the NAO were 0.57 during the period 1962–2004 and 0.74 during 1980–2004 (Hordoir and Meier 2010; Hordoir et al. 2013). Days-to-months variability O(0.1 Sv) in North Sea—Baltic Sea exchange far exceeds the mean Baltic Sea outflow of the order 0.01 Sv or any trend therein.

North Sea outflows and inflows (plus net precipitation minus evaporation) have to balance on a time scale of just a few days. Off-shelf flow is persistent in the Norwegian Trench and in a bottom layer below the poleward along-slope flow (Holt et al. 2009; Huthnance et al. 2009). A modelled time series for 1958–1997 (Schrum and Sigismund 2001) shows an average outflow of about 2 Sv, little clear trend but consistency with the above interannual variations in inflow.

A MyOcean (project) reanalysis of the region 40°–65°N by 20°W–13°E for the period 1984–2012 was undertaken with the NEMO model version 3.4 (Madec 2008; for details on this application see MyOcean 2014). Transports normal to transects were calculated following NOOS (2010): averaging flow over 24.8 h to give a tidal mean at each model point across the transect; then area-weighting for transports, separating the mean negative and mean positive flows. For the Norway–Shetland transect, flow in the west is dominantly into the North Sea and makes a significant contribution to exchange with the wider Atlantic; circulation is partially density-driven during summer and confined to the coastal waters east of Shetland. Mean inflow is 0.56 Sv with significant seasonality and interannual variability but no obvious trend. In the east sector of the Norway–Shetland transect, flow is both into and out of the North Sea, strongly steered by the Norwegian Trench and includes the Norwegian Coastal Current, resulting in a larger outflow than inflow. Mean net flow is 1.3 Sv (SD 0.97 Sv) representing large seasonal and interannual variability, especially in the outflow.

Net circulation within the North Sea is shown schematically in Fig. 1.7. Tidal currents are important, primarily semi-diurnal with longer-period modulation (Sect. 1.4.4); locally values exceed 1.2 m s^{-1} in the Pentland Firth, off East Anglia and in Dover Strait. Other important current contributions are due to winds (Sect. 1.4.3 shows

representative flow patterns) and to differences in density (Sect. 1.4.2) including estuarine outflows (e.g. van Alphen et al. 1988), varying on time scales from hours to seasons (e.g. Turrell et al. 1992) to decades. Hence flows can be very variable in time; they also vary strongly with location.

Wind forcing is the most variable factor; water transports in one storm (typically in winter; time-scale hours to a day) can be significant relative to a year's total. 50-year return values for currents in storm surges have been estimated at 0.4–0.6 m s^{-1} in general, but exceed 1 m s^{-1} locally off Scottish promontories, in Dover Strait, west of Denmark and over Dogger Bank (Flather 1987). These extreme currents are directed anti-clockwise around the North Sea near coasts, and into the Skagerrak.

In summer-stratified areas (Sect. 3.2.4) cold bottom water is nearly static (velocity tends to zero at the sea bed due to friction). Between stratified and mixed areas, relatively strong density gradients are expected to drive near-surface flows anti-clockwise around the dense bottom water (Hill et al. 2008). These flows, of the order 0.3 m s^{-1} but sometimes >1 m s^{-1} in the Norwegian Coastal Current, are liable to baroclinic instability developing meanders, scale 5–10 km (e.g. Badin et al. 2009; their model shows eddy variability increasing in late summer with increased stratification). Such meanders are prominent north of Scotland over the continental slope and off Norway where the fresher surface layer increases stratification.

When a region of freshwater influence (ROFI) is stratified, cross-shore tidal currents may develop; for example, according to de Boer et al. (2009) surface currents rotate clockwise and bottom currents anti-clockwise in the Rhine ROFI when stratified. These authors also found cyclical upwelling there due to tidal currents going offshore at the surface and onshore below.

The winter mean circulation of the North Sea is organised in one anti-clockwise gyre with typical mean velocities of about 10 cm s^{-1} (Kauker and von Storch 2000). On shorter time scales the circulation is highly variable. Kauker and von Storch (2000) identified four regimes. Two are characterised by a basin-wide gyre with clockwise (15 % of the time) or anti-clockwise (30 % of the time) orientation. The other two regimes are characterised by the opposite regimes of a bipolar pattern with maxima in the southern and northern parts of the North Sea (45 % of the time). For 10 % of the time the circulation nearly ceased. Kauker and von Storch (2000) found that only 40 % of the one-gyre regimes persist for longer than five days while the duration of the bipolar circulation patterns rarely exceeded five days. Accordingly, short-term variability typically dominates transports; tidal flows dominate instantaneous transports (positive and negative volume fluxes across sections) and meteorological phenomena dominate residual (net) transports.

Mean residual transports are generally smaller than their variability. Many transects show strong seasonality as meteorological conditions drive surges, river runoff and ice melt. No trend in transports has been seen in these data: limited duration of available data and large variability in the transports on time scales of days, seasons and interannually makes discerning trends difficult.

In the German Bight, anti-clockwise circulation is about twice as frequent as clockwise, and prevails during south-westerly winds typical of winter storms, giving rapid transports through the German Bight (Thiel et al. 2011, on the basis of Pohlmann 2006). Loewe (2009) associated clockwise flow with high-pressure and north-westerly weather types, anti-clockwise flow with south-westerly weather types, and flow towards the north or north-west with south-easterly weather types. However, Port et al. (2011) found that the wind-current relation changes away from the coast owing to dependence on density effects, the coastline and topography.

On longer time scales the variability of the North Sea circulation and thus transports is linked to variations in the large-scale atmospheric circulation. Emeis et al. (2015) reported results of an EOF analysis (see von Storch and Zwiers 1999) of monthly mean fields of vertically integrated volume transports derived from a multi-decadal model hindcast (Fig. 3.14; see also Mathis et al. 2015). Regions of particularly high variability include the inflow areas of Atlantic waters via the northern boundary of the North Sea and the English Channel, respectively. The time coefficient associated with the dominant EOF mode overlaid with the NAO index illustrates the relation with variability of the large-scale atmospheric circulation (Fig. 3.14). Positive EOF coefficient (intensified inflow of Atlantic waters) corresponds with a positive NAO, i.e. enhanced westerly winds, which in turn result in an intensified anti-clockwise North Sea circulation (Emeis et al. 2015); opposites also hold.

In summary, multiple forcings cause currents to vary on a range of time and space scales, including short scales relative to which measurements are sparse. Hence trends are of lesser significance and hard to discern. Moreover, causes of trends in flows are difficult to diagnose; improvements are needed in observational data (quantity and quality). Reliance is placed on models, which need improvement (in formulation, forcing) for currents other than tides and storm surges.

3.4 Mean Sea Level

Thomas Wahl, Philip Woodworth, Ivan Haigh, Ralf Weisse

Changes in mean sea level (MSL) result from different aspects of climate change (e.g. the melting of land-based ice, thermal expansion of sea water) and climate variability (e.g.

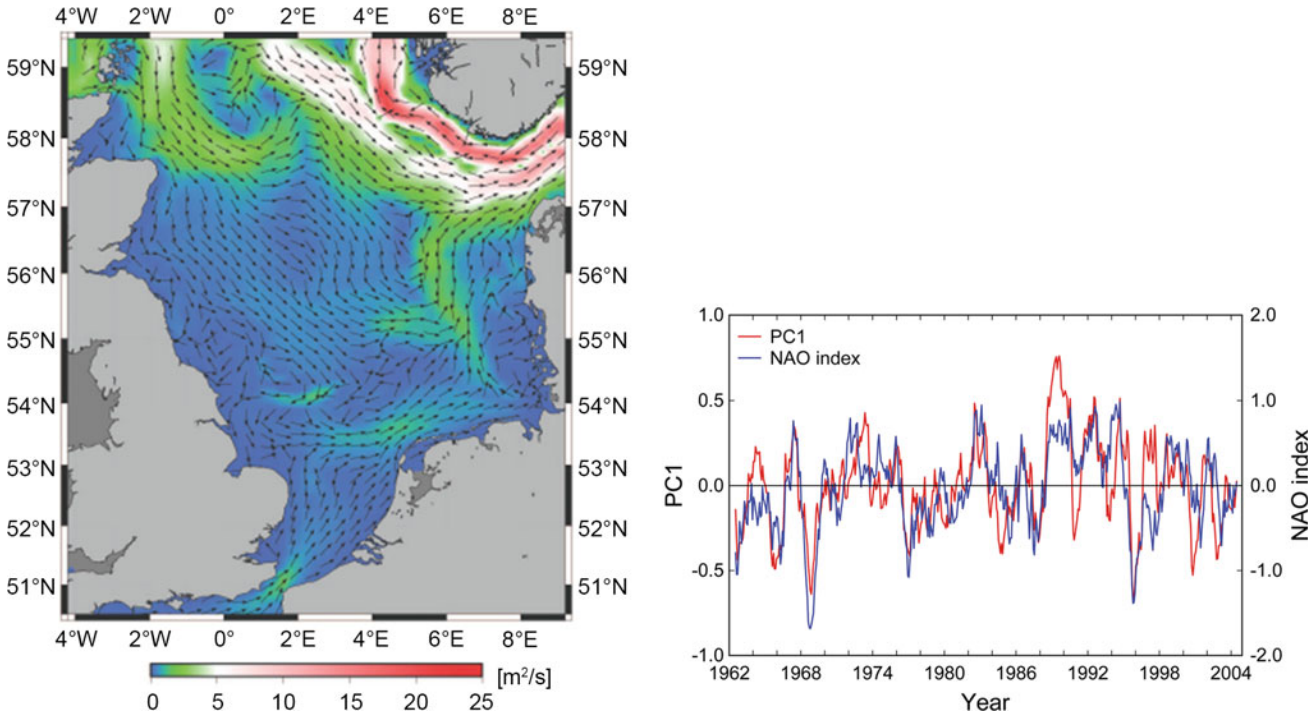

Fig. 3.14 Dominant EOF of monthly mean vertically integrated volume transports obtained from a 3D baroclinic simulation (1962–2004) explaining 75.8 % of the variability. Vectors indicate directions of transport anomalies while colours indicate magnitudes (*left* Emeis et al. 2015); Corresponding coefficient time series (*red*) and NAO index (*blue*) (*right* Hurrell et al. 2013). Shown are moving annual averages based on monthly values

changes in wind forcing related to the NAO or El Niño–Southern Oscillation) and occur over all temporal and spatial scales. MSL is sea level averaged into monthly or annual mean values, which are the parameters of most interest to climate researchers (Woodworth et al. 2011). The focus in this chapter is on the last 200 years, when direct 'modern' measurements of sea level are available from tide gauges and high precision satellite radar altimeter observations. MSL can be inferred indirectly over this period (and thousands of years earlier) using proxy records from salt-marsh sediments and the fossils within them (Gehrels and Woodworth 2013) or archaeology (e.g. fish tanks built by the Romans), and over much longer time scales (thousands to millions of years) using other paleo-data (e.g. geological records, from corals or isotopic methods).

The North Sea coastline has one of the world's most densely populated tide gauge networks, with many (>15) records spanning 100 years or longer and a few going back almost continuously to the early 19th century. The tide gauges of Brest and Amsterdam also provide some data for parts of the 18th century and are among the longest sea level records in the world. Since 1992, satellite altimetry has provided near-global coverage of MSL. The advantage of altimetry is that it records geocentric sea level (i.e. measurements relative to the centre of the Earth). By contrast, tide gauges measure the relative changes between the ocean surface and the land itself; hence, the term 'relative mean sea level' (RMSL), and it is this that is of most relevance to coastal managers, engineers and planners. Calculation from tide gauge records of changes in 'geocentric mean sea level' (sometimes referred to as 'absolute mean sea level'; AMSL) requires the removal of non-climate contributions to sea level change, which arise both from natural processes (e.g. tectonics, glacial isostatic adjustment GIA) and from anthropogenic processes (e.g. subsidence caused by ground water abstraction). Tide gauge records can be corrected using estimates of vertical land motion from (i) models which predict the main geological aspect of vertical motion, namely GIA (e.g. Peltier 2004); (ii) geological information near tide gauge sites (e.g. Shennan et al. 2012); and (iii) direct measurements made at or near tide gauge locations using continuous global positioning system (GPS) or absolute gravity (e.g. Bouin and Wöppelmann 2010). Rates of vertical land movement have also been estimated by comparing trends derived from altimetry data and tide gauge records (e.g. Nerem and Mitchum 2002; Garcia et al. 2007; Wöppelmann and Marcos 2012).

Paleo sea level data from coastal sediments, the few long (pre-1900) tide gauge records and reconstructions of MSL, made by combining tide gauge records with altimetry measurements (e.g. Church and White 2006, 2011; Jevrejeva et al. 2006, 2008; Merrifield et al. 2009), indicate that there

was an increase in the rate of global MSL rise during the late 19th and early 20th centuries (e.g. Church et al. 2010; Woodworth et al. 2011; Gehrels and Woodworth 2013). Over the last 2000 to 3000 years, global MSL has been near present-day levels with fluctuations not larger than about ±0.25 m on time scales of a few hundred years (Church et al. 2013) whereas the global average rate of rise estimated for the 20th century was 1.7 mm year^{-1} (Bindoff et al. 2007). Measurements from altimetry suggest that the rate of MSL rise has almost doubled over the last two decades; Church and White (2011) estimated a global trend of 3.2 ± 0.4 mm year^{-1} for the period 1993–2009. Milne et al. (2009) assessed the spatial variability of MSL trends derived from altimetry data and found that local trends vary by as much as −10 to +10 mm year^{-1} from the global average value for the period since 1993, due to regional effects influencing MSL changes and variability (e.g. non-uniform contributions of melting glaciers and ice sheets, density anomalies, atmospheric forcing, ocean circulation, terrestrial water storage). This highlights the importance of regional assessments. Examining whether past MSL has risen faster or slower in certain areas compared to the global average will help to provide more reliable region-specific MSL rise projections for coastal engineering, management and planning.

There have been very few region-wide studies of MSL changes in the North Sea. The first detailed study was by Shennan and Woodworth (1992), who used geological and tide gauge data from sites around the North Sea to infer secular trends in MSL in the late Holocene and 20th century (up until the late 1980s). They concluded that a systematic offset of 1.0 ± 0.15 mm year^{-1} in the tide gauge trends, compared to those derived from the geological data, could be interpreted as the regional average rate of geocentric MSL change over the 20th century; this is significantly less than global rates over this period. They also showed that part of the interannual MSL variability of the region was coherent, and they represented this as an index, created by averaging the de-trended MSL time series. Like Woodworth (1990), they found no evidence for a statistically significant acceleration in the rates of MSL rise for the 20th century.

Since then many other investigations of MSL changes have been undertaken for specific stretches of the North Sea coastline, mostly on a country-by-country basis, as for example by Araújo (2005), Araújo and Pugh (2008), Wöppelmann et al. (2006, 2008) and Haigh et al. (2009) for the English Channel; by van Cauwenberghe (1995, 1999) and Verwaest et al. (2005) for the Belgian coastline; Jensen et al. (1993) and Dillingh et al. (2010) for the Dutch coastline; Jensen et al. (1993), Albrecht et al. (2011), Albrecht and Weisse (2012) and Wahl et al. (2010, 2011) for the German coastline; Madsen (2009) for the Danish coastline; Richter et al. (2012) for the Norwegian coastline; and by Woodworth (1987) and Woodworth et al. (1999, 2009a) for the United Kingdom (UK). The most detailed analysis of 20th century geocentric MSL changes was undertaken by Woodworth et al. (2009a). They estimated that geocentric MSL around the UK rose by 1.4 ± 0.2 mm year^{-1} over the 20th century; faster (but not significantly faster at 95 % confidence) than the earlier estimate by Shennan and Woodworth (1992) for the whole North Sea and slower (but not significantly slower at 95 % confidence level) than the global 20th century rate.

A recent investigation undertaken by Wahl et al. (2013) aimed at updating the results of the Shennan and Woodworth (1992) study, using tide-gauge records that are now 20 years longer across a larger network of sites, altimetry measurements made since 1992, and more precise estimates of vertical land movement made since then with the development of advanced geodetic techniques. They analysed MSL records from 30 tide gauges covering the entire North Sea coastline (Fig. 3.15). Trends in RMSL were found to vary significantly across the North Sea region due to the influence of vertical land movement (i.e. land uplift in northern Scotland, Norway and Denmark, and land subsidence elsewhere). The accuracy of the estimated trends was also influenced by considerable interannual variability present in many of the MSL time series. The interannual variability was found to be much greater along the coastlines of the Netherlands, Germany and Denmark, compared to Norway, the UK east coast and the English Channel (Fig. 3.16).

However, using correlation analyses, Wahl et al. (2013) showed that part of the variability was coherent throughout the region, with some differences between the Inner North Sea (number 4 anti-clockwise to 26 in Fig. 3.15) and the English Channel. Following Shennan and Woodworth (1992), they represented this coherent part of the variability by means of MSL indices (Fig. 3.16). Geocentric MSL trends of 1.59 ± 0.16 and 1.18 ± 0.16 mm year^{-1} were obtained for the Inner North Sea and English Channel indices, respectively, for the period 1900–2009 (data sets were corrected for GIA to remove the influence of vertical land movement). For the North Sea region as a whole, the geocentric MSL trend was 1.53 ± 0.16 mm year^{-1}. These results are consistent with those presented by Woodworth et al. (2009a) for the UK (i.e. an AMSL trend of 1.4 ± 0.2 mm year^{-1} for the 20th century), but were significantly different from those presented by Shennan and Woodworth (1992) for the North Sea region (i.e. a geocentric MSL trend of 1.0 ± 0.15 mm year^{-1} for the period from 1901 to the late 1980s). For the 'satellite period' (i.e. 1993 to 2009) the geocentric MSL trend was estimated to be 4.00 ± 1.53 mm year^{-1} from the North Sea tide gauge records. This trend is faster but not significantly different from the global geocentric MSL trend for the same period (i.e. 3.20 ± 0.40 mm year^{-1} from satellite altimetry and

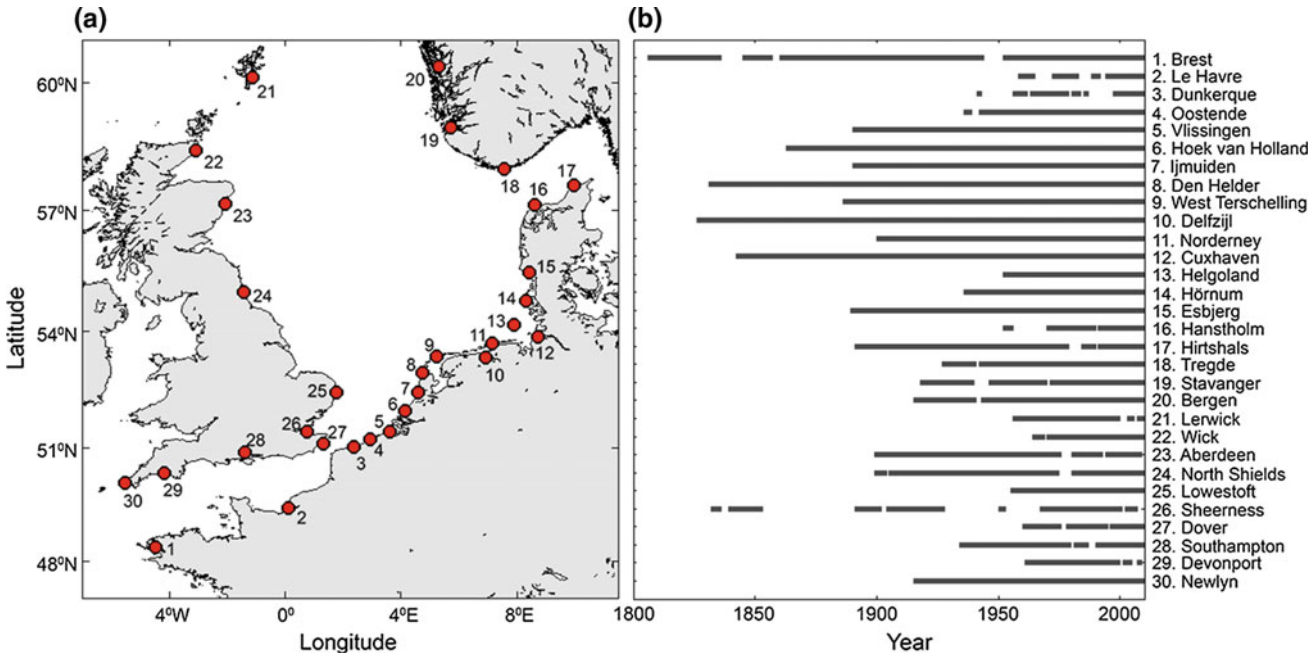

Fig. 3.15 Study area, tide gauge locations and length of individual mean sea level data sets (Wahl et al. 2013)

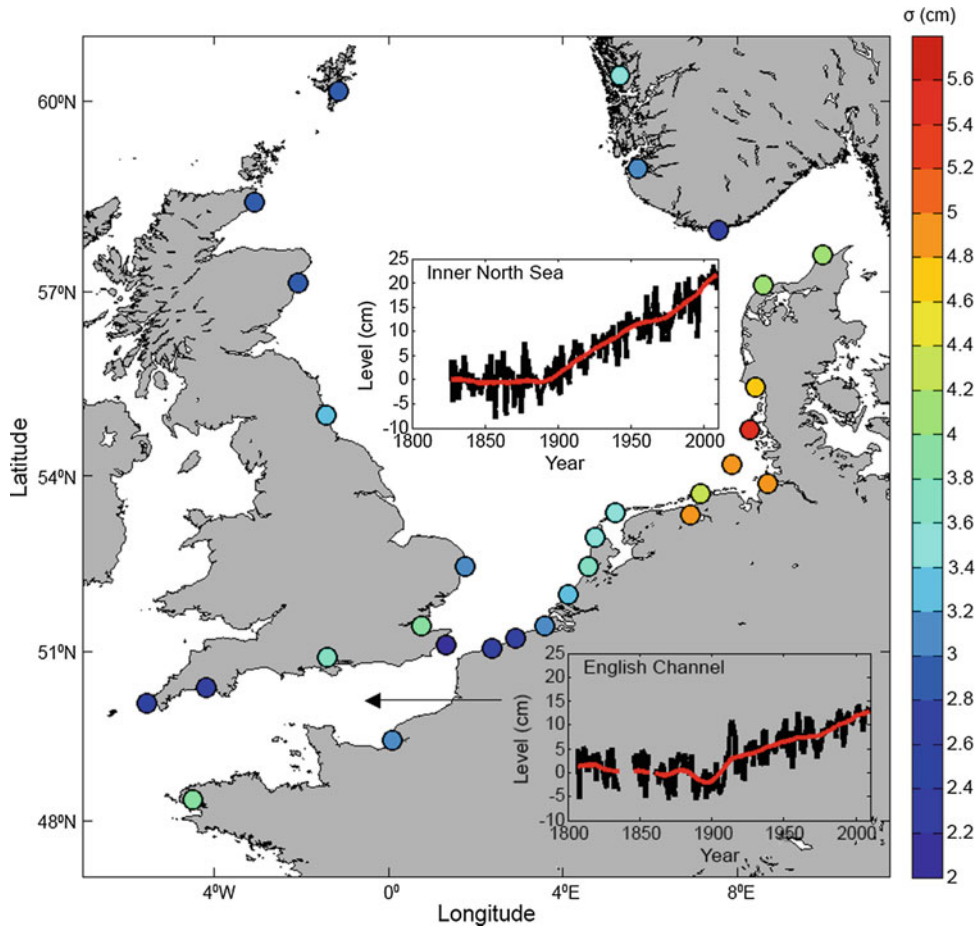

Fig. 3.16 Standard deviation from de-trended annual mean sea level (MSL) time series from 30 tide gauge sites around the North Sea; *upper inset* MSL index for the Inner North Sea (*black*) together with the non-linear sea-surface anomaly (SSA) smoothed time series (*red*); *lower inset* MSL index for the English Channel (*black*) together with the non-linear SSA smoothed time series (*red*) (after Wahl et al. 2013)

2.80 ± 0.80 mm year^{-1} from tide gauge data; Church and White 2011). In summary, the observed long-term changes in sea-level rise (SLR) in the North Sea do not differ significantly from global rates over the same period.

In recent years there has also been considerable focus on the issue of 'acceleration in rates of MSL rise'. Several methods have been applied to examine non-linear changes in long MSL time series from individual tide gauge sites and global or regional reconstructions (see Woodworth et al. 2009b, 2011 for a synthesis of these studies). Wahl et al. (2013) used singular system analysis (SSA) with an embedding dimension of 15 years for smoothing the MSL indices for the Inner North Sea and English Channel (Fig. 3.16). Periods of SLR acceleration were detected at the end of the 19th century and in the 1970s; a period of deceleration occurred in the 1950s. Several authors (e.g. Miller and Douglas 2007; Woodworth et al. 2010; Sturges and Douglas 2011; Calafat et al. 2012) suggested that these periods of acceleration/deceleration are associated with decadal MSL fluctuations arising from large-scale atmospheric changes. The recent rates of MSL rise were found to be faster than on average, with the fastest rates occurring at the end of the 20th century. These rates are, however, still comparable to those observed during the 19th and 20th centuries.

3.5 Extreme Sea Levels

Ralf Weisse, Andreas Sterl

Extreme sea levels pose significant threats (such as flooding and/or erosion) to many of the low-lying coastal areas along the North Sea coast. Two of the more recent examples are the events of 31 January/1 February 1953 and 16/17 February 1962 that caused extreme sea levels along much of the North Sea coastline and that were associated with a widespread failure of coastal protection, mostly in the UK, the Netherlands and Germany (e.g. Baxter 2005; Gerritsen 2005). Since then, coastal defences have been substantially enhanced along much of the North Sea coastline.

Extreme sea levels usually arise from a combination of factors extending over a wide range of spatial and temporal scales comprising high astronomical tides, storm surges (also referred to as meteorological residuals caused by high wind speeds and inverse barometric pressure effects) and extreme sea states (wind-generated waves at the ocean surface) (Weisse et al. 2012). On longer time scales, rising MSL may increase the risk associated with extreme sea levels as it modifies the baseline upon which extreme sea levels act; that is, it tends to shift the entire frequency distribution towards higher values.

The large-scale picture may be modified by local conditions. For example, for given wind speed and direction the magnitude of a storm surge may depend on local bathymetry or the shape of the coastline. Extreme sea states may become depth-limited in very shallow water and effects such as wave set-up (Longuet-Higgins and Stewart 1962) may further raise extreme sea levels. Moreover, there is considerable interaction among the different factors contributing to extreme sea levels, especially in shallow water. For example, for the UK coastline Horsburgh and Wilson (2007) reported a tendency for storm surge maxima to occur most frequently on the rising tide arising primarily from tide-surge interaction. Mean SLR may modify tidal patterns and several authors report changes in tidal range associated with MSL changes. For M2 tidal ranges, estimates vary from a few centimetres increase in the German Bight for a 1-m SLR (e.g. Kauker 1999) to 35 cm in the same area for a 2-m SLR (Pickering et al. 2011). So far, reasons for these differences are not elaborated on in the peer-reviewed literature.

Large sectors of the North Sea coastline are significantly affected by storm surges. A typical measure to assess the weather-related contributions relative to the overall variability is the standard deviation of the meteorological residuals (Pugh 2004). Typically, this measure varies from a few centimetres for open ocean islands hardly affected by storm surges to tens of centimetres for shallow water subject to frequent meteorological extremes (Pugh 2004). For the German Bight, values are in the order of approximately 30–40 cm indicating that storm surges provide a substantial contribution to the total sea level variability (Weisse and von Storch 2009). There is also pronounced seasonal variability with the most severe surges generally occurring within the winter season from November to February reflecting the corresponding cycle in severe weather conditions (Weisse and von Storch 2009).

Extreme sea level variability and change for Cuxhaven, Germany is illustrated in Fig. 3.17. Here a statistical approach was used to separate effects due to changes in MSL and to storm surges (von Storch and Reichardt 1997). The approach is based on the assumption that changes in MSL will be visible both in mean and in extreme sea levels as these changes tend to shift the entire frequency distribution towards higher values. Changes in the statistics of storm surges, on the other hand, will not be visible in the mean but only in the extremes. Following this idea, variations in the extremes may be analysed for example by subtracting trends in annual means from higher annual percentiles while variations and changes in the mean may be obtained by analysing the means themselves. Figure 3.17 shows the result of such an analysis for Cuxhaven, Germany. It can be inferred that the meteorological part (i.e. storm surges) shows pronounced decadal and interannual variability but no substantial long-term trend. The decadal variations are broadly consistent with observed variations in storm activity in the area (e.g. Rosenhagen and Schatzmann 2011; Weisse et al.

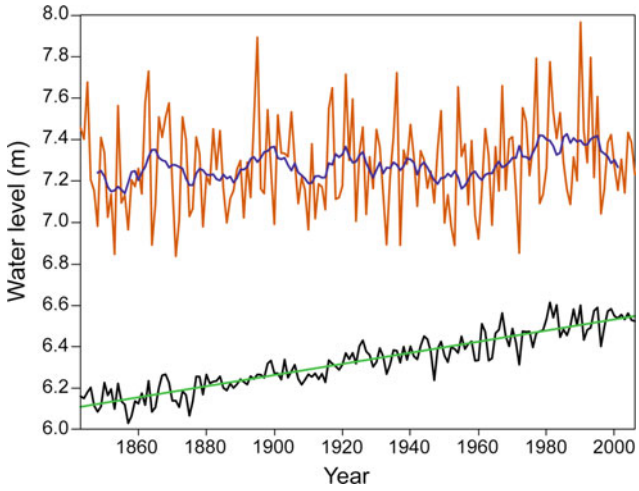

Fig. 3.17 Annual mean high water and linear trend (in m) for the period 1843–2012 at Cuxhaven, Germany (*lower*) and annual 99th percentile of the approximately twice-daily high-tide water levels at Cuxhaven after subtraction of the linear trend in the annual mean levels (*upper*); an 11-year running mean is also shown in the upper panel (redrawn and updated after von Storch and Reichardt 1997)

2012). Figure 3.17 also reveals that extreme sea levels substantially increased over the study period but that changes are primarily a consequence of corresponding changes in MSL and not of storm activity.

An alternative approach to analyse changes in extreme sea levels caused by changing meteorological conditions is by using numerical tide-surge models for hindcasting extended periods over past decades. Such hindcasts are usually set up using present-day bathymetry and are driven by observed (reanalysed) atmospheric wind and pressure fields. In such a design any observed changes in extreme sea levels result solely from meteorological changes while contributions from all other effects such as changes in MSL or local construction works are explicitly removed. Generally, and consistent with the results obtained from observations, such studies do not show any long-term trend but pronounced decadal and interannual variability consistent with observed changes in storm activity (e.g. Langenberg et al. 1999; Weisse and Pluess 2006).

In the analysis of von Storch and Reichardt (1997) annual mean high water is used as a proxy to describe changes in the mean. Climatically induced changes in annual mean high water statistics result principally from two different contributions: (i) corresponding changes in MSL and/or (ii) changes in tidal dynamics. Separating both contributions, Mudersbach et al. (2013) found for Cuxhaven from 1953 onwards that, apart from changes in MSL, extreme sea levels have also increased as a result of changing tidal dynamics. Reasons for the observed changes in tidal variation remain unclear. While increasing MSL represents a potential driver discussed by some authors (e.g. Mudersbach et al. 2013) the magnitude of the observed changes is too large compared to expectations from modelling studies (e.g. Kauker 1999; Pickering et al. 2011) and other contributions (such as those caused by local construction works) could not be ruled out (e.g. Hollebrandse 2005). Other potential reasons for changes in tidal constituents are referred to by Woodworth (2010) and Müller (2012) but have not been explored for the North Sea.

Systematic measurements of sea state parameters exist only for periods much shorter than those from tide gauges. In the late 1980s and early 1990s a series of studies analysed changes in mean and extreme wave heights in the North Atlantic and the North Sea (e.g. Neu 1984; Carter and Draper 1988; Bacon and Carter 1991; Hogben 1994). These were typically based on time series of 15 to at most 25 years and, while reporting a tendency towards more extreme sea states, all authors concluded that the time series were too short for definitive statements on longer-term changes. As for storm surges, numerical models are therefore frequently used to make inferences about past long-term changes in wave climate. Such models are either used globally (e.g. Cox and Swail 2001; Sterl and Caires 2005) or regionally for the North Sea and adjacent sea areas (e.g. WASA-Group 1998; Weisse and Günther 2007). For the North Sea, the latter found considerable interannual and decadal variability in the hindcast wave data consistent with existing knowledge on variations in storm activity.

Results from numerical studies should be complemented with those from statistical approaches. While numerical studies may represent variability and changes with fine spatial and temporal detail, the period for which such studies are possible is presently limited to a few decades. Statistical approaches may bridge the gap by providing information for longer time spans, but are usually limited in spatial and/or temporal detail. Such approaches were used by Kushnir et al. (1997), WASA-Group (1998), Woolf et al. (2002) and Vikebø et al. (2003), exploiting different statistical models between sea-state parameters and large-scale atmospheric conditions. Generally these approaches illustrate the substantial interannual and decadal variability inherent in the North Sea and North Atlantic wave climate. While longer periods are covered, the authors described periods of decreases and increases in extreme wave conditions. For example, Vikebø et al. (2003) described an increase in severe wave heights emerging around 1960 and lasting until about 1999 and concluded that this increase is not unusual when longer periods are considered. This indicates that changes extending over several decades, i.e. typical periods covered by numerical or observational based studies, should be viewed in the light of decadal variability obtained by analysing longer time series.

3.6 Carbon Dioxide, pH, and Nutrients

Helmuth Thomas, Johannes Pätsch, Ina Lorkowski, Lesley Salt, Wilfried Kühn, John Huthnance

Drivers and consequences of climate change are usually discussed from the perspective of physical processes. As such, Sects. 3.2 and 3.3 focus on aspects of physical water column properties (sea temperature, salinity and stratification) and physical interaction with adjacent water bodies (circulation and currents), and climate-change-driven alterations of these. While biogeochemical properties clearly respond to changes in physical conditions, changes can also be modulated by anthropogenic changes in the chemical conditions. These include increasing atmospheric CO_2 levels, ocean acidification as a consequence, and eutrophication/oligotrophication. Relevant time scales can co-vary with those of climate change processes, however they may also be distinctly different (e.g. Borges and Gypens 2010). Furthermore, effects of direct anthropogenic changes (such as nutrient inputs) and feedbacks between anthropogenic and climate changes (atmospheric CO_2 and warming, for example) can be synergistic (amplify each other) or antagonistic (diminish each other). Eutrophication and oligotrophication, feedbacks to changes in physical properties and their effects on productivity in the North Sea have been investigated using models (e.g. Lenhart et al. 2010; Lancelot et al. 2011). Results have been used by international bodies and regulations such as OSPAR, the European Water Framework Directive (EC 2000) and the Marine Strategy Framework Directive. A summary was recently given by Emeis et al. (2015).

The main focus of this section is on the carbonate and pH system of the North Sea and its vulnerability to climate and anthropogenic change. To address these issues, large systematic observational studies were initiated in the early 2000s by an international consortium led by the Royal Netherlands Institute of Sea Research (e.g. Thomas et al. 2005b; Bozec et al. 2006). Observational studies have been supplemented by modelling studies (e.g. Blackford and Gilbert 2007; Gypens et al. 2009; Prowe et al. 2009; Borges and Gypens 2010; Kühn et al. 2010; Liu et al. 2010; Omar et al. 2010; Artioli et al. 2012, 2014; Lorkowski et al. 2012; Wakelin et al. 2012; Daewel and Schrum 2013).

The North Sea is one of the best studied and most understood marginal seas in the world and so offers a unique opportunity to identify biogeochemical responses to climate variability and change. To better understand the sensitivity of the North Sea biogeochemistry to climate and anthropogenic change, this section first discusses some of the main responses to variability in the dominant regional climate mode—the NAO—based on observational data for 2001, 2005 and 2008. The effects of long-term perturbations on the major processes regulating biogeochemical conditions in the North Sea are then discussed based on results from multi-decadal ecosystem model runs. Observations on longer time scales exist locally off the Netherlands, Helgoland and elsewhere but are all from sites close to the coast where strong offshore gradients in nutrients and primary productivity (e.g. Baretta-Bekker et al. 2009; Artioli et al. 2014) affect CO_2.

3.6.1 Observed Responses to Variable External Forcing

In deeper areas of the North Sea, beyond the 50 m depth contour, primary production and CO_2 fixation are supported by seasonal stratification and by nutrients, which are a limiting factor and largely originate from the Atlantic Ocean (Pätsch and Kühn 2008; Loebl et al. 2009). Sinking particulate organic matter facilitates the replenishment of biologically-fixed CO_2 by atmospheric CO_2. Respiration of particulate organic matter below the surface layer releases metabolic dissolved inorganic carbon (DIC) which is either exported to the deeper Atlantic or mixed back to the surface in autumn and winter (Thomas et al. 2004, 2005b; Bozec et al. 2006; Wakelin et al. 2012). These northern areas of the North Sea act as a net annual sink for atmospheric CO_2.

By contrast, in the south (depth <50 m), the absence of stratification causes respiration and primary production to occur within the well-mixed water column. Except during the spring bloom, the effects of particulate organic carbon (POC) production and respiration cancel out and the CO_2 system is largely temperature-controlled (Thomas et al. 2005a; Schiettecatte et al. 2006, 2007; Prowe et al. 2009). Total production in this area is high in global terms; terrestrial nutrients contribute, especially in the German Bight, but in the shallow south, primary production is based largely on recycled nutrients with little net fixation of CO_2.

Beyond the biologically-mediated CO_2 controls, North Atlantic waters, flushing through the North Sea, dominate the carbonate system (Thomas et al. 2005b; Kühn et al. 2010) but may have only small net budgetary effects. The Baltic Sea outflow and river loads constitute net imports of carbon to the North Sea and modify the background conditions set by North Atlantic waters.

Basin-wide observations of DIC, pH, and surface temperature during the summers of 2001, 2005 and 2008 (Salt et al. 2013) reveal the dominant physical mechanisms regulating the North Sea pH and CO_2 system. pH and CO_2 system responses to interannual variability in climate and weather conditions (NAO, local heat budgets, wind and fluxes to or from the Atlantic, the Baltic Sea and rivers, see also Sects. 3.2 and 3.3) are also considered to be the responses that climate change will trigger. Interannual

variability appears generally more pronounced than long-term trends (e.g. Thomas et al. 2008).

The NAO index (Hurrell 1995; Hurrell et al. 2013) is commonly established for the winter months (DJF), although its impacts have been identified at various time scales. Many processes in the North Sea are reported to be correlated with the winter NAO, even if they occur in later seasons. Two aspects may explain an apparent delay between the trigger (i.e. winter NAO) and the response (the timing of the actual process): preconditioning and hysteresis (Salt et al. 2013).

An example of pre-conditioning is the water mass exchange between the North Atlantic Ocean and the North Sea. This exchange is enhanced during years of positive NAO (Winther and Johannessen 2006) and leads to an increased nutrient inventory in the North Sea and to higher annual productivity in spring and summer (Pätsch and Kühn 2008). Hysteresis can be characteristic of the North Sea's response to the NAO. Stronger westerly winds in winter, correlated with the winter NAO, push North Sea water into the Baltic Sea, a process that in turn leads to an enhanced outflow from the Baltic Sea into the North Sea in subsequent seasons (Hordoir and Meier 2010).

The bottom topographic divide of the North Sea, at about 40–50 m depth, is reflected in DIC, pH and temperature distributions (Figs. 3.18, 3.19 and 3.20) with higher DIC and temperature, and lower pH observed in the south, which is under stronger influence of terrestrial waters. In summer 2001, the year with the most negative NAO, the lowest DIC values and highest pH values were observed across the entire basin, whereas 2005 and 2008 were both characterised by higher DIC and lower pH, with some variability in these patterns across the North Sea. Summer 2005 had the coolest surface waters.

For winter NAO values, 2001 was the most negative (−1.9), 2005 was effectively neutral (0.12) and 2008 was positive (2.1). Weaker winds and circulation in the North Sea are associated with negative NAO (see Sects. 1.4.3 and 3.3.2) and reduce the upward mixing of cold winter water (Salt et al. 2013). Hence, metabolic DIC accumulated in deeper waters during the preceding autumn and winter

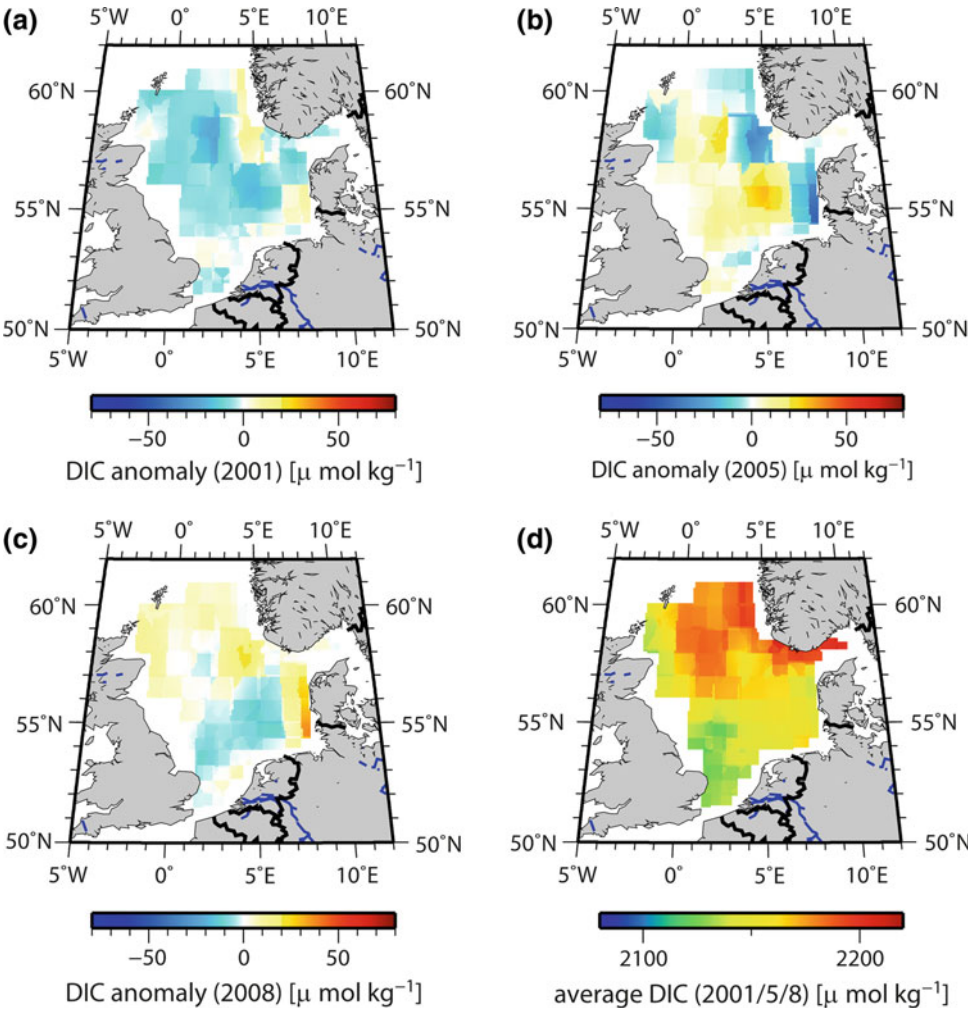

Fig. 3.18 Observed variability in surface water dissolved inorganic carbon (DIC) concentrations. All observations were made in summer (August/September) of the years 2001, 2005 and 2008 (Salt et al. 2013). Anomalies are shown relative to the average observed values for these years (also shown; figure by Helmuth Thomas, Dalhousie University, Canada)

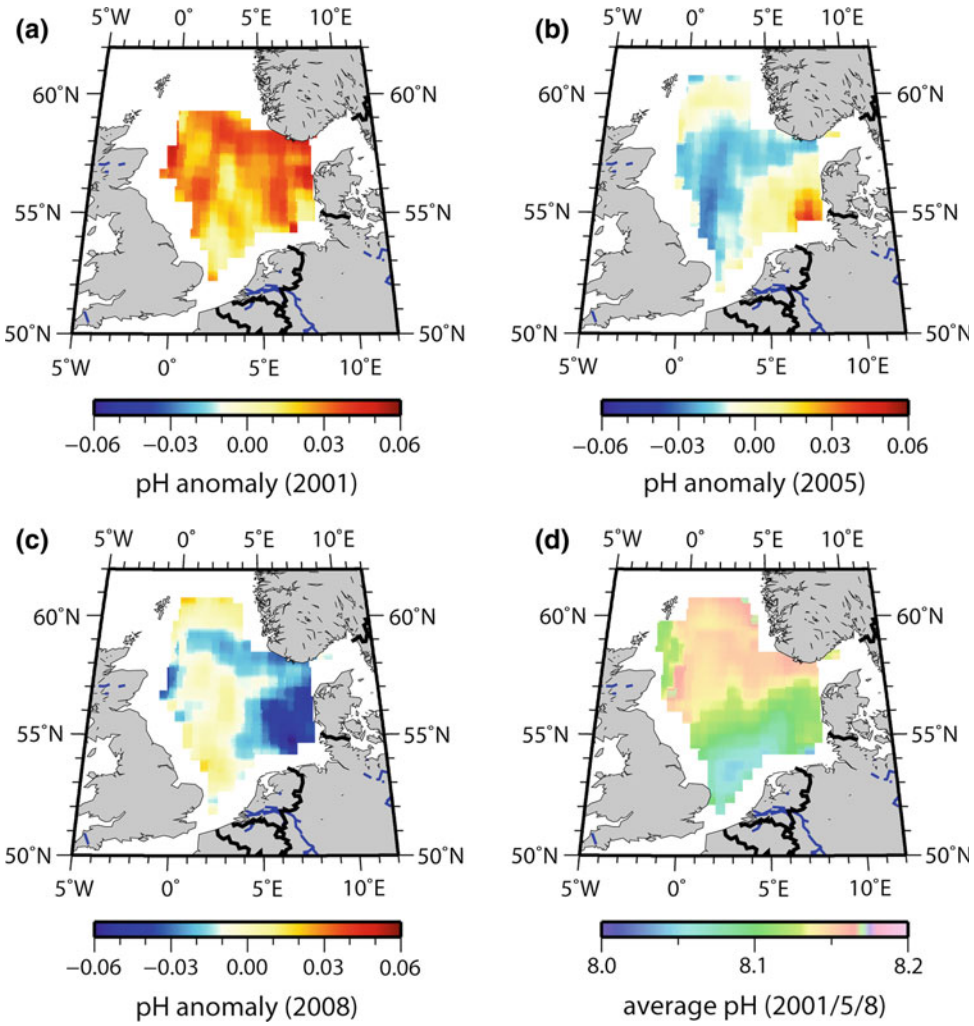

Fig. 3.19 Observed variability in surface water pH. All observations were made in summer (August/September) of the years 2001, 2005 and 2008 (Salt et al. 2013). Anomalies are shown relative to the average observed values for these years (figure by Helmuth Thomas, Dalhousie University, Canada)

(Thomas et al. 2004) was mixed into surface waters to a lesser extent in 2001 than in 2005 or 2008 when wind or circulation-driven mixing was stronger (see also Salt et al. 2013), which explained the elevated surface DIC and lower pH in 2005 and 2008 relative to 2001 (Figs. 3.18 and 3.19).

The striking difference between 2001 and 2005 in the northern North Sea (Thomas et al. 2007) was reinforced by the warmer summer with a shallower mixed layer in 2001 (Salt et al. 2013: their Fig. 5). Comparable biological activity caused the shallower mixed layer of 2001 to experience stronger biological DIC drawdown on a concentration basis, resulting in higher pH, than in 2005 (Figs. 3.18 and 3.19).

Interaction with the North Atlantic Ocean also causes variability in the CO_2 system, partly explained by NAO-dependent circulation changes (Thomas et al. 2008; Watson et al. 2009). Figure 3.21 shows the net flow of water in the first half of the three respective years. 2008 (positive NAO) has the strongest north-western inflow of DIC-enriched North Atlantic waters to the North Sea, via the Fair Isle Current and Pentland Firth, although 2001 had strong inflow from the north which recirculated out of the North Sea quickly off Norway (Lorkowski et al. 2012).

Such an influence of North Atlantic inflow is supported by strong correlations between changes in the inventories of salinity and corrected DIC (i.e. accounting for biological effects) during the periods 2001–2005 and 2005–2008 (Salt et al. 2013). Mean values of partial pressure of CO_2 (pCO_2) in the water (331.6 ppm in 2001, 352.5 ppm in 2005, 364.0 ppm in 2008) reflect the large change between 2001 and 2005 and the moderate change between 2005 and 2008. Also, strong NAO-driven anti-clockwise circulation in the North Sea in 2008 intensified the distinct characteristics of the southern and northern North Sea and sharpened the transition between them (e.g. high to low pH, see Salt et al. 2013: their Fig. 2).

Modelling results (Lorkowski et al. 2012) agree with several of these findings: a mixed layer shallower in 2001 and 2008 than in 2005, which had the coolest summer surface waters; central North Sea DIC concentrations about 10 μmol/kg less than average in 2001.

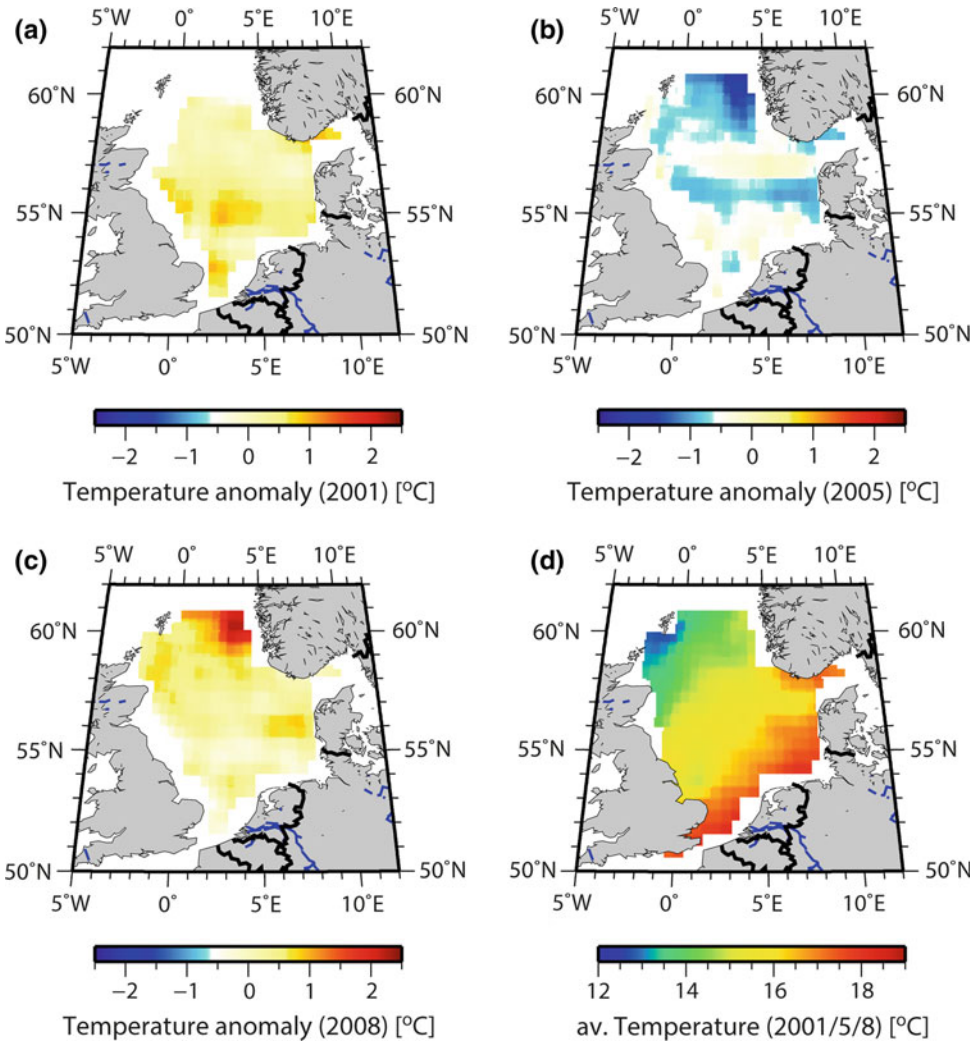

Fig. 3.20 Observed variability in sea surface temperature. All observations were made in summer (August/September) of the years 2001, 2005 and 2008 (Salt et al. 2013). Anomalies are shown relative to the average observed values for these years (figure by Helmuth Thomas, Dalhousie University, Canada)

In summary, three factors regulate the North Sea's CO_2 system and thus reveal points of vulnerability to climate change and more direct anthropogenic influences: local weather conditions (including water temperature in the shallower southern North Sea), circulation patterns, and end-member properties of relevant water masses (Atlantic Ocean, German Bight and Baltic Sea). Thus a positive NAO increases Atlantic Ocean and Baltic Sea inflow, the anti-clockwise circulation, carbon export out of the Norwegian Trench below the surface (limiting out-gassing) and hence the effectiveness of the shelf-sea CO_2 'pump' (Salt et al. 2013). If the NAO is positive together with higher SST, a shallower mixed layer favours lower surface pCO_2 and higher pH in the northern North Sea. These factors can be considered key to regulation of the North Sea's response to climate change and more direct anthropogenic influences.

3.6.2 Model-Based Interannual Variations in Nitrogen Fluxes

The North Sea is a net nitrogen sink for the Atlantic Ocean, due to efficient flushing by North Atlantic water with strong nitrogen concentrations and to large rates of benthic denitrification in the southern North Sea (Pätsch and Kühn 2008). This is the case despite large nitrogen inputs from the rivers and atmosphere. There is net production of inorganic nitrogen from organic compounds.

Pätsch and Kühn (2008) investigated nitrogen fluxes in 1995 and 1996 as the NAO shifted from very strong positive conditions in winter 1994/1995 to extreme negative conditions in winter 1995/1996. Due to enhanced ocean circulation on the Northwest European Shelf, the influx of total nitrogen from the North Atlantic was much stronger in 1995

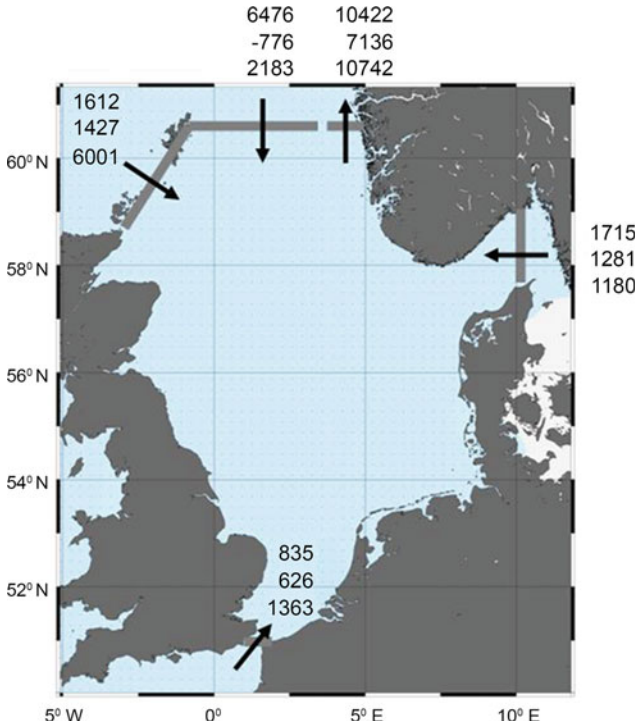

Fig. 3.21 Simulated cumulative net flux of water from 1 January to 30 June (km^3 per half year) for the years 2001 (*upper values*), 2005 (*middle values*), 2008 (*lower values*) (Lorkowski et al. 2012)

(NAO positive) than in 1996. River input of nitrogen was also larger in 1995 than 1996. While the import of organic nitrogen was similar for both years, the import of inorganic nitrogen was larger in 1995 than in 1996. The ecosystem response was stronger dominance of remineralisation over production of organic nitrogen in 1996 with negative NAO conditions.

According to this simulation, in 1996 (with extreme negative winter NAO) the net-heterotrophic state of the North Sea was stronger than in 1995. As a result, the biologically-driven air-to-sea flux of CO_2 was larger in 1995 than in 1996 (Kühn et al. 2010). In other words, in positive NAO years stronger fixation of inorganic nitrogen and inorganic carbon facilitates stronger biological CO_2 uptake. This carbon is exported into the adjacent North Atlantic in positive NAO years, as reported above. The balance between respiration and production in regulating DIC and pCO_2 conditions thus acts in synergy with the processes discussed in Sect. 3.6.1. At regional and sub-regional scales, modelling studies have investigated the concurrent impacts of eutrophication, increases in atmospheric CO_2 and climate change on the Southern Bight of the North Sea (Gypens et al. 2009; Borges and Gypens 2010; Artioli et al. 2014). The studies clearly highlight the complex effects of the individual drivers, as well as the different time scales of impact. Eutrophication, oligotrophication and temperature variability affect the CO_2 system at interannual to decadal time scales. Long-term trends of increases in atmospheric CO_2 and rising temperature have begun to cause tangible effects (e.g. Artioli et al. 2014) although, to date, these have been much less pronounced than effects at shorter time scales.

3.6.3 Ocean Acidification and Eutrophication

The interplay of the different anthropogenic and climate change processes, as well as their different, obviously overlapping time scales, can be exemplified with respect to the long-term effects of ocean acidification and the shorter-term effects of eutrophication/oligotrophication. Effects of eutrophication are closely related to the trend of ocean acidification, since both affect DIC concentrations and the DIC/A_T ratio (A_T: total alkalinity) in coastal waters, and thus CO_2 uptake capacity. Increased nutrient loads may lead to enhanced respiration of organic matter, which releases DIC and thus lowers pH. On shorter time scales, enhanced respiration overrides ocean acidification, which acts at centennial time scales (e.g. Borges and Gypens 2010; Artioli et al. 2014). (Surface-ocean pH has declined by 0.1 over the industrial era, in the North Sea as well as globally, and a hundred times faster in recent decades than during the previous 55 million years; EEA 2012).

If eutrophication-enhanced respiration of organic matter exhausts available oxygen, respiration then takes place through anaerobic pathways. Denitrification is crucial here; the biogeochemical consequences of depleted oxygen are many. Under eutrophic conditions, release of nitrate (NO_3) by enhanced respiration is controlled by the amount of available oxygen. If oxygen is depleted, NO_3 is converted to nitrogen gas (N_2). Any further input of NO_3 stimulates denitrification. The lost NO_3 is not available for biological production, thus the system is losing reactive nitrogen (Pätsch and Kühn 2008) as with eutrophication in the Baltic Sea (Vichi et al. 2004). A transition from aerobic to anaerobic processes has consequences for CO_2 uptake capacity and pH regulation: denitrification driven by allochthonous NO_3 releases alkalinity in parallel with the metabolic DIC, with a DIC/A_T ratio of 1:1.

Compared with aerobic respiration, which gives a DIC/A_T ratio of −6.6, the release of alkalinity in denitrification increases the CO_2 and pH buffer capacity of the waters, in turn buffering ocean acidification. Since denitrification is irreversible, the increased CO_2 and pH buffer capacity will persist on time scales relevant for climate change. In other words, if eutrophication yields anaerobic metabolic pathways, this constitutes a negative feedback to climate change, since more CO_2 can be absorbed from the

atmosphere, which in turn dampens the CO_2 greenhouse gas effect.

Other anaerobic pathways such as sulphate or iron reduction give even lower DIC/A_T release ratios (Chen and Wang 1999; Thomas et al. 2009); those may be reversible, however. Reduced (nitrogen-) nutrient input (i.e. oligotrophication) thus comes with a negative feedback with regard to ocean acidification: a desirable reduction in NO_3 release enhances vulnerability of the coastal ecosystem to ocean acidification, since most organic matter respiration is on or in shallow surface sediments (Thomas et al. 2009; Burt et al. 2013, 2014).

3.6.4 Variability on Longer Time Scales

Climate, CO_2 and more direct anthropogenic drivers also determine the variability of carbon fluxes in the North Sea. They can all be indicated as negative or positive feedback mechanisms for CO_2 exchange with the atmosphere and thus as feedbacks on climate change. The main direct anthropogenic impact on the carbon cycle, mostly for the southern North Sea, is the input of bio-reactive tracers, namely nutrients, via the atmosphere and rivers. Indirect anthropogenic drivers include acidification due to the ongoing increase in atmospheric pCO_2. Climate change processes (rising SST and changes in salinity distribution due to changes in circulation and winds) also induce shifts in the carbonate system and thus changes in carbon fluxes.

These anthropogenic and climate-change drivers, which act at interannual to decadal time scales, and their potential feedbacks and impacts were investigated in the model study by Lorkowski et al. (2012) for the years 1970 to 2006 (extended here to 2009). Simulation of the total system with all drivers included reproduced observations. Scenarios, mimicking anthropogenic and climate change processes, give insight into their roles and feedback mechanisms. These scenarios were generally run without biology, and with either fixed temperature or atmospheric CO_2 concentrations fixed at 1970 values. Both 'biotic' and 'abiotic' scenarios are shown here (Figs. 3.22 and 3.23, respectively), the latter to prevent biological feedbacks overshadowing the physically-driven and biogeochemically-driven responses.

The 'standard' simulation showed a decrease in CO_2 uptake from the atmosphere in the last decade (Fig. 3.22), an increase in SST by 0.027 °C year^{-1} and a decrease in winter

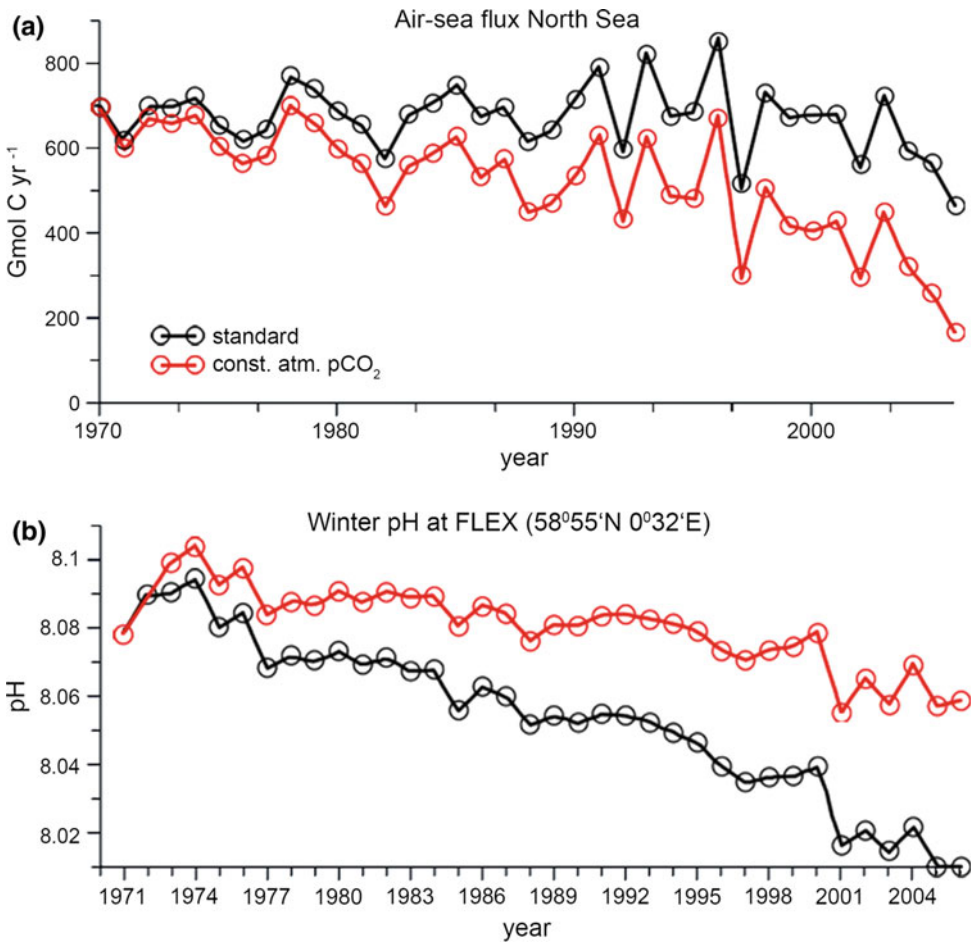

Fig. 3.22 Carbon dioxide (CO_2) air-sea fluxes for the total North Sea (*upper*, black curve reprinted from Fig. 5a in Lorkowski et al. 2012) and winter pH at one station in the northern North Sea (*lower*). Standard simulation (*black*); repeated annual cycle of atmospheric CO_2 (*red*) (figure by Helmuth Thomas, Dalhousie University, Canada)

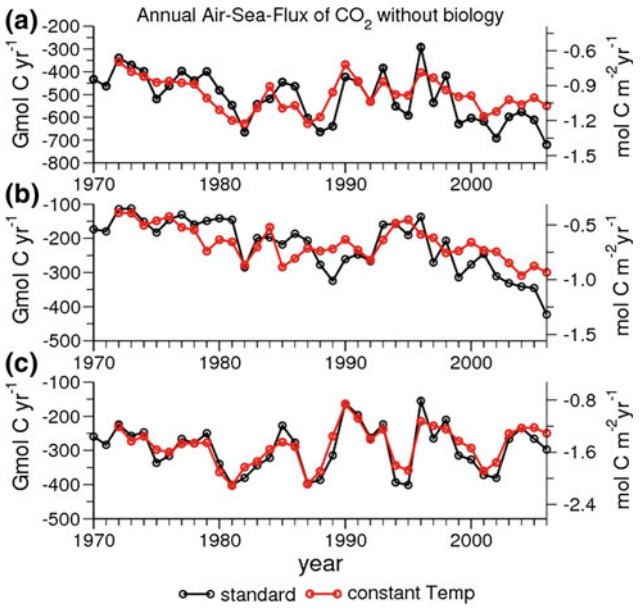

Fig. 3.23 Annual air-sea carbon dioxide (CO_2) flux for 'abiotic' simulations: total North Sea (*upper*), northern North Sea (*middle*), southern North Sea (*lower*). *Black* Results for standard conditions (Fig. 8 in Lorkowski et al. 2012); *red* results from the simulation with a repeated annual cycle of 1972 temperature. NB. Scales differ between the plots (figure by Helmuth Thomas, Dalhousie University, Canada)

pH by 0.002 year^{-1} (Lorkowski et al. 2012). Thus climate change alone (i.e. rising sea temperature) thermodynamically raises the pCO_2 and reduces CO_2 uptake in the North Sea. Furthermore, warming waters cause a lower pH, thus increased surface water acidity (Fig. 3.22).

Increasing atmospheric pCO_2 during the 'standard' simulation increases the gradient between seawater and atmospheric pCO_2 and increases the (net-) CO_2 uptake. To investigate this, the standard simulation is compared with a simulation using a repeated 1970 annual cycle of atmospheric pCO_2 (Fig. 3.22). 1970 pCO_2 (with rising temperature in common) leads to a smaller air-sea flux and less CO_2 uptake. pH decreases less than in the standard simulation (Fig. 3.22). Thus the simulations show enhanced CO_2 uptake in the North Sea as a consequence of rising atmospheric pCO_2, in turn increasing North Sea acidification as a 'local' process. This experiment also shows that for today's carbonate-system-status the increase in atmospheric CO_2 has a stronger impact on air-sea flux of CO_2 than the reduction in the buffer capacity by the ongoing acidification. This trend in acidification might be overlain on shorter time scales by advective processes (Thomas et al. 2008; Salt et al. 2013) as discussed in Sect. 3.6.1, by eutrophication (Gypens et al. 2009; Borges and Gypens 2010; Artioli et al. 2014) or by variability in biological activity.

Climate change enhances the hydrologic cycle, which means enhanced precipitation and river runoff, which drive changes in surface water salinity. Salinity decrease generally represents a dilution of DIC and A_T, with the DIC-effect dominating the A_T-effect on pCO_2 and pH (e.g. Thomas et al. 2008). Changes in salinity also alter the equilibrium conditions of the carbonate system (a minor effect): on addition of freshwater, pCO_2 decreases and pH increases. In coastal areas, precipitation-evaporation effects are confounded by changes in the mixing ratios of the dominant water masses, i.e., runoff and the oceanic end-member; higher salinity can mean a larger proportion of oceanic water relative to river runoff and vice versa. A sensitivity study, with salinity reduced by 1 (compared with the standard setup) and no biological processes, showed 10 % less outgassing, slightly counteracting the effect of rising temperature. In summary, rising temperature reduces uptake of atmospheric CO_2; increasing atmospheric pCO_2 or reduced salinity increases net uptake of atmospheric CO_2.

3.7 Oxygen

John Huthnance, Franciscus Colijn, Markus Quante

Oxygen is of concern because depletion (hypoxia) adversely affects ecosystem functioning and can lead to fish mortality. Air-sea exchange and photosynthesis tend to keep upper waters oxygenated; oxygen concentrations can be strongest in the thermocline associated with a sub-surface chlorophyll maximum (Queste et al. 2013). However, oxygen concentration near the sea bed can be reduced by organic matter respiration below stable stratification, breakdown of detrital organic matter in the sediment and lack of oxygen supply (by advection or vertical mixing). Temperature is also a factor; warmer waters can contain less oxygen but increase metabolic rates. Extra nutrients from rivers and estuaries can increase the amount of respiring organic matter. In the North Sea, most areas are well-oxygenated but some areas are prone to low oxygen concentrations near the bottom—the Oyster Grounds (central North Sea), off the Danish coast (Karlson et al. 2002) and locally near some estuaries, as in the German Bight. Climate change may influence oxygen concentrations through changes in absolute water temperature as well as through changes in temperature gradient, storm intensity and frequency, and related changes in mixing.

Data are available from the International Council for the Exploration of the Sea (ICES) for the past 100 years or so, research cruises (notably August 2010; Queste et al. 2013) and models (e.g. Meire et al. 2013; Emeis et al. 2015). The deep oxygen distribution and its relation to stratification is illustrated in Fig. 3.24.

There is strong interannual variability in the oxygen concentration of the bottom water in late summer. Published

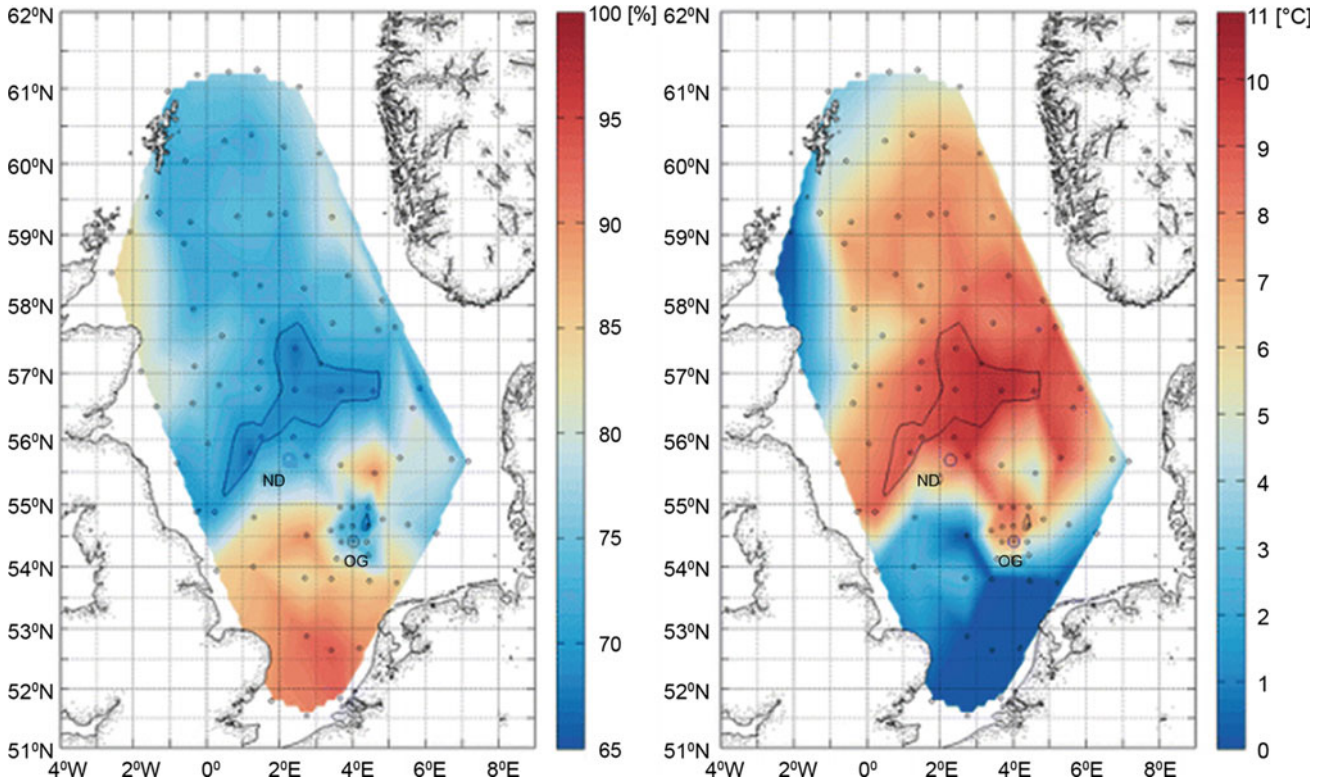

Fig. 3.24 August 2010 CTD casts for the shallowest 3 m and deepest 3 m of the water column. Deepest oxygen saturation (%, *left*) and temperature difference between surface and bottom mixed layer (°C, *right*). The 70 % saturation contour highlights similarity in the distributions (Queste et al. 2013)

oxygen minimum values vary from 65 to 220 µM (Meire et al. 2013). A value of 65 µM in the Oyster Grounds indicates that this area could be on the brink of hypoxia in exceptional years. Models suggest that it is the effect of warming on stratification, rather than on decreased oxygen solubility or enhanced respiration rates, that is the main physical factor affecting bottom oxygen concentrations (Meire et al. 2013; Emeis et al. 2015). Comparing the periods 1970–1979 and 2000–2009, Emeis et al. (2015) found the more recent period to show a longer period of stratification in the middle of the North Sea with increased apparent oxygen utilisation and a lower September oxygen minimum around 6°E 56°N. They also found decreased September oxygen concentrations in the south-eastern German Bight around 54°S. However, storms can promote sediment resuspension and subsequent oxygen consumption, such as in the Oyster Grounds (Greenwood et al. 2010). Observed changes in summer bottom temperature and oxygen concentration show a strong relation (Queste et al. 2013 and Fig. 3.25).

Climate change, for example raised water temperatures, is expected to have a negative impact on oxygen concentrations in surface waters, and deepening of the thermocline will reduce the bottom mixed layer and may cause further depletion of oxygen concentrations in deeper layers. However, quantifying temperature effects is difficult, owing to climate-related effects on nutrient inputs to the North Sea as well as on local mixing characteristics and the duration of reduced oxygen concentrations.

3.8 Suspended Particulate Matter and Turbidity

Julie Pietrzak, Alejandro Jose Souza, John Huthnance

Suspended particulate matter (SPM) is a significant agent of change in morphology, it also transports pollutants, redistributes nutrients and modifies the light climate (Capuzzo et al. 2013), hence its role in modulating primary production. Suspended particulate matter includes plankton.

3.8.1 Sources in the North Sea

The seabed is an important source of SPM in the North Sea. Rivers and cliffs are also important sources in certain areas. Cliff sources are very variable interannually.

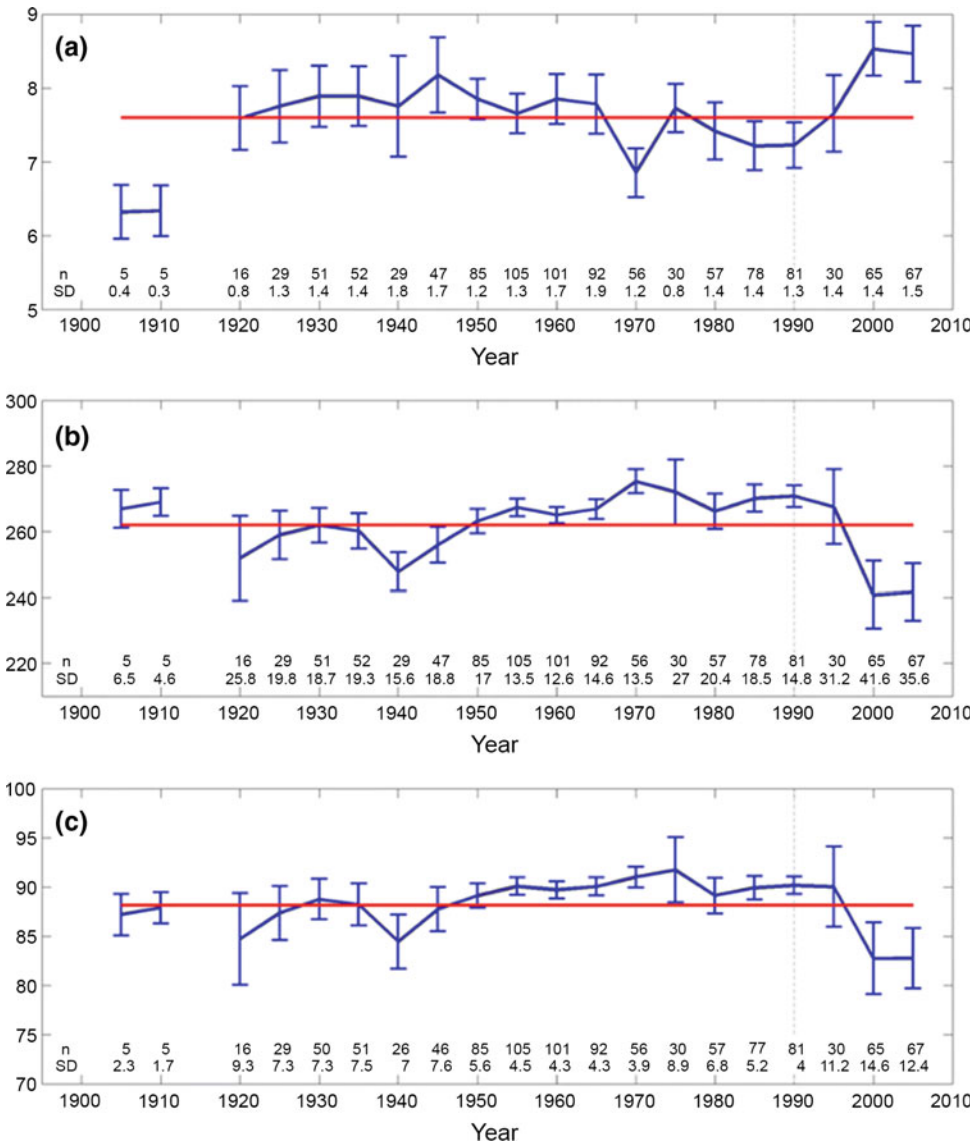

Fig. 3.25 Five-yearly values of an 11-year running mean of summer bottom-mixed-layer temperature (°C, *upper*), oxygen concentration (μmol dm^{-3}, *middle*) and oxygen saturation (%, *lower*) in the stratified central North Sea. The data are for June to September below 30 m, in regions deeper than 45 m and in grid 'squares' (1° longitude × 0.5° latitude) north of 56°N with more than five data points (total of 16,250 measurements). *Error bar* length shows two standard errors. The *horizontal line* represents the overall mean of the time series. The number of grid squares retained and the standard deviation are indicated below each data point (Queste et al. 2013)

Bottom sediment distributions in the North Sea have been reported by many authors (such as Eisma and Kalf 1987 and Nedwell et al. 1993, using data from the UK NERC North Sea Project). More recently, Dobrynin et al. (2010; Fig. 3.26) compiled a seabed fine-sediment distribution that combines in situ data (Puls et al. 1997) and satellite data (Gayer et al. 2006).

The main river sources are the Elbe, Weser, Ems, Rhine, Thames, Welland, Humber, Tees, and Tyne, as well as the Forth, Ijssel and the Nordzeekanaal. River discharge and consequently SPM load (Fig. 3.27) show strong interannual variability. For example, freshwater discharge and SPM loads for the major continental rivers (i.e. Rhine, Elbe and Weser) were much less in 2003 than in 2002, owing to the low precipitation and very high temperatures in central and western Europe in 2003 (Gayer et al. 2006).

Long-term measurements of annual mean amounts of SPM eroded from English cliffs imply the following average rates: Suffolk, 50 kg s^{-1}; Norfolk, 45 kg s^{-1}; and Holderness, 58 kg s^{-1}. SPM loads eroded from cliffs are dependent on whether storm or calm conditions occur (Fig. 3.27). According to Gayer et al. (2006) cliff erosion appears to start when significant wave heights near the coast exceed 2 m. Sediment composition suggests that SPM for alongshore transport off the Belgian and Dutch coasts is largely supplied by sediment transported through Dover Strait from the erosion of the French and British cliff coasts (Irion and Zöllmer 1999; Fettweis and van den Eynde 2003). The transport through Dover Strait largely exceeds the fluvial input by rivers such as the Rhine-Meuse estuary (de Nijs 2012). The annual sediment influx shows large interannual variations which appear to reflect differences in number and duration of storms (van Alphen 1990).

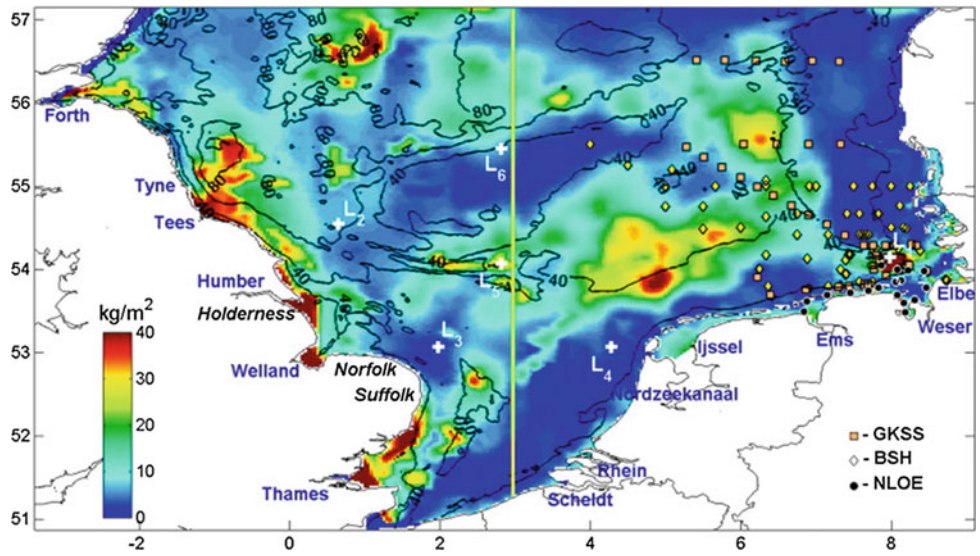

Fig. 3.26 Sea-bed fine sediment (<20 μm; settling velocities 0.01–0.1 mm s^{-1}). Distribution in kg m^{-2} shown by *colour shading*; bathymetry (m) shown by *black contour lines*. The distribution is the result of combining sediment grain analysis, satellite data and numerical model results. The map (reprinted from Dobrynin et al. 2010) also shows the most important rivers and cliffs. (Labels $L_{1\text{-}6}$ and the *vertical yellow line* are not relevant here). *Marked points* show sites of data used by Dobrynin et al. (2010)

3.8.2 Overall Distribution

Sediment is transported either as bed load (typically for coarse material) or suspended load (SPM). Advances in observational techniques, from water samples to in situ instruments (transmissometers, optical backscatter and Laser In Situ Scattering and Transmissometery—LISST) and reliable use of optical remote sensing (e.g. AVHRR, SeaWiFS, recent MODIS and MERIS) have increased understanding of SPM distribution. Remote sensing techniques provide a synoptic view of the sea surface at fine temporal (daily) and spatial (kilometre) resolution, providing information on variability in SPM distribution. The ability to estimate near-surface SPM loads, relatively continuously and at synoptic scale, has allowed study of surface SPM over seasonal cycles: for example it has been observed that high

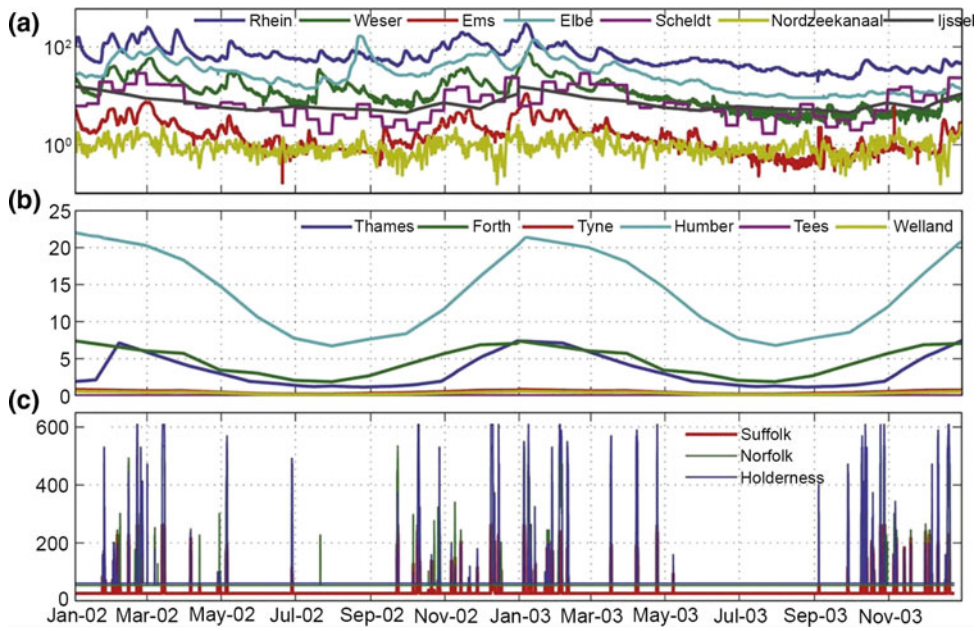

Fig. 3.27 Sources of SPM (kg s^{-1}) to the North Sea from continental Europe (*upper*), UK rivers (*middle*) and UK cliffs (*lower*) during 2002 and 2003. Each river's SPM load is the product of freshwater discharge (m^3 s^{-1}) and annual mean SPM concentration (kg m^{-3}; Gayer et al. 2004). River discharges are a combination of measured data and climatology (reprinted from Dobrynin et al. 2010)

SPM concentrations evolve during winter, with much lower values in summer (Eleveld et al. 2004, 2006, 2008). However, it should be noted that satellites provide information concerning the sea surface only. When the water column is well mixed SPM can be remotely observed at the sea surface; when it is stratified (as in the Rhine ROFI) SPM can only be observed remotely for high discharge events and close to the mouth (of the Rotterdam Waterway), see Sect. 3.8.5.

Suspension of particles off the bed needs stronger currents (including waves and turbulence) than the limit for the same particles to settle. If the currents allow settling, there is still transport until the particles reach the bed. These biases, tidal straining and current asymmetries cause net transport of SPM. Moored instruments have allowed better understanding of tidal, spring-neap and vertical variability (Jones et al. 1996).

Eleveld et al. (2008) found that annual, winter and summer remote sensing SPM observations highlighted the dominant North Sea water types as characterised by Lee (1980) in terms of salinity (see also Otto et al. 1990). Pietrzak et al. (2011; Fig. 3.28) used remote sensing images to characterise the water types in terms of SPM, relating the SPM to stratification in the southern North Sea. They found pronounced seasonal and spring-neap variability, and highlighted the significant role played by tides and winds in controlling stratification, and hence the distribution of SPM at the sea surface. Prevailing circulations (river plumes and overall anti-clockwise circulation) also influence SPM distribution. (The *southern* North Sea is emphasised fhaving

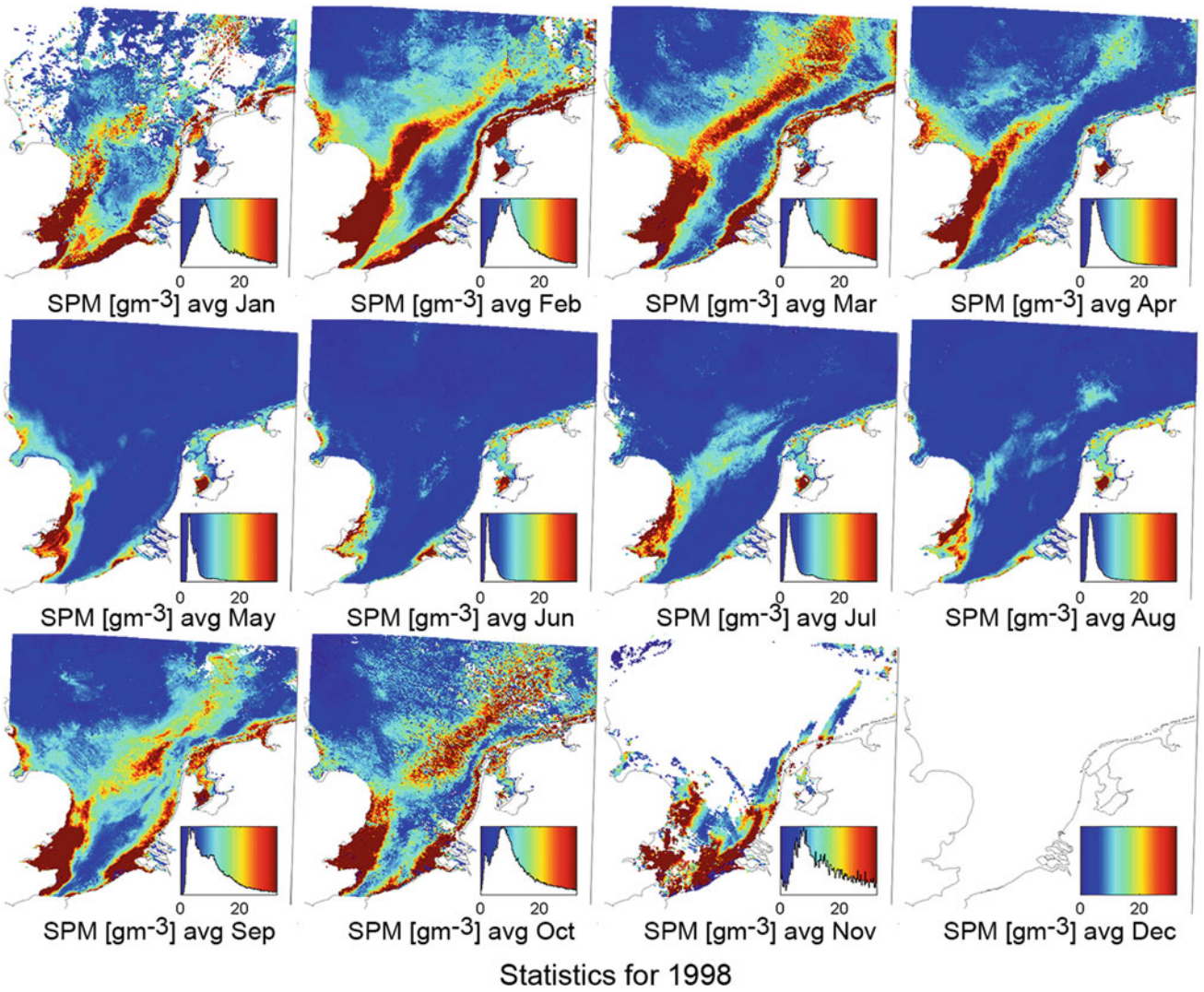

Fig. 3.28 Monthly average surface suspended particulate matter (SPM) based on SeaWiFs data from 1998 (reprinted from Pietrzak et al. 2011). The *insets* are the *colour bars* and the *white areas* the histograms of the pixel values, where the x-axis corresponds to the SPM pixel value and the y-axis to the relative frequency distribution of the pixel values

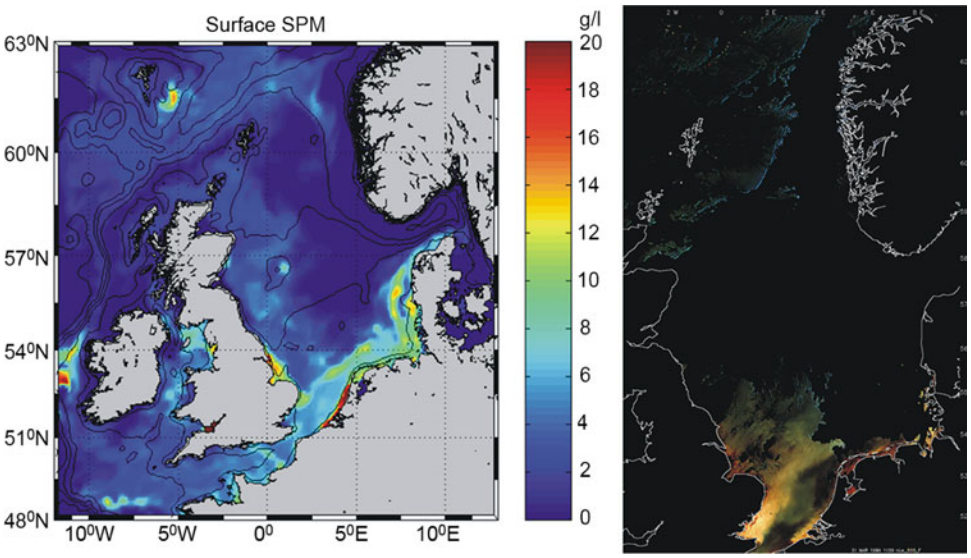

Fig. 3.29 Surface suspended particulate matter (SPM) distribution (g l^{-1}) for March from a numerical model (*left*) and satellite false colour (*right*). Areas of strong concentration qualitatively agree with areas of strong reflectance, showing the East Anglia and Rhine plumes (reprinted from Souza et al. 2007)

greater SPM concentrations than the northern North Sea due to differences in the sources, stronger currents and shallower depth, i.e. a larger Stokes number (Souza 2013), and correspondingly more studies and available data).

The waters exiting the rivers Rhine, Tees, Humber and Wash are deflected to the right under the Coriolis influence, forming classic river plumes of which the Rhine ROFI dominates the southernmost North Sea. A zone of high turbidity extends along the Belgian and Dutch coasts, primarily controlled by the Rhine ROFI which transports SPM northwards along the Dutch coast (Dronkers et al. 1990; Visser et al. 1991; de Kok 1992; de Ruijter et al. 1992; McCandliss et al. 2002). The Flemish Banks turbidity maximum off Belgium (Fig. 3.28) is present throughout the year but is much reduced in summer; studies have disagreed about its cause. Off the Dutch coast, Visser et al. (1991) and Suijlen and Duin (2001, 2002) found a local SPM minimum about 30 km offshore. In the German Bight, SPM from the Rhine ROFI appears to merge with SPM from the Weser and Elbe, before arriving in the Skagerrak (Simpson et al. 1993).

Within the North Sea, an overall anti-clockwise circulation extends south to around East Anglia, before turning into strong eastward flow at about 53°N across the southern North Sea, as a residual tidal and meteorologically-forced flow (e.g. Dyer and Moffat 1998; Holt and James 1999). Off East Anglia, this eastward flow has high turbidity (Fig. 3.29) extending from the Norfolk banks across the southern Bight to the German Bight (McCave 1987). This 'East-Anglia Plume' (Dyer and Moffat 1998) comprises southward-flowing waters from the Tees, Humber and Wash and a southern source of fresh water from the Thames (Thames waters deflect to the left, unlike those of other rivers entering the North Sea). The plume location is evident in SPM images (Fig. 3.29) and can be linked to the frontal boundary that separates well-mixed water in the southern Bight from seasonally-stratified central North Sea waters (Eisma and Kalf 1987; Hill et al. 1993), especially the Flamborough Head and Frisian Fronts.

Plume currents can be enhanced by the thermohaline circulation (jets associated with tidal mixing fronts; Hill et al. 1993). The East-Anglia Plume eventually joins the northward flow from Dover Strait and the Rhine ROFI (Prandle 1978b; Prandle et al. 1993). The plume carries an estimated annual SPM flux of 6.6 million tonnes, from English rivers and cliffs (Sündermann 1993), eastwards across the southern North Sea (Howarth et al. 1993). Both the East-Anglia Plume and the seasonal thermocline have a large impact on the transport of SPM across the southern North Sea. Holt and James (1999) found that deposition typically occurs along the 40 m depth contour. Their results are consistent with those of Eisma (1981) and Eisma and Kalf (1987), who found that the main areas of fine sediment accumulation are the Oyster Grounds and the strip along the German Bight (see also Fig. 3.26).

3.8.3 Tidal Influence

Figure 3.30 shows the spring-neap SPM cycle and highlights the important role played by tides in the surface distribution of SPM in the southern North Sea.

Deposition and erosion of sediment are related to critical values of the bed shear stress. Fine sediments are deposited when the bed shear stress is less than critical (0.1–0.2 N m^{-2}) and are typically eroded if the stress exceeds 0.4–0.5 N m^{-2} (Puls and Sündermann 1990; Holt and James 1999; Souza et al. 2007). In principle the tidal bed stress can be used to characterise regions where the tides can resuspend

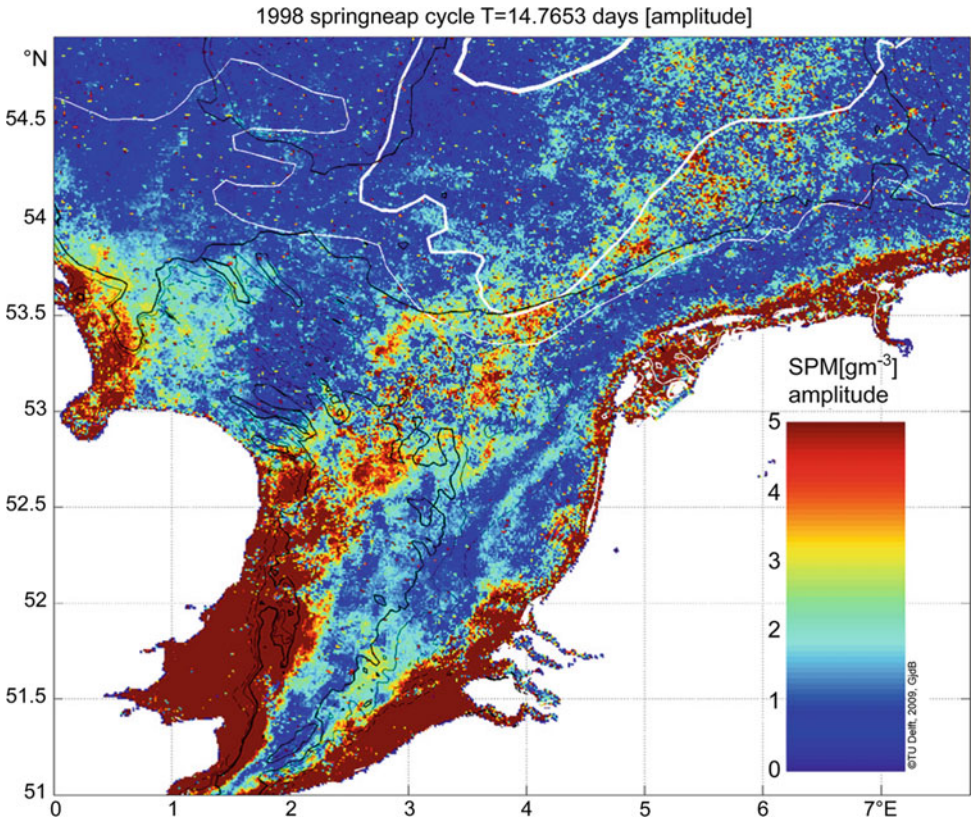

Fig. 3.30 The spring-neap harmonic using SPM images from SeaWiFS in 1998 (reprinted from Pietrzak et al. 2011). *Black lines* show bathymetry contours: 25 m (thinnest), 30 m (medium) and 35 m (thickest). *White lines* show values of the Simpson and Hunter (1974) criterion (Sect. 3.2.4): S = 1 (*thinnest line*), S = 1.5 (*medium*) and S = 2 (*thickest line*). Areas with S < 1 are well mixed

bed material. For example, in the Belgium coastal zone, the water column is always well mixed by tidal currents which also cause the SPM maxima in this zone (Lacroix et al. 2004).

Jago et al. (1993) showed typical behaviour of SPM: quarter-diurnal maxima due to tidal resuspension and semi-diurnal maxima due to tidal advection of ambient SPM concentration gradients. The result of these processes is that SPM time series show two maxima per tidal cycle, one larger than the other. SPM also responds to the spring-neap tidal cycle as shown by numerical simulations (Souza et al. 2007; see Fig. 3.31); monthly variability is also clear in the deposition of material and is present in SPM and q^2 (where q is the turbulent velocity). The model has been extensively validated using North Sea Project data including that for station CS (e.g. Holt and James 1999; Holt et al. 2005; Allen et al. 2007).

3.8.4 Wave Effects

Data from the northern Rhine ROFI after storms show a sudden increase in SPM over the entire coastal zone, suggesting local resuspension of sediment (Suijlen and Duin 2001, 2002) and an important effect of waves. Waves are strongly seasonal in the North Sea. Significant wave heights (*Hs*) in the winter half year are usually much higher than in the summer half year over the entire North Sea. For example, Dobrynin et al. (2010) showed that during 2002–2003 seasonally-averaged *Hs* was up to 1.5 m higher for the winter season.

The largest values of *Hs* are usually found in the open North Sea (e.g. Weisse and Günther 2007; Dobrynin et al. 2010), owing to a combination of topography effects with predominant wind direction and storms coming from the North Atlantic. In shallow regions, effects such as bottom boundary dissipation of waves can be significant even during the (calmer) summer, although they are usually more important during winter. For example, in winter over Dogger Bank, Dobrynin et al. (2010) found enhanced combined wave-current stress resulting in very high SPM concentrations (>50 mg l^{-1}).

3.8.5 Impact of Stratification

Stratification (Sect. 3.2) has an impact on the vertical distribution of SPM through reduced turbulence at the pycnocline. The effect of *thermal* stratification is particularly noticeable in the East-Anglia Plume around the stratified areas close to the Frisian Front. Moreover, at the 55° 30′N station shown in Fig. 3.31, as thermal stratification develops the SPM

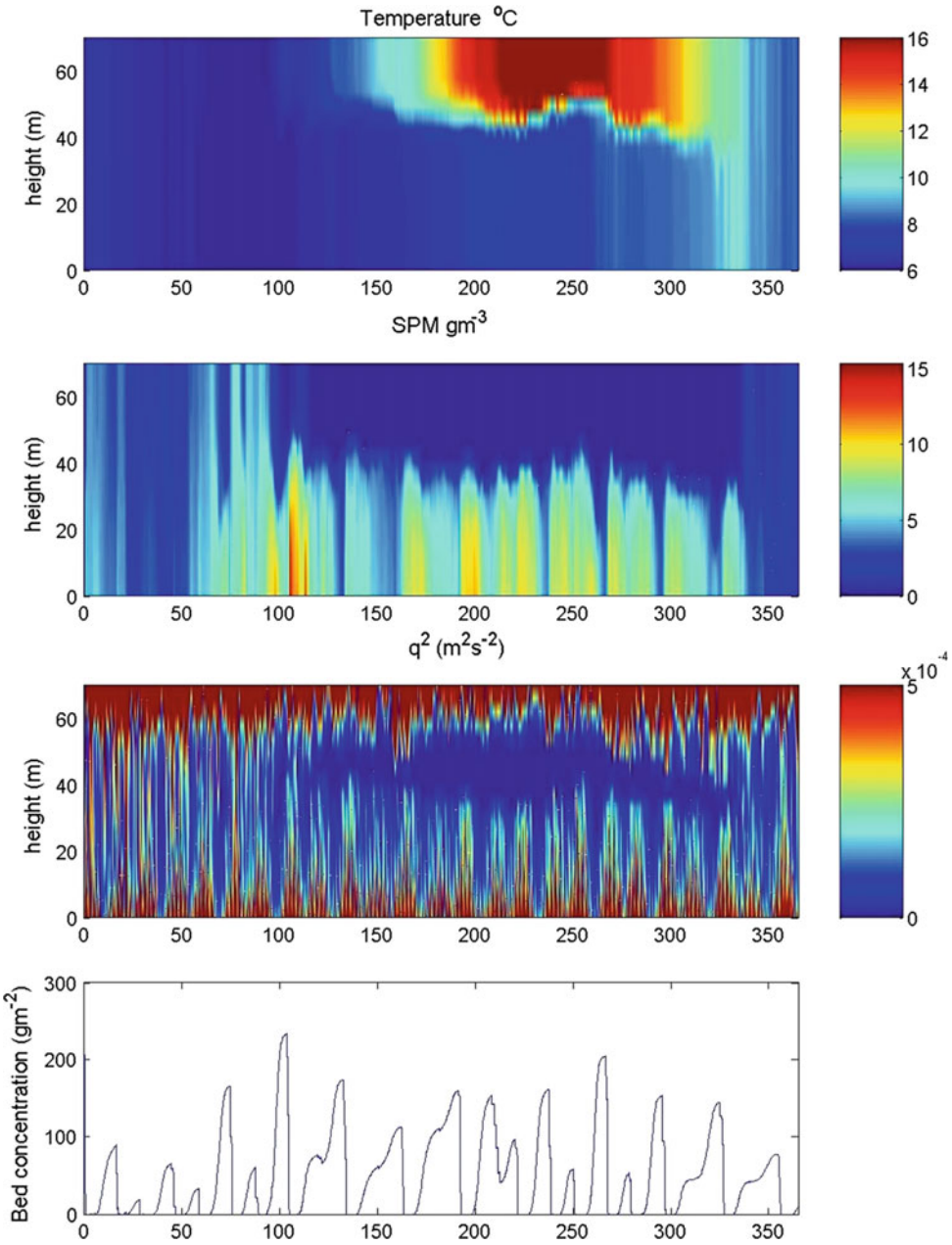

Fig. 3.31 Modelled time series at 55° 30′N 0° 50′E (North Sea Project station CS); time in days. Temperature (°C, *upper*), SPM (g m^{-3}, *upper middle*), q^2 (turbulence kinetic energy × 2, m^2 s^{-2}, *lower middle*), bed concentration (g m^{-2}, *lower*) (Souza et al. 2007)

concentrates in the lower 40 m of the water column, with values up to 15 g m^{-3}, but decreases to zero at the surface. *Haline* stratification appears to be significant especially within the Rhine ROFI and other adjacent ROFI areas such as the German Bight. The Rhine ROFI switches between well-mixed and stratified within a tidal cycle and through the spring-neap cycle (de Boer et al. 2006); haline stratification can develop at neap tides throughout the year and thermal stratification can be important in summer. As found in field studies of the Rotterdam Waterway, with stratification and reduced turbulence, any SPM advected over the salt wedge settles (de Nijs et al. 2010). Observations (e.g. Joordens et al. 2001) and numerical simulations (Fig. 3.31) show how SPM is trapped beneath the pycnocline when stratified. When the water column is mixed, turbulence and SPM can reach the surface; when a pycnocline develops, it inhibits turbulence, preventing upward flux of SPM and turbulence to the surface layer. Although de Boer et al. (2006) found differences to Heaps' model for the Rhine ROFI, cross-shore flow associated with estuarine-type circulation (Heaps 1972) tends to be offshore near the surface and onshore near the bed, giving a bias to onshore transport of settling SPM.

3.8.6 Seasonal Variability

Pleskachevsky et al. (2005) found that most SPM transport occurs in winter when cliff erosion along the English coasts is greatest. Numerical simulations of Holt and James (1999) highlighted seasonal variability of SPM. They found that SPM is only measured in time series of the water column in a series of discrete events associated with stronger winds, which resuspend bed material and mix the water column. Likewise, Souza et al. (2007) found their modelled water column to be well-mixed with very similar surface and bed SPM distributions in the East-Anglia Plume in February. In contrast, during summer the water column is stratified, almost all SPM settles out and an increase in net deposition correlates with decreased wind stress; moreover, less SPM is supplied by erosion of Holderness cliffs.

Satellite images of surface SPM show significant annual and seasonal variability (Eleveld et al. 2004, 2006, 2008; Pietrzak et al. 2011; see Fig. 3.28). Large values of surface SPM were observed in winter in Southern Bight coastal waters, especially in the Rhine ROFI, the East-Anglia Plume and Frisian Front. Summer minima occur throughout the southern North Sea, with low SPM values from April to August; in August almost all surface SPM in the Dutch coastal zone has gone. Pietrzak et al. (2011) showed the influence of the Rhine ROFI, East-Anglia Plume and fronts on the intra-annual distribution of SPM.

De Nijs (2012) found siltation rates in the Dutch waters to vary over the year and correlate with variations in sediment supply; the availability of sediment at Dover Strait and the river boundaries is typically greater between late autumn and spring. Verlaan and Spanhoff (2000) found massive siltation events, caused by storms, to occur near the mouth of the Rotterdam Waterway; a few such events determine annual siltation rates.

3.8.7 Interannual and Long-Term Variability

Strong year-to-year variation in sediment supply and required dredging near the mouth of the Rotterdam Waterway (de Nijs 2012) highlight the importance of interannual meteorological forcing.

Most long-term records of SPM are from satellites or sea-surface water samples collected along the Dutch coast (Suijlen and Duin 2001, 2002). However, near surface values vary in relation to stratification, making it difficult to use these data to infer trends or study impacts of climate change. Nevertheless, recent work continuing that of Pietrzak et al. (2011) indicates that interannual variability in wind stress, river discharge and heating due to variations in the NAO may have a pronounced impact on SPM distribution in the North Sea. Fettweis et al. (2012) classified surface SPM distributions according to 11 weather types, emphasising dependence in different locations on different hydrodynamic and wave conditions. Thus Southern Bight SPM is strongly influenced by advection, while exposure to waves favours resuspension in the central North Sea and German Bight and there is some overall positive correlation with the NAO.

Many coasts around the southern North Sea, notably the Dutch coast, are highly engineered, making it difficult to assess climate change impacts on sediment dynamics. However, supply of SPM for transport along the Belgian and Dutch coast, from French and English cliff coasts (Sect. 3.8.1), is determined by prevailing meteorological conditions and associated periods of large waves. This explains (seasonal and) interannual variations in the transport of SPM into the southern North Sea through Dover Strait. Climate-change effects on river discharge, storm tracks and associated winds and waves (intensity) are likely to affect the supply and distribution of SPM in the coastal zone and thus sediment distribution within the North Sea.

3.9 Coastal Erosion, Sedimentation and Morphology

Sytze van Heteren, John Huthnance

3.9.1 Historical Perspective

Coastal erosion is a key element of coastal behaviour and a useful—though imperfect—indicator of climate change. It is the active removal of sediment from various environments that marks the transition from sea to land, generally forcing the coastline landward. For cliffs and bluff coasts, erosion is irreversible. For sandy or muddy coasts, accretion and erosion may alternate. Coastal erosion may result in loss of land, destruction of sea defences and flooding. It has been measured for many centuries.

Coastal erosion takes place on different time scales. Long-term changes are commonly driven by relative sea-level rise and the associated creation of ‘accommodation space’ available for potential sediment accumulation. Shorter-term changes show regular patterns and irregular, partly short-lived effects of waves, tides, storm surges, slope processes and local or regional sediment dynamics. Long-term measurements enable distinction between the effects of these short- and long-term drivers, both natural and human-induced.

Systematic observation of coastal erosion, by periodically mapping or measuring the North Sea water lines and frontal dunes, started in earnest during the 17th century.

Annual coastline monitoring started in 1843, in the western Netherlands. Between 1840 and 1857, 124 oak

poles were driven about 3 m into the beach sand, initiating a network of beach poles with 1000-m spacing that spans the entire Dutch coast and still operates today. For each pole, cross-shore distances to the low- and high-water lines and dune foot have been logged annually ever since. Starting in 1965, some 1450 transects at 250-m spacing have been profiled near-annually from at least the frontal dune to about 1000 m seaward of the dune foot. Below low water, data come primarily from single-beam echo sounding. Above low-water, photogrammetry was used before 1996 and laser altimetry since.

Monitoring records for other countries bordering the North Sea are shorter, commonly limited to local or regional studies, and used mainly to assess the need for coastal maintenance and protection measures. In Denmark, soundings and levelling for coastal monitoring started in 1874 in the Thyborøn area along lines spaced 600–1000 m apart (Thyme 1990). Since 1957, the entire west coast of Jutland has been monitored for cross-shore coastline migration at least several times per decade, at similar spacing (Kystdirektoratet 2008). In Belgium, coastline changes have been monitored nationally since the late 1970s, using echo-sounding, topographic surveying, photogrammetry and laser altimetry (since the late 1990s). In the United Kingdom, one of the longest records concerns cliff behaviour at Holderness, Yorkshire, from 1951 to the present day (Brown 2008) using erosion posts, on average 500 m apart along the cliff edge. More extensive regional surveys have been conducted since 1992, when the Environment Agency started annual monitoring of winter and summer cliff and beach profile change at 1-km intervals between the Humber and Thames estuaries.

Where systematic monitoring networks to quantify behaviour of the entire coastline do not exist, useful information on local or regional coastal erosion is provided by analyses of historical to recent maps, aerial photographs (extensively used in mapping since the Second World War) and satellite images. In Germany, series of maps were analysed by Mroczek (1980) to deduce rates of erosion or accretion for the North Sea coast over more than one hundred years. In Britain, maps from the late 16th century provide the oldest former positions of coastal bluffs and cliffs.

Detail on evidence for (possibly varying) coastal erosion rates is given in E-Supplement Sect. S3.4.

3.9.2 Understanding Coastal Erosion: State, Variability and Trends

Erosion is widespread along the central and southern parts of the North Sea coastline, with about 25 % of the Danish-to-Scottish coastline eroding. Farther north, erosion is rare. Erosion percentages for the North Sea part of the coastline of countries bordering the North Sea vary widely. On a country-by-country basis, the percentage eroding is as follows: UK (22 %), France (76 %), Belgium (40 %), Netherlands (30 %), Germany (14 %), Denmark, north to Skagen (57 %), Sweden, south to Marstrand (0 %), and Norway (0 %). The data were calculated from EUrosion/EMODnet data (http://onegeology-europe.brgm.fr/geoportal/viewer.jsp) and the values are approximate. They exclude areas with no data (e.g. back-barrier shorelines are excluded for some countries like the Netherlands) and the Skagerrak is included.

In Norway, the coastline is mostly rocky. Combined with limited and only recent relative sea-level rise, there is no significant coastline change. In Sweden, Rydell et al. (2004) showed that erosion is limited to very few small areas with pocket beaches and bluffs in Västra Götaland County.

In Denmark, coastal erosion affects most of the North Sea shoreline, as summarised by Sørensen (2013). Much of the northern Jutland headland coast has eroded about 2–4 m $year^{-1}$ over the last 20 years, with maximum erosion in central bays and maximum deposition on the north-western side of eroding headlands (Christiansen and Bowman 1990). The central west coast, which is dominated by barrier beaches and bounded by glacial bluffs, has been the most vulnerable, with natural erosion rates of 2–8 m $year^{-1}$. Only the southernmost barrier beaches around Vejers, between Nymindegab and Blaavands Huk, are accreting naturally (Aagaard 2011). Horns Rev, which marks the southern end of the barrier-beach coast, acts as a natural groyne, protecting the island coast farther south from wave attack (Meesenburg 1996). This coast is in overall sediment balance, with parts of the barrier islands growing seaward, supplied by sediment from north and south (Sørensen 2013). Here, the southern ends of the islands are the most vulnerable to erosion.

Storm surges induce the most prominent changes along the Danish North Sea coast (Fruergaard et al. 2013). They lead to ephemeral and permanent barrier breaching, and drive the episodic transfer of large volumes of sediment from dunes and beaches to the nearshore and shoreface. During subsequent healing phases, which may last several decades, much of this sediment returns to the coast. South of Blavands Huk, persistent onshore migration of nearshore bars, governed by high-energy dissipative conditions, explains long-term coastline behaviour (Aagaard et al. 2004). Bar welding widens the beach and temporarily increases the amount of sand available for aeolian transport. Two trends can be observed on the Danish coast. First, most natural changes in coastal erosion are overprinted by increasing beach and shoreface nourishment (Fig. 3.32). Second, natural changes seem to indicate a switch to or acceleration of coastal erosion.

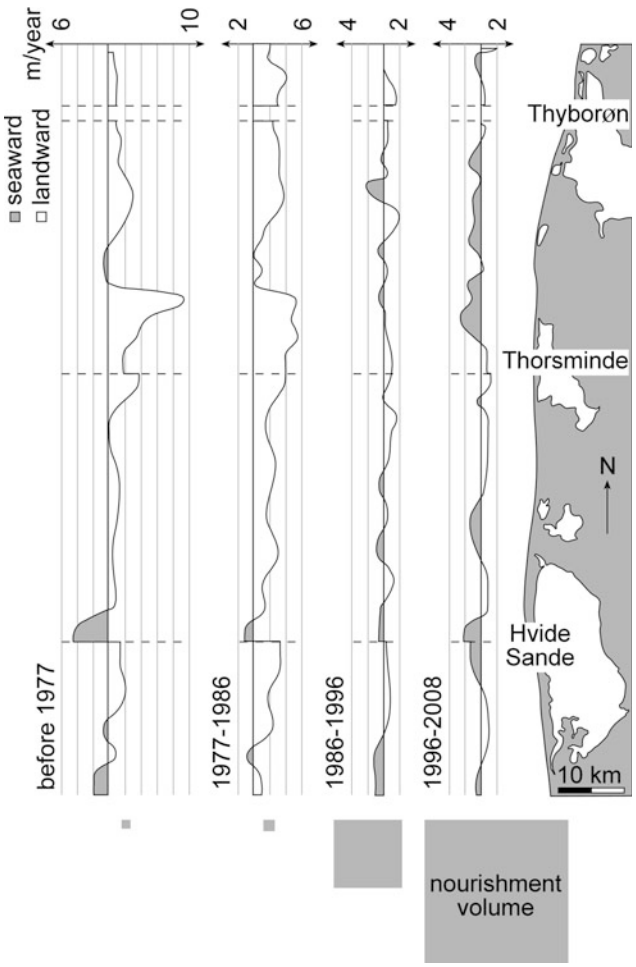

Fig. 3.32 West Jutland coastline advance/retreat rates for four periods and corresponding nourishment volumes (2.5 million m^3 $year^{-1}$ is represented by the *large box*). The 'y'-axis is located along the coast as in the sketch map; *horizontal lines* are at lagoon entrances (Sørensen 2013)

Along the German North Sea coast, erosion has had the most impact on the barrier-island coasts in the north and west, away from the central estuaries. At present, erosion occurs only along the 100 km of the coastal length that is not protected by dikes. Rates vary between <1 and 8 m $year^{-1}$. Most erosion has resulted from storm surges (Kelletat 1992) which have also reshaped the overall barrier and back-barrier morphology. Eroded sediments are partially regained during subsequent fair-weather periods, after temporary storage in the nearshore zone, and may be redistributed on neighbouring coasts. Through spit progradation, Sylt (one of the North Frisian Islands) has been growing northwards and southwards.

Acceleration of erosion along the German North Sea coast over the last 120 years is evident. Dette and Gärtner (1987) found average loss on the west coast of Sylt to have increased from 0.9 m $year^{-1}$ in the period 1870–1952 to 1.5 m $year^{-1}$ in the period 1952–1984, in spite of increasing efforts to protect the coast (Fig. 3.33). It is tempting to link this increase to acceleration of sea-level rise, but an increase in extreme events, with warmer, stormier winters, must also be considered (Salman et al. 2004).

The Dutch long-term monitoring record, starting in 1843, shows that the central (Holland) coastline receded relatively moderately (about 1 m $year^{-1}$) throughout the 19th and 20th centuries (van der Meulen et al. 2013). During this period, the coastline became increasingly defended by groynes and seawalls, which stabilised the coastline but resulted in steepening of the nearshore zone and the shoreface. Monitoring data also show that major storms have caused interruptions of long-term trends. Short-lived and rapid recession is commonly followed by extended post-storm periods of little erosion or even recovery, after which erosion resumes at the pre-storm rate (Fig. 3.34). Along the southwestern estuarine coast, erosion is linked to nearshore channel activity alongside island heads. Figure 3.35 shows long-term coastal erosion in North-Holland reversed by large-scale nourishment.

The west-Frisian islands fringing the Wadden Sea show large spatial and temporal differences in coastal erosion and accretion, similar to those observed along the German coast; local processes clearly overprint the long-term regional trend in coastal behaviour (Oost et al. 2012). Island growth and dune development reflect sand supply from the ebb deltas and shoreface, with episodes of rapid accretion linked to bars merging with the islands. Coastal erosion and dune scarping are associated with exposure to high-energy waves, as ebb-tidal deltas shift, or to strong currents, as marginal flood channels are forced toward the coast. The adjacent barrier islands of Ameland and Schiermonnikoog showed opposite behaviour during the last 150 years: Ameland receded and extended only slightly in a longshore direction, whereas Schiermonnikoog shifted seawards and accreted eastwards by more than 6 km (Oost 1995).

In Belgium, beaches and dunes showed long-term erosion until human intervention intensified (Charlier 2013). Currently, the dune foot is growing seaward in most places, aided by sand nourishments and hard coastal-protection structures (De Wolf 2002). Beaches behave more heterogeneously. West of Oostende, most are stable or show slight accretion. East of Oostende, erosive, stable and accretionary stretches alternate (De Wolf 2002).

In France, beach accretion is most usual southwest of Dunkerque, beach erosion between Dunkerque and the French-Belgian border (Bryche et al. 1993). Swell action is responsible for coastline recession of about 0.75 m $year^{-1}$ (Clabaut et al. 2000). Detailed topographic surveys of the upper beaches and dune fronts fringing the French North Sea indicate that periods of greater storminess do not necessarily result in more rapid retreat or more general coastal erosion. Here, coastline behaviour at a decade-to-century time scale

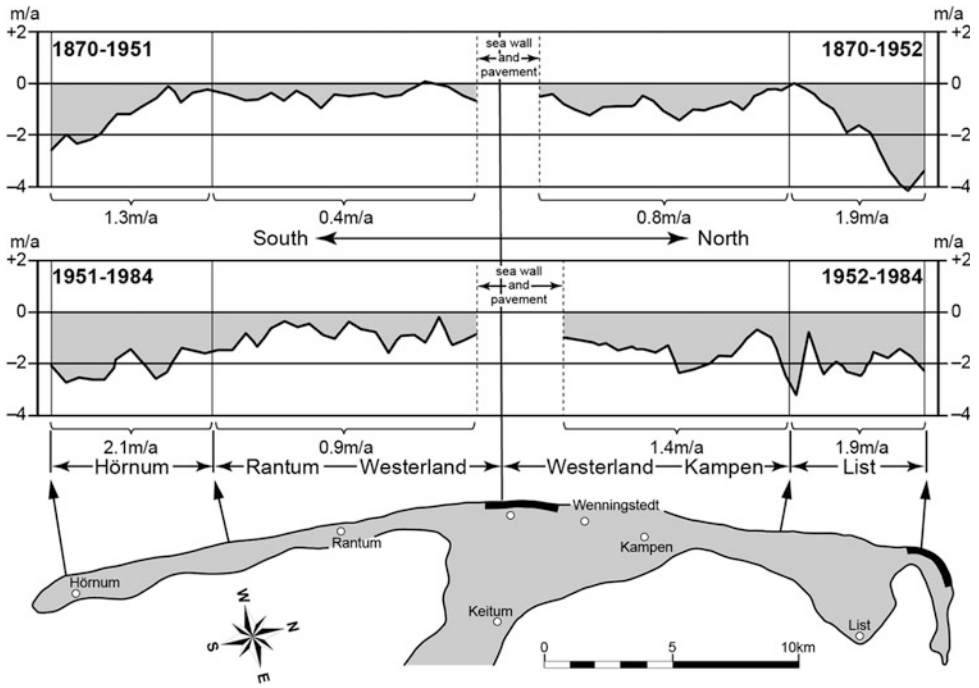

Fig. 3.33 Annual rates of coastal change on the west coast of Sylt island from 1870 to 1951/52, and from 1951/52 to 1984 (Besch 1987)

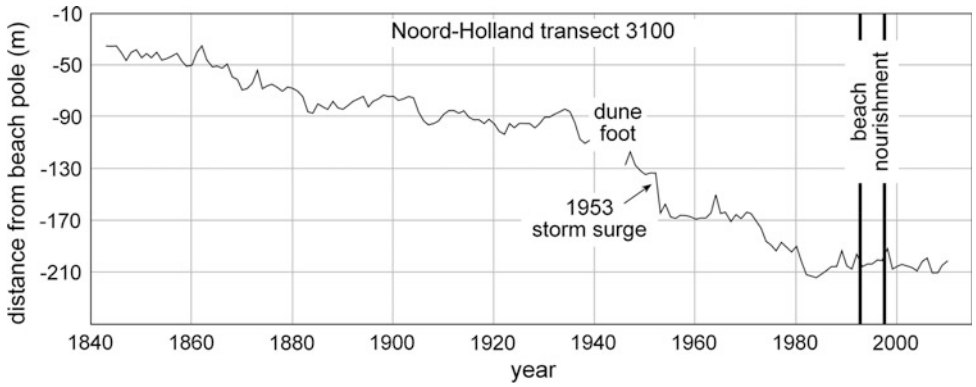

Fig. 3.34 Long-term erosion of the western Dutch coast just north of Bergen aan Zee, from annual monitoring data. The major effect of the 1953 record storm surge is clearly visible. It was followed by 20 years of relative stability before the pre-storm trend of coastal erosion continued (figure by Sytze van Heteren, Geological Survey of the Netherlands)

also depends on occurrences of high water levels (Vasseur and Héquette 2000), on local sediment budgets and on nearshore bathymetry (Ruz and Meur-Férec 2004; Chaverot et al. 2005). Although net loss of sediment from coastal systems prevails, see Fig. 3.36 for example, some coastline recession is counterbalanced by sand accumulation on top of the dunes and on their land-facing slopes (Clabaut et al. 2000).

The North Sea coasts of England and Scotland are dominated by cliffs and bluffs, with shorter stretches of pebble beaches, several estuaries, dwindling tidal flats and few dunes. The English areas at risk of erosion are mostly those where the North Sea is fringed by beaches or bluffs (Blott et al. 2013). Coastal erosion percentages are estimated as 27 % for north-eastern England, 56 % for Yorkshire and Humber, 9 % for Lincolnshire, 13 % for Norfolk to Essex and 31 % for south-eastern England (EUROSION 2004). Intertidal zones of saltmarsh and mudflat have been disappearing at a typical loss rate of 1–1.5 % per year over a period of more than 50 years. This loss is linked, though not solely attributable, to coastal squeeze. The lateral recession rates of coastal cliffs and bluffs vary with rock type (French 2001). In Scotland, most cliffs consist of resistant rock; significant erosion is limited to beaches.

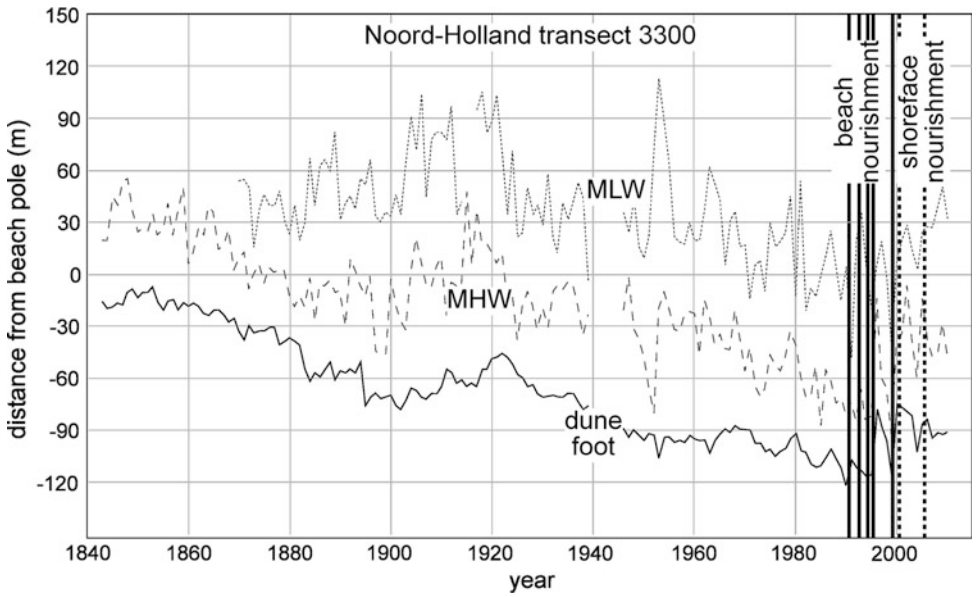

Fig. 3.35 Long-term coastal erosion at the Bergen aan Zee monitoring station in North-Holland, reversed with the advent of large-scale nourishment (*vertical lines on the right*) in the 1990s. The dune foot (*solid line*) receded more than 100 m between 1850 and 1990, as indicated by its distance to the beach pole. Similar patterns, although more diffuse, are shown by the mean-high-water (*dashed line*) and mean-low-water (*dotted*) lines (data from Deltares, figure by Sytze van Heteren, Geological Survey of the Netherlands)

Frontal dunes along beaches show average erosion rates of 1 m year^{-1} (Pye et al. 2007). Bluffs are particularly common in east Yorkshire, Humberside and East Anglia; they show very variable spatial and temporal erosion patterns, a function of complex glacial geology. Changes are episodic with no discernible trend. At Dunwich, for example, phases of accelerated coastal retreat (e.g. 1863–1880, 2.57 m year^{-1}; 1903–1919, 3.53 m year^{-1}) have alternated with periods of relative stability (e.g. 1826–1863, 0.06 m year^{-1}; 1882/3–1903, 0.08 m year^{-1}; Carr 1979). Landslides, protection by shingle beaches, cliff or bluff material, pore-water pressure and hydrodynamics all play a role (Brooks and Spencer 2010). These factors interact with longer-term drivers, including shifts in dominant weather patterns and changes in

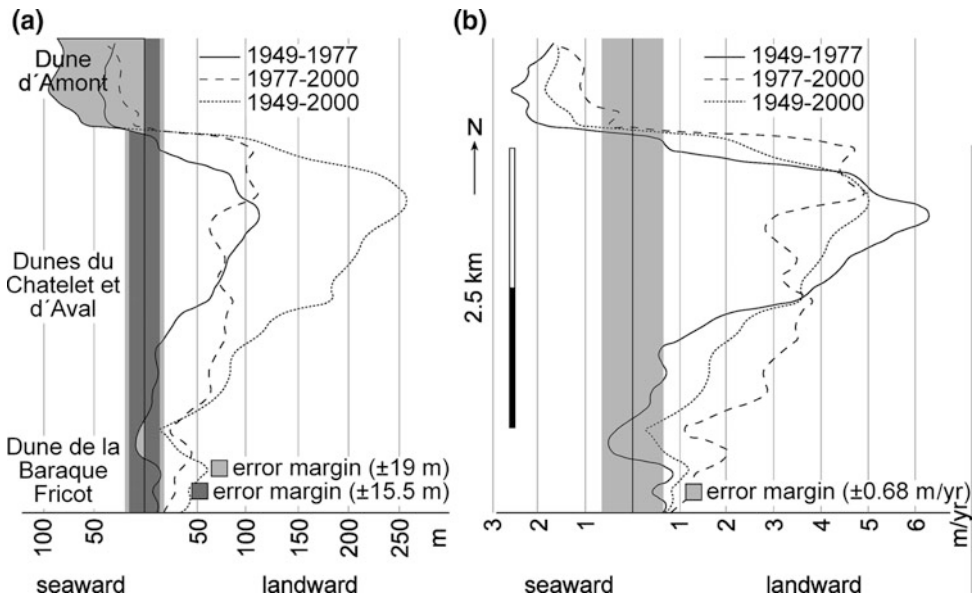

Fig. 3.36 Coastline evolution in the Bay of Wissant from 1949 to 2000 (*left*) and mean rates of coastline evolution for 1949–1977, 1977–2000 and 1949–2000 (*right*) (Aernouts and Héquette 2006)

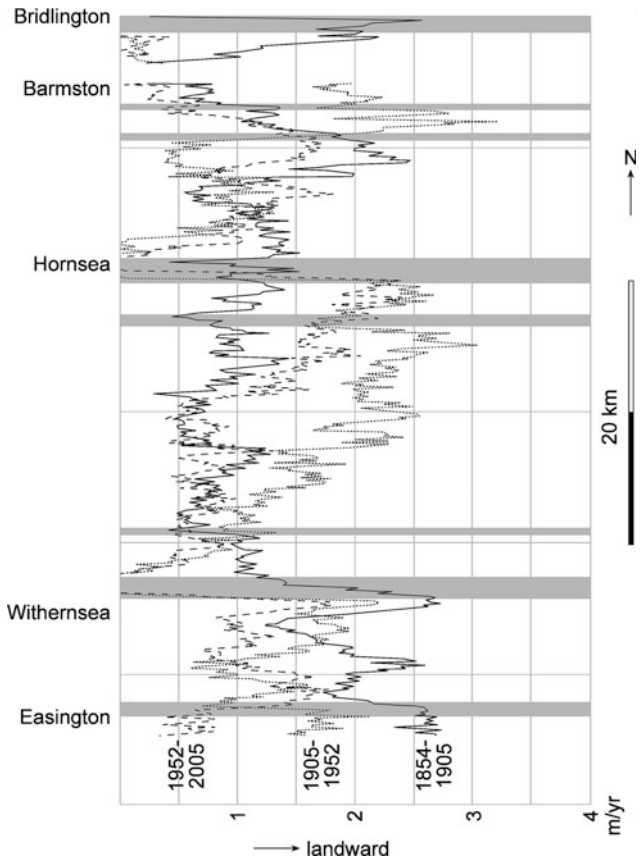

Fig. 3.37 Cliff-top retreat rates at Holderness calculated in three approximate 50-year periods. Areas defended in 2005 are in *grey*. Retreat rates vary within each zone (Brown 2008)

the rate of relative sea-level rise. As receding bluffs and cliffs expose new material, they may steepen, flatten or even disappear (Brooks and Spencer 2010). Feedbacks also operate. Large landslides provide the steep coast with temporary protection from the sea. Longshore drift of eroded sand and gravel leads to net accumulation at nearby beaches.

The Holderness bluff coast (Fig. 3.37) was eroded by more than 300 m in 150 years (Valentin 1954). At Happisburgh rates of erosion increased to average about 8 m year^{-1} in 1992–2004 (Poulton et al. 2006), significantly faster than the long-term averages of 0.9 m year^{-1} for North Norfolk in 1880–1967 (Cambers 1976; Thomalla and Vincent 2003), 2.3–3.5 m year^{-1} for Benacre–Southwold and 0.9 m year^{-1} for Dunwich–Minsmere in 1883–2008 (Brooks and Spencer 2010).

3.9.3 Offshore Morphology

3.9.3.1 History and Evidence

Long bathymetric time series (many decades to centuries) are rare and generally localised in the context of port approaches and dredging (for navigation) or aggregate extraction. 200-year records of an ebb-tidal delta in the Deben estuary, eastern England, and a 180-year record in the outer Thames estuary, have been analysed (Burningham and French 2006, 2011). Horrillo-Caraballo and Reeve (2008) interpreted sandbank configurations off Great Yarmouth using historic charts over a 150-year period. There are no field studies relating such series to climate-dependent factors (e.g. wave heights).

Van der Molen et al. (2004) numerically modelled millennial-scale morphodynamics of an idealised, semi-enclosed, energetic tidal shelf sea with dimensions and tidal characteristics resembling the Southern Bight of the North Sea. Several local process studies have related morphological change to wider-scale sediment transport and to tides, wind-driven flows and waves, for example eight years of current profile monitoring at Marsdiep inlet, Netherlands (Buijsman and Ridderinkhof 2008a, b) and a 1977–2003 sidescan sonar and multibeam backscatter record in the German Bight (Diesing et al. 2006).

3.9.3.2 Features

The English Channel is shallow and tidally dominated with waves mainly from the west-southwest during storms; it has limited sediment sources and is marked by extensive reworking of a relatively thin sediment cover (Paphitis et al. 2010). The central Channel seabed is covered by coarse-grained material. Wide areas are occupied by sand-sized sediments with various bedforms: ripples, sandwaves, longitudinal bedforms and sandbanks. Fine-grained sediments are confined to coastal embayments, rias, estuaries and open-coast intertidal flats (Paphitis et al. 2010).

Sandbanks occur widely in the North Sea (Knaapen 2009); they dominate the southern North Sea except near the mouth of the Rhine. In some areas, bank crests comprise fine sand whereas troughs comprise material too coarse to be moved by local tidal currents alone: such as shoreface-connected ridges off the East Frisian barrier-island coast (Son et al. 2012) and banks off Thorsminde (west Denmark; Anthony and Leth 2002). Sand-waves also occur widely, most commonly around sand banks. There is an extensive field of large sand-waves off the Netherlands.

3.9.3.3 Dynamics

Van der Molen (2002) modelled the influence of tides, wind and waves on net sand transport in the present southern North Sea. Results showed that wind-driven flow and waves only contribute significantly to net sand transport by tides when acting together where tidal currents are small. However, various combinations of forcing dominate net sand transport in different regions of the southern North Sea. Tides dominate in the southern, middle and north-western parts of the Southern Bight and in the region of The Wash.

Tides, wind-driven flow and waves are all important in the north-eastern part of the Southern Bight. Wind-driven flow and waves dominate north of the Frisian Islands, in the German Bight and on Dogger Bank. In the Channel, Reynaud et al. (2003) inferred predominant control by tidal dynamics, with mobile sediments in the central and eastern Channel, and longer-term influence of sea-level rise.

Contrasts in sand-wave character are related to differences in the relative importance of suspended load transport and of tidal currents and waves near the bed (Van Dijk and Kleinhans 2005; stronger tidal residual currents tend to cause faster sand-wave migration, waves tend to flatten sand-wave crests). In Marsdiep inlet, sand-waves typically migrate in the flood direction and not necessarily with predicted bedload and suspended load transport; Buijsman and Ridderinkhof (2008b) hypothesised that advection of suspended sand and lag effects may govern sand-wave migration.

Tidal sandbank height (60–90 % of water depth) and shape are controlled by the mode of sediment transport and hydrodynamic conditions (Roos et al. 2004). Bedload transport under symmetrical tidal conditions leads to high spiky banks. Profiles are lowered and smoothed by relaxation of suspended sediment, wind-wave stirring and tidal asymmetry; this last factor also causes profiles to be asymmetric. Thus strong tidal currents and their residuals, with enhancement of bed stress by waves, are the main hydrodynamic agents for (long-term changes in) sandbank morphology. Examples are off Great Yarmouth (Horrillo-Caraballo and Reeve 2008), Westhinder sandbank (Deleu et al. 2004) and Kwinte Bank (Giardino et al. 2010) off Belgium, the outer troughs of shoreface-connected ridges off the East Frisian barrier-island coast (Son et al. 2012). Near the mouth of the river Rhine, freshwater outflow affects the direction of tidal ellipses and residual flow, suppressing the formation of open ridges (Knaapen 2009). Other studies of local system dynamics (E-Supplement Sect. S3.4.1) emphasise the role of tidal asymmetries with wave-enhanced transport, and show that shoals evolve, in some cases cyclically.

3.9.3.4 Evolution in Relation to Climate

Idealised simulations (Van der Molen et al. 2004) suggest that a basin resembling the Southern Bight may be expected to export sediment, deepen and expand by accumulation of eroded sediment in the deeper waters to the north, owing to asymmetry in the amphidromic tidal velocities. Sea-level changes affect tidal wavelength, hence this sediment distribution, and deepening reduces evolution rate. However, changes in sea level and tides are small relative to average water depths on time scales of decades to a century (Sect. 3.4).

In practice, repeat surveys tend to show stability of larger (kilometre-scale) features or patterns over periods of nine months (off Thorsminde on the Danish west coast; Anthony and Leth 2002), some years (e.g. Son et al. 2012) or even decades (Diesing et al. 2006). There is no clear evidence of any regionally coherent response to large-scale historical forcing such as sea-level rise. However, harbour or dike works and large-scale dredging induce wider change, such as to Texel inlet (Elias et al. 2006) and Kwinte Bank (Degrendele et al. 2010). Detecting abiotically-induced climate-related changes in morphological evolution could only be expected where the influence of storms and waves is significant in net sediment transport, namely in the north-east of the Southern Bight (notably the German Bight) and on Dogger Bank (van der Molen 2002).

Climate-related change is more likely where benthic organisms play an important role in the development and dynamics of bedforms, as so-called ‘ecosystem engineers’. Although no field studies exist that link changes in benthic habitats and indicator species to bedform development and mobility, an increasing number of modelling studies suggest that such a link exists. Borsje et al. (2009) showed that including the abundance of three dominant eco-engineers (*Lanice conchilega*, *Tellina fabula*, *Echinocardium cordatum*) gives a more accurate prediction of sand-wave occurrence on the Dutch continental shelf than modelling without biology. Very little work has been done on eco-engineers, climate change and seabed morphology; this is an important subject for future research.

3.10 Sea Ice

Natalija Schmelzer, Jürgen Holfort, Ralf Weisse

In the North Sea, ice does not form in every winter season. Ice formation generally depends on the weather regimes prevailing over Europe and their temporal stability, and on the morphological characteristics of the North Sea.

Typically, in autumn and winter, prevailing westerly weather regimes bring relatively mild air masses from the Atlantic Ocean into the North Sea area. These weather regimes also cause inflows of relatively warm, high-salinity Atlantic water into the North Sea, preventing or delaying the seasonal cooling of North Sea water and hence ice formation. By contrast, easterly weather regimes cause rapid cooling of the water.

Large stationary high-pressure zones over northern Scandinavia and the European polar seas, and stable anti-cyclonic regimes over eastern Europe, are particularly effective in this respect. The extent and duration of ice cover in the North Sea are governed by the number, intensity, and length of freezing periods and by the timing of their occurrence. The North Sea comprises open sea areas, Wadden Sea areas, and tributaries; these play an important role in the

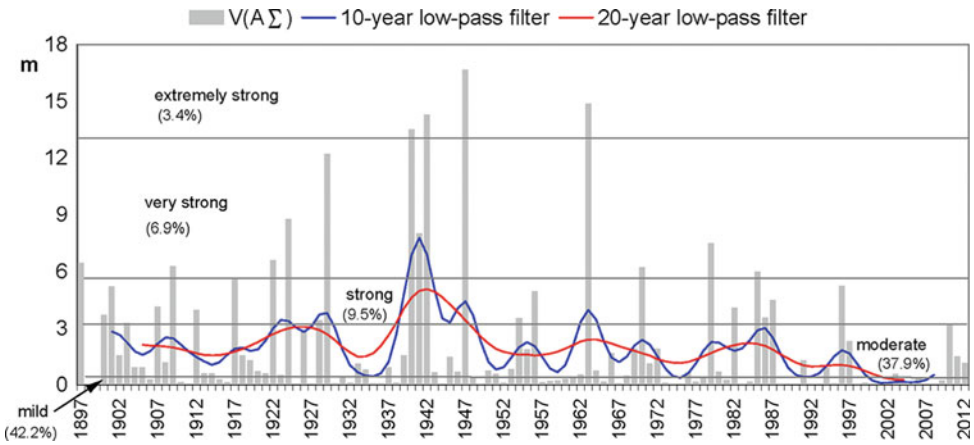

Fig. 3.38 Annual accumulated areal ice volume $V_{A\Sigma}$ on the German North Sea coast for 1897 to 2012 (update from http://www.bsh.de/de/Meeresdaten/Beobachtungen/Eis/Eiswinter2010_11.pdf)

development of ice conditions. Peer-reviewed literature on long-term changes in sea-ice conditions in the North Sea is sparse.

For the German North Sea coast, ice winters are classified on the basis of the accumulated areal ice volume $V_{A\Sigma}$ (in metres)

$$V_{A\Sigma} = \frac{1}{n}\sum_{j}\sum_{k}(NH)_{jk} \tag{3.1}$$

where n denotes the number of observations (stations); N is the fractional ice concentration varying between 0 and 1; and H represents ice thickness in metres at station $k = 1...n$ on day j when there is ice (Koslowski 1989). Available data allow the classification of different types of ice winter on the German North Sea coast for the period 1897–2012 (Fig. 3.38).

In the past 52 years (1961–2012), 26 (50 %) winter seasons on the North Sea coast were very weak or weak, 18 (35 %) were moderate and eight (15 %) were strong, very strong or extremely strong. In comparison with the 116-year time span shown in Fig. 3.38, the occurrence of extremely strong and very strong ice winters has decreased while there has been a simultaneous increase in winters with low ice-cover conditions.

Ice formation on the tidal flats of the Wadden Sea normally begins in mid- to late January (BSH 2008). Ice-cover duration varies widely, in space and time. In moderate ice winters, ice occurs on 10–20 days in the sheltered inner coastal waters of the North Frisian Wadden Sea, and on up to 10 days in open navigation channels, which is comparable to ice formation in the East Frisian Wadden Sea.

In strong and very strong ice winters, ice cover in the sheltered navigation channels of the North Frisian Wadden Sea lasts from 55 to 75 days on average, and in open navigation channels from 45 to 55 days, similar to the East Frisian Wadden Sea. In near-shore tidal flats, the most common type of ice is fast ice or rafted/ridged ice; in outer tidal flats, ice floes and slash or shuga predominate, kept in motion by wind and tidal forces.

In the open part of the German Bight, the remaining heat content of North Sea water in early winter is so large that ice rarely forms. Shuga and ice floes occurred in offshore waters to the west and northwest of Helgoland in about 8 % of all winter seasons, being last observed in late January 1970 and before that in February and March 1963; they do not originate near Helgoland but are carried there from the coastal area by tidal currents and by easterly winds persisting for long periods. In the offshore waters of the German Bight off the North and East Frisian islands, ice forms only in very strong or extremely strong ice winters.

Level ice thicknesses reach 10–15 cm in most winters, 15–30 cm in strong ice winters, and as much as 30–50 cm in very strong ice winters. The higher ice thickness categories are most likely to occur in February and early March. Ice thickness data refer to level ice, which occurs primarily in the form of ice cakes and small- to medium-sized floes. A typical phenomenon caused by tidal influences in areas of the Wadden Sea is rafting and ridging of initially level ice, which may cause ice walls several metres high. In such areas, floebits of about 1–3 m thickness comprising frozen ice cakes and small to medium-sized floes of coarse compacted ice are also likely to occur, especially in winters with long freezing periods.

Thawing causes rapid retreat of ice in south-eastern North Sea coastal areas. Westerly winds push warmer, high-salinity North Sea water toward the coast, accelerating the melting process started by meteorological influences. Ice in south-eastern North Sea coastal waters normally melts completely by the end of February. In very strong to extremely strong ice winters during which maximum ice formation is not reached until mid-February, the last remnants of ice may melt as late as the end of March.

The frequency of ice occurrence has decreased since 1961, analogous to the development of ice conditions in the western Baltic Sea (Schmelzer and Holfort 2012). Although

there is presently a trend toward milder ice winters, strong to extremely strong ice winters in the area of the western Baltic Sea and North Sea are still likely in the future (Vavrus et al. 2006; Kodra et al. 2011).

3.11 Wadden Sea

Justus van Beusekom

3.11.1 Background

The Wadden Sea, fringing the coast of the south-eastern North Sea, is the largest coherent tidal flat system of the temperate world. Its outstanding geological and biological importance makes it a world nature heritage site (Reise et al. 2010). The Wadden Sea is the result of the intricate interplay of tidal forces, sediment supply and moderate sea-level rise (Reise 2013). Since its beginning some 8000 years ago, the Wadden Sea has been increasingly affected by humans (Lotze et al. 2005). Around 1000 years ago, coastal people started to transform the coast, ultimately embanking about half of the original Wadden Sea (Reise 2005).

Owing to this coastal squeeze, hydrodynamic forces increased leading to a loss of fine material (Flemming and Nyandwi 1994). Accelerated sea-level rise may also have contributed to increased hydrodynamics and a loss of mudflats (Dolch and Hass 2008). Also, the estuaries intersecting the Wadden Sea have dramatically changed due to diking and dredging (Reise 2005).

The Wadden Sea receives large amounts of riverine fresh water, either directly as (branches of) rivers debouch into it (e.g. IJsselmeer, Ems, Weser, Elbe, Eider, Varde A) or indirectly (especially from the Rhine and Maas). River water from the Rhine and Maas is transported to the Wadden Sea along with residual North Sea currents flowing predominantly anti-clockwise around the North Sea. Thus, nutrient and contaminant loads can be imported into the Wadden Sea and large amounts may be present. Given this background, three interacting aspects of environmental quality are addressed in this section: SPM, nutrients and contaminants.

3.11.2 Suspended Matter Dynamics

The Wadden Sea is characterised by relatively high SPM concentrations compared to the North Sea. To maintain these gradients, some type of accumulation process must be active (Postma 1954). Earlier explanations focusing on Wadden Sea processes included the biases described at the end of Sect. 3.8 (see also Postma 1954; van Straaten and Kuenen 1957; Burchard et al. 2008). Biological interactions such as filter-feeding or microphytobenthic microfilms (Staats et al. 2001; Andersen et al. 2010) increase the retention efficiency of the Wadden Sea. Thus the Wadden Sea proper can be regarded as an effective 'keeper' of SPM (van Beusekom et al. 2012), at least on a seasonal scale.

The North Sea, on the other hand, can be seen as the 'pusher' (van Beusekom et al. 2012) of suspended organic matter into the Wadden Sea via estuarine-type circulation (see Sect. 3.8.5; Postma 1981). The Wadden Sea is heterotrophic: locally-produced and imported organic matter is remineralised (Postma 1984) as supported by carbon budgets (van Beusekom et al. 1999). The ecological importance of organic matter import from the North Sea for the productivity of the Wadden Sea was discussed by Verwey (1952).

Changes have occurred in SPM dynamics in the Wadden Sea and its intersecting estuaries: De Jonge et al. (2014) showed that dredging of the Ems estuary caused a regime shift in hydrodynamics leading to hyperturbid conditions. Dredging of the Rhine estuary and subsequent dumping along the Dutch coast ultimately led to increased SPM concentrations in the western Dutch Wadden Sea (de Jonge and de Jong 2002). SPM dynamics were related to riverine runoff and de Jonge and de Jong (2002) suggested that increased runoff due to global climate change will enhance SPM dynamics in the Dutch Wadden Sea.

3.11.3 Changes in Nutrient and Organic Matter Dynamics

Riverine nutrient discharges are the main drivers of Wadden Sea eutrophication. Historic nutrient concentrations for the Rhine, compiled by van Bennekom and Wetsteijn (1990), show a clear increase in concentrations after the Second World War and a decrease since the mid-1980s due to the implementation of wastewater treatment and better agricultural practice (e.g. de Jong 2000) (see also Chaps. 11 and 13).

Increased nutrient availability has led to increased primary production and increased turnover of organic matter and nutrients. Changes in primary production are demonstrated by the Marsdiep time series (western Dutch Wadden Sea) initiated by Cadée (Cadée and Hegeman 2002), showing an increase in primary production until the 1990s and then a decrease. Present levels are about 120–200 g C m^{-2} $year^{-1}$ in the western and northern Wadden Sea (Loebl et al. 2007; Philippart et al. 2007). Most monitoring programmes started in the 1980s or later, thus only documenting changes after the maximum eutrophication had occurred. Summer chlorophyll levels are a good proxy for Wadden-Sea-wide eutrophication, correlating with riverine

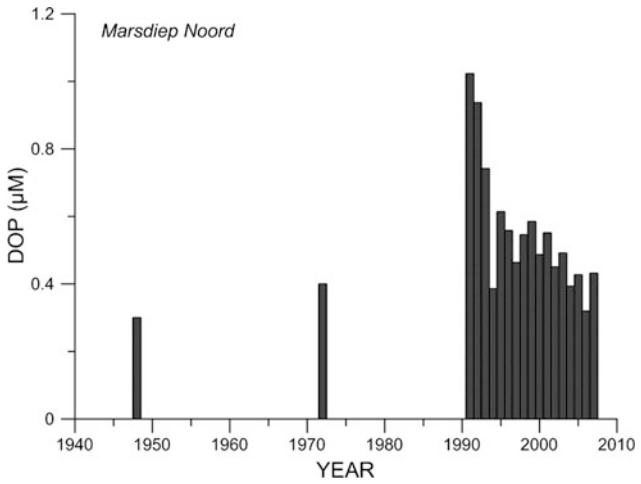

Fig. 3.39 Long-term changes in summer concentration of dissolved organic phosphorus in the Marsdiep area (western Dutch Wadden Sea) (figure by Justus van Beusekom after van Beusekom and de Jonge 2012)

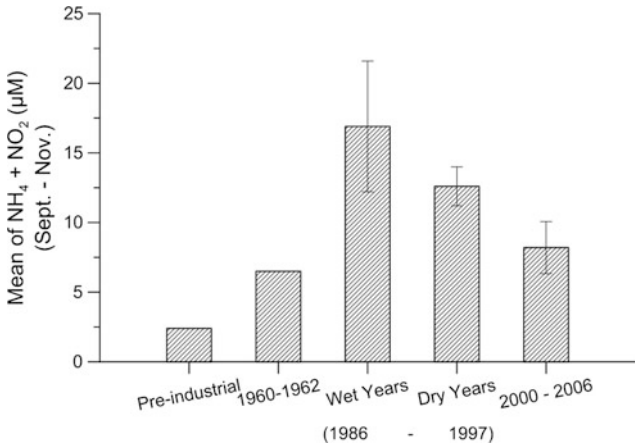

Fig. 3.40 Mean autumn ammonium and nitrite (µM) during pre-industrial times, in 1960–1962 (Postma 1966), in the five wettest (1986–1988, 1994, 1995) and five driest (1991–1993, 1996, 1997) years between 1986 and 1997, and in 2000–2006 in the western Dutch Wadden Sea (figure by Justus van Beusekom after van Beusekom and de Jonge 2002, updated with data from van Beusekom et al. 2009b). For the latter three groups, the standard deviation is shown

nutrient discharges (van Beusekom et al. 2009a) and demonstrating a gradual decrease in eutrophication.

Changes in organic matter and nutrient turnover covering both the increase and decrease in eutrophication are again best demonstrated for the western Dutch Wadden Sea. De Jonge and Postma (1974) documented a two- to three-fold increase in phosphate and particulate and dissolved organic phosphorus concentrations between the 1950s and 1972 (Fig. 3.39). Between 1961 (Postma 1966) and the 1990s, autumn levels of ammonium and nitrite (indicating organic matter turnover; van Beusekom and de Jonge 2002) also increased about two- to five-fold depending on whether wet years with high riverine loads or dry years with low riverine loads are compared (Fig. 3.40). From the 1990s, dissolved organic phosphorus levels and autumn ammonium and nitrite levels have decreased (van Beusekom et al. 2009a; van Beusekom and de Jonge 2012) as chlorophyll levels and riverine nutrient loads generally decreased.

Since the mid-1980s, several monitoring programmes have covered the entire Wadden Sea. These data document large regional differences in eutrophication. In general, levels are higher in the southern Wadden Sea than in the northern Wadden Sea, but some overlap exists (van Beusekom et al. 2009a). These differences are also captured by summer chlorophyll levels (average May–September) and autumn ammonium and nitrite levels (average September–November) suggesting that both parameters are useful proxies for describing Wadden Sea eutrophication. At a few stations only, dissolved nutrients are monitored and show the same spatial differences: high values in the Dutch Wadden Sea and low values in the northern Wadden Sea (Sylt; van Beusekom and de Jonge 2012).

The factors responsible for the regional differences are not yet known. Van Beusekom et al. (2012) suggested two possibilities: differences in the amount of imported organic matter or the size of the receiving tidal basins. Evidence was presented to show that the size of the receiving tidal basin, in particular the distance between barrier islands and the mainland, may lead to a dilution of the import signal, whereas in narrow basins with a small distance between the islands the imported organic matter is concentrated.

The general decrease in eutrophication has resulted in lower chlorophyll levels and, in the northern Wadden Sea, to a decrease in green macroalgae (van Beusekom et al. 2009a) and has possibly contributed to an increase in seagrass (Reise and Kohlus 2008).

3.11.4 Contaminants

Within the framework of the Wadden Sea Quality Status Reports, Bakker et al. (2009) presented an overview of hazardous substances. Dissolved heavy metal concentrations in the Wadden Sea (mercury, cadmium, copper, zinc and lead) are not monitored and the focus is on sediment contamination. The main reduction in riverine heavy metal loads—the principal source for the Wadden Sea—was during the 1980s and 1990s. Notable decreases were observed in the river Elbe after the end of the German Democratic Republic. Since then heavy metal concentrations have remained similar or decreased slightly. Sediment concentrations of mercury and lead still pose a risk in a majority of Wadden Sea sub-regions.

Xenobiotic compounds in the Wadden Sea are a major concern because most are persistent, bio-accumulative and

toxic (Bakker et al. 2009). In general, riverine inputs and environmental concentrations have decreased. For instance, a ban on tributyltin (TBT) has proved very successful, but effects can still be observed, for example on snails. Polychlorinated biphenyls (PCBs) are still widespread but concentrations are decreasing. Levels of lindane and DDT are also decreasing, but occasional erosion of old deposits leads to fluctuating concentrations in the Wadden Sea. Of particular future concern (as possible hormone disruptors) are newly developed xenobiotics, which include flame retardants, perfluorinated sulfonates and phthalates. These substances are not regularly monitored and little is known about their ecological effects.

3.11.5 Relevance of Climate Change

Climate change is expected to affect the sediment composition of the Wadden Sea: directly by sea-level rise (e.g. Dolch and Hass 2008) and indirectly by altered wind regimes (de Jonge and van Beusekom 1995). It is an open question whether sediment import into the Wadden Sea can compensate for increased sea-level rise or whether the Wadden Sea will ultimately drown (CPSL 2010). Nevertheless, sea-level rise will necessitate new strategies for coastal protection with yet unknown consequences for dikes, hydrodynamics and morphology (Reise 2013).

Climate change will drive complex and interacting effects on Wadden Sea water quality. One aspect of climate change is weather extremes. Extreme high river flows may transport large amounts of toxic substances to the Wadden Sea affecting filter feeders and fish (Einsporn et al. 2005). Likewise, increased nutrient fluxes during high river flows or extreme wet years lead to greater organic matter turnover (Fig. 3.40). De Jonge and de Jong (2002) suggested that increased river runoff will increase SPM levels in the Wadden Sea.

Higher temperatures will have complex and interacting effects on organic matter turnover in the Wadden Sea (Reise and van Beusekom 2008). For instance, higher temperatures enhance zooplankton dynamics (Martens and van Beusekom 2008) but suppress spring phytoplankton blooms through enhanced grazing (van Beusekom et al. 2009a). In general, higher temperatures are expected to enhance organic matter turnover with as yet unknown effects on the Wadden Sea food web.

3.12 Summary

In general, temperature variability on all time scales to multi-decadal tends to obscure longer-term trends. This variability is probably a greater source of uncertainty than lack of surface temperature data. Nevertheless, evidence of exceptional warming, especially since the 1980s, is very strong. In adjacent Atlantic waters (Faroe-Shetland Channel) and the northern North Sea, there has been a positive temperature anomaly of more than one standard deviation in most years since the mid-1990s; more than two standard deviations in a majority of years between 2002 and 2010 (Hughes et al. 2011). The temperature rise is not uniform in space, with largest rises (exceeding 1 °C since the end of the 19th century) in the south-east. Models provide some evidence of increasing duration of summer stratification away from estuarine outflow regions.

Shorter-term variations in salinity exceed any climate-related changes.

The Atlantic Meridional Overturning Circulation is very variable with no clear trend to date. However, changes in northern inflow to the North Sea correlate with changes in the NAO. Otherwise currents are highly variable on various time scales (tides, winds, seasonal density), and one storm can be significant compared to a year's integrated transport. The evidence is strong, coming from models as much as from measurements; however, observations are sparse at any one time and brief relative to climate-change time scales.

Over the past 100 to 120 years, absolute mean sea level in the North Sea rose by about 1.6 mm year^{-1}, comparable to the rates of global mean sea-level rise. Extreme sea levels have increased over the past 100–150 years in the North Sea, mainly due to a rise in mean sea level. Evidence for changes in sea level is very strong. Waves and storm surges (resulting from the weather) show pronounced variation on time scales of years and decades but no substantial long-term trend.

Carbon dioxide, pH and nutrients basin-wide are influenced by the circulation pattern, especially inflow from the Atlantic, local weather conditions (correlating with the NAO) and properties of component water masses. However, measurements on long time scales relating to climate change are only local, made close to the coast and affected by strong offshore gradients. There is net CO_2 uptake from the atmosphere, attributable to areas stratified in summer. The North Sea is a net nitrogen sink for the Atlantic. Model results suggest a long-term decrease in pH with relatively large variability due to shorter-term changes of circulation.

Higher temperatures tend to reduce oxygen concentrations near the surface; at depth, concentrations depend on vertical mixing for which variable weather is an important driver where depletion is a concern.

Suspended matter and turbidity are very variable, influenced by river inputs, seasons, tidal resuspension and advection (spring-neap modulation), waves and stratification. The North Sea is generally turbid in the unstratified south with transport to the north-east.

Coastal erosion is extensive but irregular; where it occurs, long-term rates are often 1 m year^{-1} or more. Some sectors

accrete. Climate-related change in evolving morphology is not yet known.

Ice occurrence is restricted to shallow waters of the southern and eastern North Sea and has decreased over the last 50 years. Nevertheless, some severe ice winters are still expected in future.

In the Wadden Sea, higher temperatures are expected to enhance organic matter turnover.

Much work has focused on detecting long-term change in the North Sea region, either from measurements or model results. In other regions, there have been attempts to attribute such changes to, for example, anthropogenic forcing (e.g. Barkhordarian et al. 2012). However, comparable studies are still missing for the North Sea. Such studies are urgently needed to assess consistency between observed changes and current expectations, in order to increase the level of confidence in projections of expected future conditions.

Acknowledgments Figures 3.6, 3.9, 3.10 are reproduced under the Open Government Licence v3.0: www.nationalarchives.gov.uk/doc/open-government-licence/version/3.

References

Aagaard T (2011) Sediment transfer from beach to shoreface: The sediment budget of an accreting beach on the Danish North Sea Coast. Geomorphology 135:143–157

Aagaard T, Davidson-Arnott R, Greenwood B, Nielsen J (2004) Sediment supply from shoreface to dunes: Linking sediment transport measurements and long-term morphological evolution. Geomorphology 60:205–224

Aernouts D, Héquette A (2006) L'évolution du rivage et des petits-fonds en baie de Wissant pendant le XXe siècle (Pas-de-Calais, France). Géomorphologie: relief, processus, environnement [online]: http://geomorphologie.revues.org/477; doi:10.4000/geomorphologie.477

Albrecht F, Weisse R (2012) Pressure effects on past regional sea level trends and variability in the German Bight. Ocean Dyn 62:1169–1186

Albrecht F, Wahl T, Jensen J, Weisse R (2011) Determining sea level change in the German Bight. Ocean Dyn 61:2037–2050

Albretsen J, Aure J, Sætre R, Danielssen DS (2012) Climatic variability in the Skagerrak and coastal waters of Norway. ICES J Mar Sci 69:758–763

Alheit J, Pohlmann T, Casini M, Greve W, Hinrichs R, mathis M, O'driscoll K, Vorberg R, Wagner C (2012) Climate variability drives anchovies and sardines into the North and Baltic Seas. Prog Oceanogr 96:128–139

Allen JI, Holt JT, Blackford J, Proctor R (2007) Error quantification of a high-resolution coupled hydrodynamic-ecosystem coastal-oceanmodel: Part 2. Chlorophyll-a, nutrients and SPM. J Mar Sys 68:381–404

Andersen TJ, Lanuru M, van Bernem C, Pejrup M, Riethmueller R (2010) Erodibility of a mixed mudflat dominated by microphytobenthos and *Cerastoderma edule*, East Frisian Wadden Sea, Germany. Estuar, Coastal Shelf Sci 87:197–206.

Anthony D, Leth JO (2002) Large-scale bedforms, sediment distribution and sand mobility in the eastern North Sea off the Danish west coast. Mar Geol 182:247–263

Araújo I (2005) Sea level variability: Examples from the Atlantic coast of Europe. Ph.D. Thesis, University of Southampton, United Kingdom

Araújo I, Pugh DT (2008) Sea levels at Newlyn 1915–2005: Analysis of trends for future flooding risks. J Coast Res 24(sp3):203–212

Artioli Y, Blackford JC, Butenschön M, Holt JT, Wakelin SL, Thomas H, Borges AV, Allen JI (2012) The carbonate system in the North Sea: sensitivity and model validation. J Mar Sys 102–104:1–13

Artioli Y, Blackford JC, Nondal G, Bellerby RGJ, Wakelin SL, Holt JT, Butenschön M, Allen JI (2014) Heterogeneity of impacts of high CO_2 on the North Western European Shelf. Biogeosciences 11:601–612

Bacon S, Carter D (1991). Wave climate changes in the North Atlantic and the North Sea. Int J Climatol 11:545–558

Badin G, Williams RG, Holt JT, Fernand LJ (2009) Are mesoscale eddies in shelf seas formed by baroclinic instability of tidal fronts? J Geophys Res 114:C10021, doi:10.1029/2009JC005340

Bakker J, Lüerßen G, Marencic H, Jung K (2009) Hazardous substances. In: Thematic Report 5.1 In: Marencic H, de Vlas J (eds) Quality Status Report 2009, Wadden Sea Ecosystem. No 25. Common Wadden Sea Secretariat, Trilateral Monitoring and Assessment Group, Wilhelmshaven, Germany

Baretta-Bekker JG, Baretta JW, Latuhihin MJ, Desmit X, Prins TC (2009) Description of the long-term (1991–2005) temporal and spatial distribution of phytoplankton carbon biomass in the Dutch North Sea. J Sea Res 61:50–59

Barkhordarian A, Bhend J, von Storch H (2012) Consistency of observed near surface temperature trends with climate change projections over the Mediterranean region. Clim Dyn 38:1695–1702

Baxter P (2005) The East Coast Great Flood, 31 January–1 February 1953: A summary of the human disaster. Phil Trans R Soc A 363:1293–1312

Becker GA, Frohse A, Damm P (1997) The Northwest European shelf temperature and salinity variability. German J. Hydr. (Ocean. Dynamics) 49:135–151

Berx B, Hansen B, Østerhus S, Larsen KM, Sherwin T, Jochumsen K (2013) Combining in-situ measurements and altimetry to estimate volume, heat and salt transport variability through the Faroe Shetland Channel. Ocean Sci 9:639–654

Besch H-W (1987) Sylt-Naturräumliche Gliederung und Umwandlung durch Meer und Mensch. In: Hofmeister B, Voss F (eds), Beiträge zur Geographie der Küsten und Meere - Sylt 1986 und Berlin 1987. Berliner Geogr. Studien 25

Beszczynska-Möller A, Dye SR (eds) (2013) ICES Report on Ocean Climate 2012. ICES Coop Res Rep 321

Bindoff NL, Willebrand J, Artale V, Cazenave A, Gregory J, Gulev S, Hanawa K, Le Quéré C, Levitus S, Nojiri Y, Shum CK, Talley LD, Unnikrishnan A (2007) Observations: Oceanic climate change and sea level. In: Solomon, S., Qin, D., Manning, M., Chen, Z.,

Marquis, M., Averyt, K.B., Tignor M., Miller H.L (eds) Climate Change 2007: The Physical Science Basis. Contribution of Working Group I to the Fourth Assessment Report of the Intergovernmental Panel on Climate Change. Cambridge University Press

Blackford JC, Gilbert FJ (2007) pH variability and CO_2 induced acidification in the North Sea. J. Mar Sys 64:229–241

Blott SJ, Duck RW, Phillips MR, Pontee NI, Pye K, Williams A (2013) Great Britain. In: Pranzini E, Williams A (eds) Coastal Erosion and Protection in Europe. Routledge, Abingdon, pp. 173–208

Borges AV, Gypens N (2010) Carbonate chemistry in the coastal zone responds more strongly to eutrophication than to ocean acidification. Limnol Oceanogr 55:346–353

Borsje BW, Hulscher SJMH, Herman PMJ, De Vries MB (2009) On the parameterization of biological influences on offshore sand wave dynamics. Ocean Dyn 59:659–670

Bouin MN, Wöppelmann G (2010) Land motion estimates from GPS at tide gauges: A geophysical evaluation. Geophys J Int 180:193–209

Bozec Y, Thomas H, Schiettecatte L-S, Borges AV, Elkalay K, de Baar HJW (2006) Assessment of the processes controlling the seasonal variations of dissolved inorganic carbon in the North Sea. Limnol Oceanogr 51:2746–2762

Brooks SM, Spencer T (2010) Temporal and spatial variations in recession rates and sediment release from soft rock cliffs, Suffolk coast, UK. Geomorphology 124:26–41

Brown S (2008) Soft cliff retreat adjacent to coastal defences, with particular reference to Holderness and Christchurch Bay, UK. PhD Thesis University of Southampton

Bryche A, de Putter B, De Wolf P (1993) French and Belgian Coast from Dunkirk to De Panne: a case study of transborder cooperation in the framework of the Interreg initiative of the European community. In: Coastal Zone: Proceedings of the Symposium on Coastal and Ocean Management

BSH (2008) Umweltbericht zum Raumordnungsplan für die deutsche ausschließliche Wirtschaftszone (AWZ) Teil Nordsee. Bundesamt für Seeschiffahrt und Hydrographie (BSH)

Buijsman MC, Ridderinkhof H (2008a) Long-term evolution of sand waves in the Marsdiep inlet. I: High-resolution observations. Cont Shelf Res 28:1190–1201

Buijsman MC, Ridderinkhof H (2008b) Long-term evolution of sand waves in the Marsdiep inlet. II: Relation to hydrodynamics. Cont Shelf Res 28:1202–1215

Burchard H, Flöser G, Staneva J, Badewien TH, Riethmüller R (2008) Impact of density gradients on net sediment transport into the Wadden Sea. J Phys Oceanogr 38:566–587

Burningham H, French J (2006) Morphodynamic behaviour of a mixed sand-gravel ebb-tidal delta: Deben estuary, Suffolk, UK. Mar Geol 225:23–44

Burningham H, French J (2011) Seabed dynamics in a large coastal embayment: 180 years of morphological change in the outer Thames estuary. Hydrobiologia 672:105–119

Burt WJ, Thomas H, Fennel K, Horne E (2013) Sediment-water column fluxes of carbon, oxygen and nutrients in Bedford Basin, Nova Scotia, inferred from 224Ra measurements. Biogeosci 10:53–66

Burt WJ, Thomas H, Pätsch J, Omar AM, Schrum C, Daewel U, Brenner H, de Baar HJW (2014) Radium isotopes as a tracer of sediment-water column exchange in the North Sea. Glob Biogeochem Cyc 28, doi:10.1002/2014GB004825

Cadée GC, Hegeman J (2002) Phytoplankton in the Marsdiep at the end of the 20th century; 30 years monitoring biomass, primary production, and Phaeocystis blooms. J Sea Res 48:97–110

Calafat FM, Chambers DP, Tsimplis MN (2012) Mechanisms of decadal sea level variability in the Eastern North Atlantic and the Mediterranean Sea. J Geophys Res 117 C09022, doi:10.1029/2012JC008285

Cambers G (1976) Temporal scales in coastal erosion systems. Trans Inst British Geographers 1:246–256

Capuzzo E, Painting SJ, Forster RM, Greenwood N, Stephens DT, Mikkelsen OA (2013) Variability in the sub-surface light climate at ecohydrodynamically distinct sites in the North Sea. Biogeochemistry 113:85–103

Carr AP (1979) Sizewell-Dunwich Banks Field Study. Topic Report: 2. Long-term changes in the coastline and offshore banks. Report 89, Institute of Oceanographic Sciences, Taunton

Carter D, Draper L (1988). Has the north-east Atlantic become rougher? Nature 332:494

Chafik L (2012) The response of the circulation in the Faroe-Shetland Channel to the North Atlantic Oscillation. Tellus A 64:18423, doi:10.3402/tellusa.v64i0.18423

Charlier RH (2013) Belgium. In: Pranzini E, Williams A (eds) Coastal Erosion and Protection in Europe. Routledge, Abingdon, pp. 158–172

Chaverot S, Héquette A, Cohen O (2005) Evolution of climatic forcings and potentially eroding events on the coast of Northern France. Proceedings 5th International Conference on Coastal Dynamics, Barcelona, Spain, April 2005, Cd-Rom, 11 p.

Chen C-TA, Wang S-L (1999) Carbon, alkalinity and nutrient budgets on the East China Sea continental shelf. J Geophys Res 104:20675–20686

Christiansen C, Bowman D (1990) Long-term beach and shoreface changes, NW Jutland, Denmark: effects of a change in wind direction. In: Beukema JJ et al. (eds) Expected Effects of Climatic Change on Marine Coastal Ecosystems, pp. 113–122

Church JA, White NJ (2006) A 20th century acceleration in global sea-level rise. Geophys Res Lett 33: L01602, doi:10.1029/2005GL024826

Church JA, White NJ (2011) Sea-level rise from the late 19th to the early 21st Century. Surveys in Geophysics 32:585–602

Church J, Aarup T, Woodworth P, Wilson W, Nicholls R, Rayner R, Lambeck K, Mitchum G, Steffen K, Cazenave A, Blewitt G, Mitrovica J, Lowe J (2010). Sea-level rise and variability: synthesis and outlook for the future. In: Church J, Woodworth P, Aarup T, Wilson S (eds) Understanding Sea-level Rise and Variability. Wiley & Sons

Church JA, Clark PU, Cazenave A, Gregory JM, Jevrejeva S, Levermann A, Merrifield MA, Milne GA, Nerem RS, Nunn PD, Payne AJ, Pfeffer WT, Stammer D, Unnikrishnan AS (2013) Sea level change. In: Climate Change 2013: The Physical Science Basis. Contribution of Working Group I to the Fifth Assessment Report of the Intergovernmental Panel on Climate Change. Stocker TF, Qin D, Plattner G-K, Tignor M, Allen SK, Boschung J, Nauels A, Xia Y, Bex V, Midgley PM (eds.). Cambridge University Press

Clabaut P, Chamley H, Marteel H (2000) Évolution récente des dunes littorales à l'est de Dunkerque (Nord de la France) [Recent coastal dunes evolution, East of Dunkirk, Northern France]. Géomorphologie: relief, processus, environnement 6:125–136

Corten A, van de Kamp G (1996) Variation in the abundance of southern fish species in the southern North Sea in relation to hydrography and climate. ICES J Mar Sci 53:1113–1119

Cox AT, Swail VR (2001) A global wave hindcast over the period 1958–1997: Validation and climate assessment. J Geophys Res 106C:2313–2329

CPSL (2010) Third Report. The role of spatial planning and sediment in coastal risk management. Wadden Sea Ecosystem No. 28. Common Wadden Sea Secretariat, Trilateral Working Group on Coastal Protection and Sea Level Rise (CPSL), Wilhelmshaven, Germany: 1-51

Cunningham S, Marsh R, Wood R, Wallace C, Kuhlbrodt T, Dye S (2010) Atlantic Heat Conveyor (Atlantic Meridional Overturning

Circulation). In MCCIP Annual Report Card 2010-11, MCCIP Science Review, 14 pp, www.mccip.org.uk/arc
Daewel U, Schrum C (2013) Simulating long-term dynamics of the coupled North Sea and Baltic Sea ecosystem with ECOSMO II: Model description and validation. J Mar Sys 119–120:30–49
de Boer GJ, Pietrzak JD, Winterwerp JC (2006) On the vertical structure of the Rhine region of freshwater influence. Ocean Dyn 56:198–216
de Boer GJ, Pietrzak JD, Winterwerp JC (2009) SST observations of upwelling induced by tidal straining in the Rhine ROFI. Cont Shelf Res 29:263–277
de Jong F (2000) Marine Eutrophication in Perspective. On the Relevance of Ecology for Environmental Policy. Springer
de Jonge VN, de Jong DJ (2002) 'Global change' Impact of inter-annual variation in water discharge as a driving factor to dredging and spoil disposal in the river Rhine system and of turbidity in the Wadden Sea. Est Coast Shelf Sci 55:969–991
de Jonge VN, Postma H (1974) Phosphorus compounds in the Dutch Wadden Sea. Netherland J Sea Res 8:139–153
de Jonge VN, van Beusekom JEE (1995) Wind-induced and tide-induced resuspension of sediment and microphytobenthos from tidal flats in the Ems estuary. Limnol Oceanogr 40:766–778
de Jonge VN, Schuttelaars HM, van Beusekom JEE, Talke SA, de Swart HE (2014) The influence of channel deepening on estuarine turbidity levels and dynamics, as exemplified by the Ems estuary. Est Coast Shelf Sci 139:46–59
de Kok JM (1992) A three-dimensional finite difference model for computation of near- and far-field transport of suspended matter near a river mouth. Cont Shelf Res 12:625–642
de Nijs MAJ (2012) On sedimentation processes in a stratified estuarine system. PhD Thesis, Delft University of Technology
de Nijs MAJ, Winterwerp JC, Pietrzak JD (2010) The effects of internal flow structure on sediment entrapment in the Rotterdam Waterway. J Phys Oceanogr 40:2357–2380
de Ruijter WPM, Van der Giessen A, Groenendijk FC (1992) Current and density structure in the Netherlands coastal zone. In: Prandle D (ed) Coast Estuar Studies 40: Dynamics and exchanges in estuaries and the coastal zone. AGU, Washington, USA
De Wolf P (2002) Kusterosie en verzanding van het Zwin. In: Van Lancker V et al. (eds) Colloquium Kustzonebeheer vanuit geo-ecologische en economische invalshoek. Oostende (B), 16–17 May 2002. Genootschap van Gentse Geologen (GGG)- Vlaams lnstituut van de Zee (VLIZ). VLIZ Special Publication 10: Oostende, Belgium
Degrendele K, Roche M, Schotte P, Van Lancker V, Bellec V, Bonne W (2010) Morphological evolution of the Kwinte Bank central depression before and after the cessation of aggregate extraction. J Coast Res SI 51:77–86
Deleu S, Van Lancker V, Van den Eynde D, Moerkerke G (2004) Morphodynamic evolution of the kink of an offshore tidal sandbank: the Westhinder Bank (Southern North Sea). Cont Shelf Res 24:1587–1610
Dette HH, Gärtner J (1987) Erfahrungen mit der Versuchssand-vorspülung vor Hörnum im Jahre 1983. Die Küste 45:209–258
Dickson RR, Meincke J, Malmberg SA, Lee AJ (1988) The "Great Salinity Anomaly" in the northern North Atlantic 1968–1982. Prog Oceanogr 20:103–151
Diesing M, Kubicki A, Winter C, Schwarzer K (2006) Decadal scale stability of sorted bedforms, German Bight, southeastern North Sea. Cont Shelf Res 26:902–916
Dillingh D, Fedor B, de Ronde J (2010) Definitiezeespiegelstijgingvoorbepalingsuppletiebehoefte. Deltares Report 1201993-002, Delft
Dobrynin M, Gayer G, Pleskachevsky A, Günther H (2010) Effect of waves and currents on the dynamics and seasonal variations of suspended particulate matter in the North Sea. J Mar Sys 82:1–20
Dolch T, Hass HC (2008) Long-term changes of intertidal and subtidal sediment composition in a tidal basin in the northern Wadden Sea (SE North Sea). Helgol Mar Res 62:3–11
Dronkers J, Van Alphen JSLJ, Borst JC (1990) Suspended sediment transport processes in the southern North Sea. In: Cheng RT (ed) Residual Currents and Long Term Transport. Springer
Dye SR, Hughes SL, Tinker J, Berry DI, Holliday NP, Kent EC, Kennington K, Inall M, Smyth T, Nolan G, Lyons K, Andres O, Beszczynska-Möller A (2013a) Impacts of climate change on temperature (air and sea). MCCIP Science Review 2013:1–12. doi:10.14465/2013.arc01.001-012
Dye SR, Holliday NP, Hughes SL, Inall M, Kennington K, Smyth T, Tinker J, Andres O, Beszczynska-Möller A (2013b) Climate change impacts on the waters around the UK and Ireland: Salinity. MCCIP Science Review 2013:60–66
Dyer KR, Moffat TJ (1998) Fluxes of suspended matter in the East Anglian plume Southern North Sea. Cont Shelf Res 18:1311–1331
EC (2000) Directive of the European Parliament and of the council 2000/60/EC establishing a framework for community action in the field of water policy, European Union. The European Parliament, The Council, PE-CONS 3639/1/00 REV 1 EN
EEA (2012) Climate Change, Impacts and Vulnerability in Europe 2012. European Environment Agency, Copenhagen
Einsporn S, Broeg K, Koehler A (2005) The Elbe flood 2002 – toxic effects of transported contaminants in flatfish and mussels of the Wadden Sea. Mar Poll Bull 50:423–429
Eisma D (1981) Supply and deposition of suspended matter in the North Sea. In: Nio S-D, Shüttenhelm RTE, Van Weering TJCE (eds), Holocene marine sedimentation in the North Sea basin. Special Publication 5 of the International Association of Sedimentologists. Blackwell Scientific Publishers
Eisma D, Kalf J (1987) Dispersal, concentration and deposition of suspended matter in the North Sea. J Geol Soc London 144:161–178
Eleveld MA, Pasterkamp R, Van der Woerd HJ (2004) A survey of total suspended matter in the southern North Sea based on the 2001 SeaWiFS data. EARSeL eProceedings 3:166–178, www.eproceedings.org
Eleveld MA, Pasterkamp R, van der Woerd HJ, Pietrzak J (2006) Suspended particulate matter from SeaWiFS data: statistical validation, and verification against the physical oceanography of the southern North Sea. Ocean Optics OOXVIII, (9–14 Oct 2006, Montreal)
Eleveld MA, Pasterkamp R, van der Woerd HJ, Pietrzak JD (2008) Remotely sensed seasonality in the spatial distribution of sea-surface suspended particulate matter in the southern North Sea. Estuarine Coast Shelf Sci 80:103–113
Elias EPL, Cleveringa J, Buijsman MC, Roelvink JA, Stive MJF (2006) Field and model data analysis of sand transport patterns in Texel Tidal inlet (the Netherlands). Coast Eng 53:505–529
Ellett DJ, Martin JHA (1973) The physical and chemical oceanography of the Rockall Channel. Deep-Sea Res. 20:585–625
Emeis K-C, van Beusekom J, Callies U, Ebinghaus R, Kannen A, Kraus G, Kröncke I, Lenhart H, Lorkowski I, Matthias V, Möllmann C, Pätsch J, Scharfe M, Thomas H, Weisse R, Zorita E (2015) The North Sea – a shelf sea in the Anthropocene. J Mar Sys 141:18-33
EUROSION (2004) Living with Coastal Erosion in Europe: Sediment and Space for Sustainability. Part II – Maps and Statistics. Online at: www.eurosion.org/reports-online/part2.pdf
Fettweis M, van den Eynde D (2003) The mud deposits and the high turbidity in the Belgian-Dutch coastal zone, southern bight of the North Sea. Cont Shelf Res 23:669–691

Fettweis M, Monbaliu J, Baeye M, Nechad B, van den Eynde D (2012) Weather and climate induced spatial variability of surface suspended particulate matter concentration in the North Sea and the English Channel. Method Oceanogr 3–4:25–39

Flather RA (1987) Estimates of extreme conditions of tide and surge using a numerical model of the north-west European continental shelf. Estuarine, Coast Shelf Sci 24:69–93

Flemming B, Nyandwi N (1994) Land reclamation as a cause of fine-grained sediment depletion in backbarrier tidal flats (southern North Sea). Netherlands J Aquat Ecol 28:299–307

Folland CK, Parker DE (1995) Correction of instrumental biases in historical sea surface temperature data. Quart J Roy Met Soc 121:319–367

French PW (2001) Coastal Defences - Processes, Problems and Solutions. Routledge

Fruergaard M, Andersen TJ, Johannessen PN, Nielsen LH, Pejrup M (2013) Major coastal impact induced by a 1000-year storm event. Scientific Reports 3: no. 1051, doi:10.1038/srep01051

Garcia D, Vigo I, Chao BF, Martinez MC (2007) Vertical crustal motion along the Mediterranean and Black Sea coast derived from ocean altimetry and tide gauge data. Pure Appl Geophys 164:851–863

Gayer G, Dick S, Pleskachevsky A, Rosental W (2004) Modellierung von Schwebstofftransporten in Nordsee und Ostsee. Berichte des BSH 36. BSH, Hamburg

Gayer G, Dick S, Pleskachevsky A, Rosenthal W (2006) Numerical modelling of suspended matter transport in the North Sea Ocean Dyn 56:62–77

Gehrels WR, Woodworth PL (2013) When did modern rates of sea-level rise start? Global and Plan Change 100:263–277

Gerritsen H (2005) What happened in 1953? The big flood in the Netherlands in retrospect. Phil Trans R Soc A 363:1271–1291

Giardino A, Van den Eynde D, Monbaliu J (2010) Wave effects on the morphodynamic evolution of an offshore sand bank. J Coast Res 51:127–140

Greenwood N, Parker ER, Fernand L, Sivyer DB, Weston K, Painting SJ, Kröger S, Forster RM, Lees HE, Mills DK, Laane RWPM (2010) Detection of low bottom water oxygen concentrations in the North Sea; implications for monitoring and assessment of ecosystem health. Biogeosciences 7:1357–1373

Gypens N, Borges AV, Lancelot C (2009) Effect of eutrophication on air-sea CO_2 fluxes in the coastal Southern North Sea: a model study of the past 50 years. Glob Change Biol 15:1040–1056

Haekkinen S, Rhines PB, Worthen DL (2011). Warm and saline events embedded in the meridional circulation of the northern North Atlantic. J Geophys Res 116: C03006, doi:10.1029/2010JC006275

Haigh ID, Nicholls RJ, Wells NC (2009) Mean sea-level trends around the English Channel over the 20th century and their wider context. Cont Shelf Res 29:2083–2098

Hátún H, Sando A, Drange H, Bentsen M (2005) Seasonal to decadal temperature variations in the Faroe–Shetland inflow waters. In: Drange H, Dokken T, Furevik T, Gerdes R, Berger W (eds) The Nordic Seas: an Integrated Perspective: Oceanography, Climatology, Biogeochemistry, and Modeling. American Geophysical Union, pp. 239–250

Heaps NS (1972) Estimation of density currents in Liverpool Bay. Geophys J Roy Astron Soc 30:415–432

Henriksen P (2009) Long-term changes in phytoplankton in the Kattegat, the Belt Sea, the Sound and the western Baltic Sea. J Sea Res 61:114–123

Heyen H, Dippner JW (1998) Salinity variability in the German Bight in relation to climate variability. Tellus 50A:545–556

Hill AE, James ID, Linden PF, Matthews JP, Prandle D, Simpson JH, Gmitrowicz EM, Smeed DA, Lwiza KMM, Durazo R, Fox AD, Bowers DG (1993) Dynamics of tidal mixing fronts in the North Sea. Phil Trans Roy Soc London A 343:431–446

Hill AE, Brown J, Fernand L, Holt J, Horsburgh KJ, Proctor R, Raine R, Turrell WR (2008) Thermohaline circulation of shallow tidal seas. Geophys Res Lett 35:L11605, doi:10.1029/2008GL033459

Hjøllo SS, Skogen MD, Svendsen E (2009) Exploring currents and heat within the North Sea using a numerical model. J Mar Sys 78:180–192

Hogben N (1994) Increases in wave heights over the North Atlantic: a review of the evidence and some implications for the naval architect. Trans Roy Inst Naval Arch W5:93–101.

Hollebrandse FAP (2005) Temporal development of the tidal range in the Southern North Sea. Ph.D. Thesis, Delft University of Technology, Netherlands

Holliday NP (2003) Air-sea interaction and circulation changes in the northeast Atlantic. J Geophys Res 108:C3259, doi:10.1029/2002JC001344

Holliday NP, Cunningham SA (2013) The Extended Ellett Line: Discoveries from 65 years of marine observations west of the UK. Oceanography 26:156–163

Holliday NP, Hughes SL, Bacon S, Beszczynska-Möller A, Hansen B, Lavín A, Loeng H, Mork KA, Østerhus S, Sherwin T, Walczowski W (2008) Reversal of the 1960s – 1990s freshening trend in the North Atlantic and Nordic Seas. Geophys Res Lett 35: L03614, doi:10.1029/2007GL032675

Holliday NP, Hughes SL, Beszczynska-Möller A (eds) (2009) ICES Report on Ocean Climate 2008. ICES Coop Res Rep 298

Holliday NP, Hughes SL, Dye S, Inall M, Read J, Shammon T, Sherwin T, Smyth T (2010) Salinity. In: MCCIP Annual Report Card 2010-11, MCCIP Science Review, www.mccip.org.uk/arc

Holliday NP, Hughes SL, Borenäs K, Feistel R, Gaillard F, Lavìn A, Loeng H, Mork KA, Nolan G, Quante M, Somavilla R (2011) Long-term physical variability in the North Atlantic Ocean. In: Reid PC, Valdés L (eds) ICES Status Report on Climate Change in the North Atlantic. ICES Coop Res Rep 310: 21–46.

Holt JT, James ID (1999) A simulation of the southern North Sea in comparison with measurements from the North Sea Project Part 2, Suspended Particulate Matter. Cont Shelf Res 19:1617–1642

Holt J, Proctor R (2008) The seasonal circulation and volume transport on the northwest European continental shelf: a fine-resolution model study. J Geophys Res 113:C06021, doi:10.1029/2006JC004034

Holt JT, Allen JI, Proctor R, Gilbert F (2005) Error quantification of a high resolution coupled hydrodynamic–ecosystem coastal–ocean model: part 1 model overview and assessment of the hydrodynamics. J Mar Sys 57:167–188

Holt J, Wakelin SL, Huthnance JM (2009) The down-welling circulation of the northwest European continental shelf: a driving mechanism for the continental shelf carbon pump. Geophys Res Lett 36:L14602, doi:10.1029/2009GL038997

Holt J, Hughes S, Hopkins J, Wakelin SL, Holliday NP, Dye S, González-Pola C, Hjøllo SS, Mork KA, Nolan G, Proctor R, Read J, Shammon T, Sherwin T, Smyth T, Tattersall G, Ward B, Wiltshire K (2012) Multi-decadal variability and trends in the temperature of the northwest European continental shelf: A model-data synthesis. Prog Oceanogr 106:96–117

Hordoir R, Meier HEM (2010) Freshwater fluxes in the Baltic Sea: A model study. J Geophys Res 115:C08028, doi:10.1029/2009JC005604

Hordoir R, Dieterich C, Basu C, Dietze H, Meier HEM (2013) Freshwater outflow of the Baltic Sea and transport in the Norwegian Current: A statistical correlation analysis based on a numerical experiment. Cont Shelf Res 64:1–9

Horrillo-Caraballo JM, Reeve DE (2008) Morphodynamic behaviour of a nearshore sandbank system: The Great Yarmouth Sandbanks, UK. Mar Geol 254:91–106
Horsburgh K, Wilson C (2007) Tide-surge interaction and its role in the distribution of surge residuals in the North Sea. J Geophys Res 112: C08003, doi:10.1029/2006JC004033
Howarth MJ, Dyer KR, Joint IR, Hydes DJ, Purdie DA, Edmunds H, Jones JE, Lowry RK, Moffat TJ, Pomroy AJ, Proctor R (1993) Seasonal cycles and their spatial variability. Phil Trans Roy Soc Lond A 343:383–403
Hughes SL, Holliday NP, Beszczynska-Möller A (eds) (2011) ICES Report on Ocean Climate 2010. ICES Coop Res Rep 309
Hughes SL, Holliday NP, Gaillard F, ICES Working Group on Oceanic Hydrography (2012) Variability in the ICES/NAFO region between 1950 and 2009: observations from the ICES Report on Ocean Climate. ICES J Mar Sci 69:706–719
Hurrell JW (1995) Decadal trends in the North Atlantic Oscillation: Regional temperatures and precipitation. Science 269:676–679
Hurrell JW, National Center for Atmospheric Research Staff (eds) (2013) The Climate Data Guide: Hurrell North Atlantic Oscillation (NAO) Index (station-based). https://climatedataguide.ucar.edu/climate-data/hurrell-north-atlantic-oscillation-nao-index-station-based
Huthnance JM, Holt JT, Wakelin SL (2009) Deep ocean exchange with west-European shelf seas. Ocean Sci 5:621–634
Irion G, Zöllmer V (1999) Clay mineral associations in fine-grained surface sediments of the North Sea. J Sea Res 41:119–128
Ivchenko V, Wells N, Aleynik D, Shaw A (2010) Variability of heat and salinity content in the North Atlantic in the last decade. Ocean Sci 6:719–735
Iversen SA, Skogen MD, Svendsen E (2002) Availability of horse mackerel (*Trachurus trachurus*) in the north-eastern North Sea, predicted by the transport of Atlantic water. Fish Oceanogr 11:245–250
Jago CF, Bale AJ, Green MO, Howarth MJ, Jones SE, McCave IN, Millward GE, Morris AW, Rowden AA, Williams JJ, Hydes D, Turner A, Huntley D, Van Leussen W (1993) Resuspension processes and seston dynamics, southern North Sea [and discussion]. Phil Trans Roy Soc London A 343:475–491
Janssen F (2002) Statistische Analyse mehrjähriger Variabilität der Hydrographie in Nord- und Ostsee. Dissertation Fachbereich Geowissenschaften, Universität Hamburg, Germany
Jensen J, Hofstede J, Kunz H, De Ronde J, Heinen P, Siefert W (1993) Long-term water level observations and variations. Coastal Zone '93, Coastlines of the Southern North Sea
Jevrejeva S, Grinsted A, Moore JC, Holgate S (2006) Nonlinear trends and multiyear cycles in sea level records. J Geophys Res 111: C09012, doi.org/10.1029/2005JC003229
Jevrejeva S, Moore JC, Grinsted A, Woodworth PL (2008) Recent global sea level acceleration started over 200 years ago? Geophys Res Lett 35:L08715, doi:10.1029/2008GL033611
Johnson GC, Gruber N (2007) Decadal water mass variations along 20 degrees W in the Northeastern Atlantic Ocean. Prog Oceanogr 73:277–295
Jones SE, Jago CF, Simpson JH (1996) Modelling suspended sediment dynamics in tidally stirred and periodically stratified waters: Progress and pitfalls. In: Pattiaratchi C (ed), Mixing in Estuaries and Coastal Seas, AGU, Coast Estuar Studies 50
Joordens JCA, Souza AJ, Visser AW (2001) The Influence of tidal straining and wind on suspended matter and phytoplankton dynamics in the Rhine outflow region. Cont Shelf Res 21:301–325
Karlson K, Rosenberg R, Bonsdorff E (2002) Temporal and spatial large-scale effects of eutrophication and oxygen deficiency on benthic fauna in Scandinavian and Baltic waters – a review. Oceanogr Mar Biol 40:427–489
Kauker F (1999) Regionalization of climate model results for the North Sea. Ph.D. Thesis, Universität Hamburg, Germany
Kauker F, von Storch H (2000) Statistics of "synoptic circulation weather" in the North Sea as derived from a multiannual OGCM simulation. J Phys Oceanogr 30:3039–3049
Kelletat D (1992) Coastal erosion and protection measures at the German North Sea coast. J Coast Res 8:699–711
Kennedy JJ, Rayner NA, Smith RO, Saunby M, Parker DE (2011a) Reassessing biases and other uncertainties in sea-surface temperature observations since 1850 part 1: measurement and sampling errors. J Geophys Res 116:D14103, doi:10.1029/2010JD015218
Kennedy JJ, Rayner NA, Smith RO, Saunby M, Parker DE (2011b) Reassessing biases and other uncertainties in sea-surface temperature observations since 1850, part 2: biases and homogenisation. J Geophys Res 116:D14104, doi:10.1029/2010JD015220
Kent EC, Taylor PK, Truscott BS, Hopkins JS (1993) The accuracy of voluntary observing ship's meteorological observations – Results of the VSOP-NA. J Atmos Oceanic Tech 10:591–608
Kent EC, Kennedy JJ, Berry DI, Smith RO (2010) Effects of instrumentation changes on ocean surface temperature measured in situ. Climate Change 1:718–728
Kirby RR, Beaugrand G, Lindley JA, Richardson AJ, Edwards M, Reid PC (2007) Climate effects and benthic-pelagic coupling in the North Sea. Mar Ecol-Prog Ser 330:31–38
Knaapen MAF (2009) Sandbank occurrence on the Dutch continental shelf in the North Sea. Geo-Mar Lett 29:17–24
Kodra E, Steinhaeuser K, Ganguly AR (2011) Persisting cold extremes under 21st-century warming scenarios. Geophys Res Lett 38: L08705, doi:10.1029/2011GL047103
Koslowski G (1989) Die flächenbezogene Eisvolumensumme, eine neue Maßzahl für die Bewertung des Eiswinters an der Ostseeküste Schleswig-Holsteins und ihr Zusammenhang mit dem meteorologischen Charakter des meteorologischen Winters. Dt Hydrogr Z 42:61–80
Kühn W, Pätsch J, Thomas H, Borges AV, Schiettecatte L-S, Bozec Y, Prowe F (2010) Nitrogen and carbon cycling in the North Sea and exchange with the North Atlantic - a model study Part II. Carbon budget and fluxes. Cont Shelf Res 30:1701–1716
Kushnir Y, Cardone VJ, Greenwood JG, Cane MA (1997) The recent increase in North Atlantic wave heights. J. Climate 10:2107–2113
Kystdirektoratet (2008) Vestkysten 2008. Kystdirektoratet, Lemvig
Lacroix G, Ruddick K, Ozer J, Lancelot C (2004) Modelling the impact of the Scheldt and Rhine/Meuse plumes on the salinity distribution in Belgian waters (southern North Sea). J Sea Res 52:149–163
Lancelot C, Thieu V, Polard A., Garnier J, Billen G, Hecq W, Gypens N (2011) Ecological and economic effectiveness of nutrient reduction policies on coastal *Phaeocystis* colony blooms in the Southern North Sea: an integrated modeling approach. Sci Tot Env 409:2179–2191
Langenberg H, Pfizenmayer A, von Storch H, Sündermann J (1999) Storm-related sea level variations along the North Sea coast: natural variability and anthropogenic change. Cont Shelf Res 19:821–842
Latif M, Böning C, Willebrand J, Biastoch A, Dengg J, Keenlyside N, Schweckendiek U, Madec G (2006) Is the thermohaline circulation changing? J Climate 19:4631–4637
Lee AJ (1980) North Sea: Physical oceanography. In: Banner FT, Collins MB, Massie KS (eds) The North-West European Shelf Seas: The seabed and the sea in motion. 2. Physical and chemical oceanography, and physical resources. Elsevier Oceanography Series, 24B, pp. 467–493
Lenhart H-J, Mills DK, Baretta-Bekker H, van Leeuwen SM, van der Molen J, Baretta JW, Blaas M, Desmit X, Kűhn W, Lacroix G, Los HJ, Ménesguen A, neves R, Proctor R, Ruardij P, Skogen MD, Vanhoutte-Brunier A, Villars MT, Wakelin S (2010) Predicting the

consequences of nutrient reduction on the eutrophication status of the North Sea. J Mar Sys 81:148–170
Leterme SC, Pingree RD, Skogen MD, Seuront L, Reid PC, Attrill MJ (2008) Decadal fluctuations in North Atlantic water inflow in the North Sea 1958–2003: impacts on temperature and phytoplankton populations. Oceanologia 50:59–72
Liu KK, Atkinson L, Quinones R, Talaue-McManus L (eds) (2010) Carbon and Nutrient Fluxes in Continental Margins. Springer
Loebl, M., Dolch T, van Beusekom JEE (2007) Annual dynamics of pelagic primary production and respiration in a shallow coastal basin. J Sea Res 58:269–282
Loebl M, Colijn F, Beusekom JEE, Baretta-Bekker JG, Lancelot C, Philippart CJM, Rousseau V (2009) Recent patterns in potential phytoplankton limitation along the NW European continental coast. J Sea Res 61:34–43
Loewe P (ed) (2009) System Nordsee – Zustand 2005 im Kontext langzeitlicher Entwicklungen. Report 44, Bundesamt für Seeschiff-fahrt und Hydrographie, Hamburg and Rostock
Longuet-Higgins M, Stewart R (1962) Radiation stress and mass transport in gravity waves, with application to 'surf beats'. J Fluid Mech 13:481–503
Lorkowski I, Pätsch J, Moll A, Kühn W (2012) Interannual variability of carbon fluxes in the North Sea from 1970 to 2006 – Competing effects of abiotic and biotic drivers on the gas-exchange of CO_2. Estuar Coast Shelf Sci 100:38–57
Lotze HK, Reise K, Worm B, van Beusekom JEE, Busch M, Ehlers A, Heinrich D, Hoffmann RC, Holm P, Jensen C, Knottnerus OS, Langjanki N, Prummel W, Vollmer M, Wolff WJ (2005) Human transformation of the Wadden Sea ecosystem through time: a synthesis. Helgol Mar Res 59:84–95
Lozier MS, Stewart NM (2008) On the temporally varying northward penetration of Mediterranean Overflow Water and eastward penetration of Labrador Sea Water. J Phys Oceanogr 38:2097–2103
Madec G (2008) NEMO reference manual, ocean dynamics component, Institut Pierre-Simon Laplace, technical report
Madsen KS (2009) Recent and future climatic changes in temperature, salinity, and sea level of the North Sea and the Baltic Sea. PhD Thesis, Niels Bohr Institute, University of Copenhagen
Martens P, van Beusekom JEE (2008) Zooplankton response to a warmer northern Wadden Sea. Helg Mar Res 62:67–75
Mathis M, Elizalde A, Mikolajewicz U, Pohlmann T (2015) Variability patterns of the general circulation and sea water temperature in the North Sea. Prog Oceanogr 135:91–112
McCandliss RR, Jones SE, Hearn M, Latter R, Jago CF (2002) Dynamics of suspended particles in coastal waters (southern North Sea) during a spring bloom. J Sea Res 47:285–302
McCarthy G, Frajka-Williams E, Johns WE, Baringer MO, Meinen CS, Bryden HL, Rayner D, Duchez A, Roberts C, Cunningham SA (2012) Observed interannual variability of the Atlantic meridional overturning circulation at 26.5 degrees N. Geophys Res Lett 39: L19609, doi:10.1029/2012GL052933
McCave IN (1987) Fine sediment sources and sinks around the East Anglian Coast. J Geol Soc London 144:149–152
McQuatters-Gollop A, Raitsos DE, Edwards M, Pradhan Y, Mee LD, Lavender SJ, Attrill MJ (2007) A long-term chlorophyll data set reveals regime shift in North Sea phytoplankton biomass unconnected to nutrient trends. Limnol Oceanogr 52:635–648
Meesenburg H (1996) Man's role in changing the coastal landscapes in Denmark. GeoJournal 39:143–151
Meire L, Soetaert KER, Meysman FJR (2013) Impact of global change on coastal oxygen dynamics and risk of hypoxia. Biogeosciences 10:2633–2653
Merrifield M, Merrifield S, Mitchum G (2009) An anomalous recent acceleration of global sea level rise. J Clim 22:5772–5781
Meyer EMI, Pohlmann T, Weisse R (2011) Thermodynamic variability and change in the North Sea (1948–2007) derived from a multidecadal hindcast. J Mar Sys 86:35–44
Miller L, Douglas BC (2007) Gyre-scale atmospheric pressure variations and their relation to 19th and 20th century sea level rise. Geophys Res Lett 34:L16602, http://dx.doi.org/10.1029/2007GL030862
Milne GA, Gehrels WR, Hughes CW, Tamisiea ME (2009) Identifying the causes of sea-level change. Nat Geosci 2:471–478
Mork KA, Skagseth Ø (2010) A quantitative description of the Norwegian Atlantic Current by combining altimetry and hydrography. Ocean Sci 6:901–911
Mroczek P (1980) Zu einer Karte der Veränderungen der Uferlinie der deutschen Nordseeküste in den letzten 100 Jahren im Maßstab 1:200.000
Mudersbach C, Wahl T, Haigh I, Jensen J (2013) Trends in high sea levels of German North Sea gauges compared to regional mean sea level changes. Cont Shelf Res, 65:111–120
Müller M (2012) The influence of changing stratification conditions on barotropic tidal transport and its implications for seasonal and secular changes of tides. Cont Shelf Res 47:107–118
MyOcean (2014) Atlantic-European North West Shelf – Ocean Physics Reanalysis from Met Office (1985-2012). http://www.myocean.eu/web/69-myocean-interactive-catalogue.php?option=com_csw&view=details&product_id=NORTHWESTSHELF_REANALYSIS_PHYS_004_009
Nedwell DB, Parkes RJ, Upton AC, Assinder DJ (1993) Seasonal fluxes across the sediment-water interface, and processes within sediments. Phil Trans Roy Soc London A 343:519–529
Nerem RS, Mitchum GT (2002) Estimates of vertical crustal motion derived from differences of TOPEX/POSEIDON and tide gauge sea level measurements. Geophys Res Lett 29: http://dx.doi.org/10.1029/2002GL015037
Neu H (1984) Interannual variations and longer-term changes in the sea state of the North Atlantic. J Geophys Res 89:6397–6402
NOOS (2010) NOOS Activity: Exchange of computed water, salt and heat transport across selected transects. North West European Shelf Operational Oceanographic System (NOOS). www.noos.cc/fileadmin/user_upload/exch_transports_NOOS-BOOS_2010-11-11.pdf
Omar AM, Olsen A, Johannessen T, Hoppema M, Thomas H, Borges AV (2010) Spatio-temporal variations of fCO_2 in the North Sea. Ocean Sci 6:77–89
Oost AP (1995) Dynamics and sedimentary development of the Dutch Wadden Sea with emphasis on the Frisian Inlet; a study of the barrier islands, ebb-tidal deltas and drainage basins. Thesis, Utrecht, Geologica Ultraiectina, 126
Oost AP, Hoekstra P, Wiersma A, Flemming B, Lammerts EJ, Pejrup M, Hofstede J, van der Valk B, Kiden P, Bartholdy J, van der Berg MW, Vos PC, de Vries S, Wang ZB (2012) Barrier island management: Lessons from the past and directions for the future. Ocean Coast Manage 68:18–38
Orvik KA, Skagseth Ø (2005) Heat flux variations in the eastern Norwegian Atlantic Current toward the Arctic from moored instruments, 1995–2005. Geophys Res Lett 32:L14610, doi:10.1029/2005GL023487
Otto L, Zimmerman JTF, Furnes GK, Mork M, Saetre R, Becker G (1990) Review of the physical oceanography of the North Sea. Netherlands J Sea Res 26:161–238
Paphitis D, Bastos AC, Evans G, Collins MB (2010) The English Channel (La Manche): evolution, oceanography and sediment dynamics – a synthesis. In: Whittaker JE, Hart MB (eds) Micropalaeontology, Sedimentary Environments and Stratigraphy: a tribute to Dennis Curry (1921–2001). pp. 99–132

Pätsch J, Kühn W (2008) Nitrogen and carbon cycling in the North Sea and exchange with the North Atlantic – a model study. Part I. Nitrogen budget and fluxes. Cont Shelf Res 28:767–787
Pawlowicz R, McDougall T, Feistel R, Tailleux R (2012) Preface: An historical perspective on the development of the Thermodynamic Equation of Seawater – 2010. Ocean Sci 8:161–174
Peltier WR (2004) Global glacial isostasy and the surface of the ice-age earth: The ICE-5G(VM2) model and GRACE. Ann Rev Earth Planet Sci 32:111–149
Philippart CJM, Beukema JJ, Cadée GC, Dekker R, Goedhart PW, van Iperen JM, Leopold MF, Herman PNJ (2007) Impact of nutrient reduction on coastal communities. Ecosystems 10:96–119
Pickering M, Wells N, Horsburgh K, Green J (2011) The impact of future sea-level rise on the European Shelf tides. Cont Shelf Res 35:1–15
Pietrzak JD, de Boer GJ, Eleveld M (2011) Mechanisms controlling the intra-annual mesoscale variability of SST and SPM in the southern North Sea. Cont Shelf Res 31:594–610
Pleskachevsky A, Gayer G, Horstmann J, Rosenthal W (2005) Synergy of satellite remote sensing and numerical modeling for monitoring of suspended particulate matter. Ocean Dyn 55:2–9
Pohlmann T (2006) A meso-scale model of the central and southern North Sea: consequences of an improved resolution. Cont Shelf Res 26:2367–2385
Port A, Gurgel K-W, Stanev J, Schulz-Stellenfleth J, Stanev EV (2011) Tidal and wind-driven surface currents in the German Bight: HFR observations versus model simulations. Ocean Dyn 61:1567–1585
Postma H (1954) Hydrography of the Dutch Wadden Sea. Archives néerlandaises de Zoologie 10:405–511
Postma H (1966) The cycle of nitrogen in the Wadden Sea and adjacent areas. Netherlands J Sea Res 3:186–221
Postma H (1981) Exchange of materials between the North Sea and the Wadden Sea. Mar Geol 40:199–215
Postma H (1984) Introduction to the symposium on organic matter in the Wadden Sea. Neth Inst S 10:15–22
Poulton CVL, Lee JR, Jones LD, Hobbs PRN, Hall M (2006) Preliminary investigation into monitoring coastal erosion using terrestrial laser scanning: case study at Happisburgh, Norfolk, UK. Bull Geol Soc Norfolk 56:45–65
Prandle D (1978a) Monthly-mean residual flows through Dover Strait, 1949–1972. J Mar Biol Assoc UK 58:965–973
Prandle D (1978b) Residual flows and elevations in the Southern North Sea. Proc Roy Soc Lond A 259:189–228
Prandle D, Player R (1993) Residual current through the Dover Strait measured by HF radar. Estuar Coast Shelf Sci 37:635–653
Prandle D, Loch SG, Player RJ (1993) Tidal flow through the Straits of Dover. J Phys Oceanogr 23:23–37
Prandle D, Ballard G, Flatt D, Harrison AJ, Jones SE, Knight PJ, Loch S, McManus J, Player R, Tappin A (1996) Combining modelling and monitoring to determine fluxes of water, dissolved and particulate metals through the Dover Strait. Cont Shelf Res 16:237–257
Prowe F, Thomas H, Pätsch J, Kühn W, Bozec Y, Schiettecatte L-S, Borges AV, de Baar HJW (2009) Mechanisms controlling the air–sea CO_2 flux in the North Sea. Cont Shelf Res 29:1801–1808
Pugh D (2004) Changing Sea Levels: Effects of Tides, Weather and Climate. Cambridge University Press
Puls W, Sündermann J (1990) Simulation of suspended sediment dispersion in the North Sea. Coast Estuar Studies 38:356–372
Puls W, Pohlmann T, Sündermann J (1997) Suspended particulate matter in the southern North Sea: application of a numerical model to extend NERC North Sea project data interpretation. Deutsche Hydrografische Zeitschrift 49:307–327
Pye K, Saye SE, Blott SJ (2007) Sand Dune Processes and Management for Flood and Coastal Defence. Part 2. Sand Dune Processes and Morphology. Joint Defra/Environment Agency Flood and Coastal Erosion Risk Management R & D Programme, R & D Technical report FD1302/TR
Queste BY, Fernand L, Jickells TD, Heywood KJ (2013) Spatial extent and historical context of North Sea oxygen depletion in August 2010. Biogeochemistry 113:53–68
Rayner NA, Parker DE, Horton EB, Folland CK, Alexander LV, Rowell DP, Kent EC, Kaplan A (2003) Global analyses of sea surface temperature, sea ice, and night marine air temperature since the late nineteenth century. J Geophys Res 108(D14):4407, doi:10.1029/2002JD002670
Reise K (2005) Coast of change: habitat loss and transformations in the Wadden Sea. Helgoland Mar Res 59:9–21
Reise K (2013) A Natural History of the Wadden Sea. Riddled by Contingencies. Wadden Academy, Leeuwarden, NL
Reise K, Kohlus J (2008) Seagrass recovery in the Northern Wadden Sea? Helgoland Mar Res 62:77–84
Reise K, van Beusekom JEE (2008) Interactive effects of global and regional change on a coastal ecosystem. Helgoland Mar Res 62:85–91
Reise K, Baptist M. Burbridge P, Dankers NMJA, Fischer L, Flemming BW, Oost AP, Smit C (2010) The Wadden Sea – A Universally Outstanding Tidal Wetland. Wadden Sea Ecosystem 29:7–24
Reynaud JY, Tessier B, Auffret JP, Berné S, de Baptist M, Marsset T, Walker P (2003) The offshore Quaternary sediment bodies of the English Channel and its Western Approaches. J Quat Sci 18:361–371
Richter K, Nilsen JEØ, Drange H (2012) Contributions to sea level variability along the Norwegian coast for 1960–2010. J Geophys Res 117:C05038, http://dx.doi.org/10.1029/2011JC007826
Robinson IS (1976) Theoretical analysis of use of submarine cables as electromagnetic oceanographic flowmeters. Phil Trans Roy Soc Lond A 280:355–396
Roos PC, Hulscher SJMH, Knaapen MAF, Van Damme RM (2004) The cross-sectional shape of tidal sandbanks: Modeling and observations. J Geophys Res 109:F02003, doi:10.1029/2003JF000070
Rosenhagen G, Schatzmann M (2011) Das Klima der Metropolregion auf Grundlage meteorologischer Messungen und Beobachtungen. In: von Storch H, Claussen M (eds) Klimabericht für die Metropolregion Hamburg. Springer
Ruz MH, Meur-Férec C (2004) Influence of high water levels on aeolian sand transport: upper-beach/dune evolution on a macrotidal coast, Wissant Bay, Northern France. Geomorphology 60:73–87
Rydell B, Angerud P, Hågeryd A-C (2004) Omfattning av stranderosion i Sverige Översiktlig kartläggning av erosionsförhållanden: Metodik och redovisning. Varia 543, Statens Geotekniska Institut, Linköping
Salman A, Lombardo S, Doody P (2004) Living with coastal erosion in Europe: Sediment and Space for Sustainability. EUROSION.
Salt L, Thomas H, Prowe AEF, Borges AV, De Baar HJW (2013) Variability of North Sea pH and CO_2 in response to North Atlantic Oscillation forcing. J Geophys Res (Biogeosciences) 118:1584–1592
Schiettecatte L-S, Gazeau F, Van der Zee C, Brion N, Borges AV (2006) Time series of the partial pressure of carbon dioxide (2001–2004) and preliminary inorganic carbon budget in the Scheldt plume (Belgian coast waters). Geochem Geophy Geosy 7:Q06009. doi:10.1029/2005GC001161
Schiettecatte L-S, Thomas H, Bozec Y, Borges AV (2007) High temporal coverage of carbon dioxide measurements in the Southern Bight of the North Sea. Mar Chem 106:161–173
Schmelzer N, Holfort J (eds) (2012) Climatological Ice Atlas for the western and southern Baltic Sea (1961–2010). BSH Hamburg und Rostock

Schrum C, Sigismund F (2001) Modellkonfiguration des Nordsee/Ostsee-Modells. 40-Jahres NCEP Integration. Ber Zent Meeres- Klimaforsch Univ Hamburg B(4)
Sharples J, Ross ON, Scott BE, Greenstreet SPR, Fraser H (2006) Inter-annual variability in the timing of stratification and the spring bloom in the North-western North Sea. Cont Shelf Res 26:733–751
Sharples J, Holt J, Dye S (2010) Shelf sea stratification. In: MCCIP Annual Report Card 2010-11, MCCIP Science Review, www.mccip.org.uk/arc
Shennan I, Woodworth PL (1992) A comparison of late Holocene and twentieth century sea level trends from the UK and North Sea region. Geophys J Int 109:96–105
Shennan I, Milne G, Bradley S (2012) Late Holocene vertical land motion and relative sea-level changes: lessons from the British Isles. J Quart Sci 27:64–70
Sherwin TJ, Read JF, Holliday NP, Johnson C (2012) The impact of changes in North Atlantic Gyre distribution on water mass characteristics in the Rockall Trough. ICES J Mar Sci 69:751–757
Simpson JH, Hunter JR (1974) Fronts in the Irish Sea. Nature 250: 404–406
Simpson JH, Bos WG, Schirmer F, Souza AJ, Rippeth TP, Jones SE, Hydes D (1993) Periodic stratification in the Rhine ROFI in the North Sea. Oceanol Acta 16:23–32
Smeed DA, McCarthy GD, Cunningham SA, Frajka-Williams E, Rayner D, Johns WE, Meinen CS, Baringer MO, Moat BI, Duchez A, Bryden HL (2014) Observed decline of the Atlantic meridional overturning circulation 2004–2012. Ocean Sci 10:29–38
Smith TM, Reynolds RW (2002) Bias corrections for historical sea surface temperatures based on marine air temperatures. J Climate 15:73–87
Smyth TJ, Fishwick JR, Al-Moosawi L, Cummings DG, Harris C, Kitidis V, rees A, Martinez-Vicente V, Woodward EMS (2010) A broad spatio-temporal view of the Western English Channel observatory. J Plankton Res 32:585–601
Son CS, Flemming BV, Bartholomae A, Chun SS (2012) Long-term changes in morphology and textural sediment characteristics in response to energy variation on shoreface-connected ridges off the East Frisian barrier-island coast, southern North Sea. J Sed Res 82:385–399
Sørensen P (2013) Denmark. In: Pranzini E, Williams A (eds) Coastal erosion and protection in Europe. Routledge
Southward AJ (1960) On changes of sea temperature in the English Channel. J Mar Biol Assoc UK 42:275–375
Souza AJ (2013) On the use of the Stokes number to explain frictional tidal dynamics and water column structure in shelf seas. Ocean Sci 9:391–398
Souza A, Holt J, Proctor R (2007) Modelling SPM on the NW European Shelf Seas. In: Balson PS, Collins MB (eds) Coastal and Shelf Sediment Transport. Geol Soc London, Spec Publ 274:147–158
Staats N, de Deckere EMGT, de Winder B, Stal LJ (2001) Spatial patterns of benthic diatoms, carbohydrates and mud on a tidal flat in the Ems-Dollard estuary. Hydrobiologia 448:107–115
Sterl A, Caires S (2005) Climatology, variability and extrema of ocean waves. The web-based KNMI/ERA-40 Wave Atlas. Int J Climatol 25:963–977
KNMI/ERA-40 Wave Atlas. Int J Climatol 25:963–977
Sturges W, Douglas BC (2011) Wind effects on estimates of sea level rise. J Geophys Res 116:C06008, http://dx.doi.org/10.1029/2010JC006492
Suijlen JM, Duin RNM (2001) Variability of near-surface total suspended-matter concentrations in the Dutch coastal zone of the North Sea: Climatological study on the suspended matter concentrations in the North Sea. Report RIKZ/OS/2001.150X. RIKZ, The Hague, Netherlands
Suijlen JM, Duin RNM (2002) Atlas of near-surface total suspended matter concentrations in the Dutch coastal zone of the North Sea. Report RIKZ/2002.059. RIKZ, The Hague, Netherlands
Sundby S, Drinkwater K (2007). On the mechanisms behind salinity anomaly signals of the northern North Atlantic. Progr Oceanogr 73:190–202
Sündermann J (1993) Suspended particulate matter in the North Sea: Field observations and model simulations. Phil Trans Roy Soc Lond A 343:423–430
Thiel M, Hinojosa IA, Joschko T, Gutow L (2011) Spatio-temporal distribution of floating objects in the German Bight (North Sea). J Sea Res 65:368–379
Thomalla F, Vincent CE (2003) Beach response to shore-parallel breakwaters at Sea Palling, Norfolk, UK. Estuar, Coast Shelf Sci 56:203–212
Thomas H, Bozec Y, Elkalay K, deBaar HJW (2004) Enhanced open ocean storage of CO_2 from shelf sea pumping. Science 304:1005–1008
Thomas H, Bozec Y, Elkalay K, deBaar HJW, Borges AV, Schiettecatte L-S (2005a) Controls of the surface water partial pressure of CO_2 in the North Sea. Biogeosciences 2:323–334
Thomas H, Bozec Y, de Baar HJW, Elkalay K, Frankignoulle M, Schiettecatte L-S, Kattner G, Borges AV (2005b) The carbon budget of the North Sea. Biogeosciences 2:87–96
Thomas H, Prowe F, van Heuven S, Bozec Y, deBaar HJW, Schiettecatte L-S, Suykens K, Koné K, Borges AV, Lima ID, Doney SC (2007) Rapid decline of the CO_2 buffering capacity in the North Sea and implications for the North Atlantic Ocean. Global Biogeochem Cy 21:GB4001, doi:10.1029/2006GB002825
Thomas H, Prowe F, Lima ID, Doney SC, Wanninkhof R, Greatbatch RJ, Corbière A, Schuster U (2008) Changes in the North Atlantic Oscillation influence CO_2 uptake in the North Atlantic over the past 2 decades. Global Biogeochem Cy 22: doi:10.1029/2007GB003167
Thomas H, Schiettecatte L-S, Suykens K, Koné YJM, Shadwick EH, Prowe F, Bozec Y, de Baar HJW, Borges AV (2009) Enhanced ocean carbon storage from anaerobic alkalinity generation in coastal sediments. Biogeosciences 6:267–274
Thyme F (1990) Beach nourishment on the west coast of Jutland. J Coast Res 6:201–210
Tsimplis MN, Shaw AGP, Flather RA, Woolf DK (2006) The influence of the North Atlantic Oscillation on the sea-level around the northern European coasts reconsidered: the thermosteric effects. Phil Trans Roy Soc London A 364:845–856
Turrell WR, Henderson EW, Slesser G, Payne R, Adams RD (1992) Seasonal changes in the circulation of the northern North Sea. Cont Shelf Res 12:257–286
UKMMAS (2010) Charting Progress 2 Feeder Report: Ocean Processes. Huthnance J (ed.). Department for Environment Food and Rural Affairs on behalf of UKMMAS (UK Marine Monitoring and Assessment Strategy)
Valentin H (1954) Land loss at Holderness. Reprinted in 1971: Steers JA (ed) Applied coastal geomorphology. Macmillan, London
van Aken HM (2008) Variability of the water temperature in the western Wadden Sea on tidal to centennial time scales. J Sea Res 60:227–234
van Aken HM (2010) Meteorological forcing of long-term temperature variations of the Dutch coastal waters. J Sea Res 63:143–151
van Alphen JSLJ (1990) A mud balance for Belgian-Dutch coastal waters between 1969 and 1986. Netherlands J Sea Res 25:19–30
van Alphen JSLJ, de Ruijter WPM, Borst JC (1988) Outflow and three-dimensional spreading of Rhine river water in the Netherlands coastal zone. In: Dronkers J, van Leussen W (eds) Physical Processes in Estuaries. Springer

van Bennekom AJ, Wetsteijn FJ (1990) The winter distribution of nutrients in the southern bight of the North Sea (1961–1978) and in the estuaries of the Scheldt and the Rhine/Meuse. Netherlands J Sea Res 25:75–87

van Beusekom JEE, de Jonge VN (2002) Long-term changes in Wadden Sea nutrient cycles: importance of organic matter import from the North Sea. Hydrobiologia 475/476:185–194

van Beusekom JEE, de Jonge VN (2012) Dissolved organic phosphorus: An indicator of organic matter turnover? Estuar Coast Shelf Sci 108:29–36

van Beusekom JEE, Brockmann UH, Hesse KJ, Hickel W, Poremba K, Tillmann U (1999) The importance of sediments in the transformation and turnover of nutrients and organic matter in the Wadden Sea and German Bight. German J Hydrogr 51:245–266

van Beusekom JEE, Bot P, Carstensen J, Goebel J, Lenhart H, Pätsch J, Petenati T, Raabe T, Reise K, Wetsteijn B (2009a) Eutrophication. Thematic Report 6 in: Marencic H, de Vlas J (eds) Quality Status Report 2009, Wadden Sea Ecosystem. No 25. Common Wadden Sea Secretariat, Trilateral Monitoring and Assessment Group, Wilhelmshaven, Germany

van Beusekom JEE, Loebl M, Martens P (2009b) Distant riverine nutrient supply and local temperature drive the long-term phytoplankton development in a temperate coastal basin. J Sea Res 61:26–33

van Beusekom JEE, Buschbaum C, Reise K (2012) Wadden Sea tidal basins and the mediating role of the North Sea in ecological processes: scaling up of management? Ocean Coast Manage 68:69–78

van Cauwenberghe C (1995) Relative sea level rise: further analyses and conclusions with respect to the high water, the mean sea and the low water levels along the Belgian coast. Report 37, HydrografischeDienst der Kust

van Cauwenberghe C (1999) Relative sea level rise along the Belgian coast: analyses and conclusions with respect to the high water, the mean sea and the low water levels. Report 46, HydrografischeDienst der Kust

van der Meulen F, Van der Valk B, Arens B (2013) The Netherlands. In Pranzini E, Williams A (eds) Coastal Erosion and Protection in Europe. Routledge, Abingdon

van der Molen J (2002) The influence of tides, wind and waves on the net sand transport in the North Sea. Cont Shelf Res 22:2739–2762

van der Molen J, Gerrits J, de Swart HE (2004) Modelling the morphodynamics of a tidal shelf sea. Cont Shelf Res 24:483–507

van Dijk TAGP, Kleinhans MG (2005) Processes controlling the dynamics of compound sand waves in the North Sea, Netherlands. J Geophys Res 110:F04S10, doi:10.1029/2004JF000173

van Hal R, Smits K, Rijnsdorp AD (2010) How climate warming impacts the distribution and abundance of two small flatfish species in the North Sea. J Sea Res 64:76–84

van Straaten LMJU, Kuenen PH (1957) Accumulation of fine-grained sediments in the Dutch Wadden Sea. Geol Mijnb 19:319–354

Vasseur B, Héquette A (2000) Storm surges and erosion of coastal dunes between 1957 and 1988 near Dunkerque (France), southwestern North Sea. Geol Soc Lond, Spec Publ 175:99–107

Vavrus S, Walsh JE, Chapman WL, Portis D (2006) The behavior of extreme cold air outbreaks under greenhouse warming. Int J Climatol 26:1133–1147

Verlaan PAJ, Spanhoff R (2000) Massive sedimentation events at the mouth of the Rotterdam Waterway. J Coast Res 16:458–469

Verwaest T, Viaene P, Verstraeten J, Mostaert F (2005) De zeespiegelstijgingmeten, begrijpen en afblokken. De Grote Rede 15:15–25

Verwey J (1952) On the ecology of cockle and mussel in the Dutch Wadden Sea. Archives néerlandaises de Zoologie 10:171–239

Vichi M, Ruardij P, Baretta JW (2004) Link or sink: a modelling interpretation of the open Baltic biogeochemistry. Biogeosciences 1:79–100

Vikebø F, Furevik T, Furnes G, Kvamstø NG, Reistad M (2003) Wave height variations in the North Sea and on the Norwegian Continental Shelf, 1881–1999. Cont Shelf Res 23:251–263

Visser M, de Ruijter WPM, Postma L (1991) The distribution of suspended matter in the Dutch coastal zone. Netherlands J Sea Res 27:127–143

von Storch H, Reichardt H (1997) A scenario of storm surge statistics for the German Bight at the expected time of doubled atmospheric carbon dioxide concentration. J Clim 10:2653–2662

von Storch H, Zwiers F (1999) Statistical Analysis in Climate Research. Cambridge University Press

Wahl T, Jensen J, Frank T (2010) On analysing sea level rise in the German Bight since 1844. Nat Hazards Earth Syst Sci 10:171–179

Wahl T, Jensen J, Frank T, Haigh ID (2011) Improved estimates of mean sea level changes in the German Bight over the last 166 years. Ocean Dyn 61:701–715

Wahl T, Haigh I, Woodworth P, Albrecht F, Dillingh D, Jensen J, Nicholls RJ, Weisse R, Wöppelmann G (2013) Observed mean sea level changes around the North Sea coastline from 1800 to present. Earth-Sci Rev 124:51–67

Wakelin SL, Holt JT, Blackford JC, Allen JI, Butenschön M, Artioli Y (2012) Modeling the carbon fluxes of the northwest European continental shelf: validation and budgets. J Geophys Res 117: C05020, doi:10.1029/2011JC007402

WASA-Group (1998) Changing waves and storms in the Northeast Atlantic? Bull Am Met Soc 79:741–760

Watson AJ, Schuster U, Bakker DCE, Bates N, Corbiere A, Gonzalez-Davila M, Friedrich T, Hauck J, Heinze C, Johannessen T, Kortzinger A, Metz N, Olaffson J, Olsen A, Oschlies A, Pfeil B, Santano-Casiano JM, Steinhoff T, Telszewski M, Rios A, Wallace DWR, Wanninkhof R (2009) Tracking the variable North Atlantic sink for atmospheric CO_2. Science 326:1391–1393

Weisse R, Günther H (2007) Wave climate and long-term changes for the Southern North Sea obtained from a high-resolution hindcast 1958–2002. Ocean Dyn 57:161–172

Weisse R, Pluess A (2006) Storm-related sea level variations along the North Sea coast as simulated by a high-resolution model 1958–2002. Ocean Dyn 56:16–25

Weisse R, von Storch H (2009) Marine Climate and Climate Change: Storms, Wind Waves and Storm Surges. Springer

Weisse R, von Storch H, Niemeyer H, Knaack H (2012) Changing North Sea storm surge climate: An increasing hazard? Ocean Coast Manag 68:58–68

Wiltshire KH, Malzahn AM, Wirtz K, Greve W, Janisch S, Mangelsdorf P, Manly BFJ, Boersma M (2008) Resilience of North Sea phytoplankton spring bloom dynamics: an analysis of long-term data at Helgoland Roads. Limnol Oceanogr 53:1294–1302

Winther NG, Johannessen JA (2006) North Sea circulation: Atlantic inflow and its destination. J Geophys Res 111:C12018, doi:10.1029/2005JC003310

Woodruff SD, Worley SJ, Lubker SJ, Ji Z, Freeman JE, Berry DI, Brohan P, Kent EC, Reynolds RW, Smith SR, Wilkinson C (2011) ICOADS Release 2.5 and Data Characteristics. Int J Climatol 31:951–967

Woodworth PL (1987) Trends in U.K. mean sea level. Mar Geod 11:57–87

Woodworth PL (1990) A search for accelerations in records of European mean sea level. Int J Climatol 10:129–143

Woodworth PL (2010) A survey of recent changes in the main components of the ocean tide. Cont Shelf Res 30:1680–1691

Woodworth PL, Tsimplis MN, Flather RA, Shennan I (1999) A review of the trends observed in British Isles mean sea level data measured by tide gauges. Geophys J Int 136:651–670

Woodworth PL, Teferle FN, Bingley RM, Shennan I, Williams SDP (2009a) Trends in UK mean sea level revisited. Geophys J Int 176:19–30

Woodworth PL, White NJ, Jevrejeva S, Holgate SJ, Gehrels WR (2009b) Evidence for the accelerations of sea level on multi-decade and century timescales. Int J Climatol 29:777–789

Woodworth PL, Pouvreau N, Wöppelmann G (2010) The gyre-scale circulation of the North Atlantic and sea level at Brest. Ocean Sci 6:185–190

Woodworth PL, Menéndez M, Gehrels WR (2011) Evidence for century-timescale acceleration in mean sea levels and for recent changes in extreme sea levels. Surv in Geophys 32:603–618

Woolf DK, Challenor PG, Cotton PD (2002) Variability and predictability of the North Atlantic wave climate. J Geophys Res 107: C3145, doi:10.1029/2001JC001124

Wöppelmann G, Marcos M (2012) Coastal sea level rise in southern Europe and the non-climate contribution of vertical land motion. J Geophys Res 117:C01007, doi:10.1029/2011JC007469

Wöppelmann G, Pouvreau N, Simon B (2006). Brest sea level record: A time series construction back to the early eighteenth century. Ocean Dyn 56:487–497

Wöppelmann G, Pouvreau N, Coulomb A, Simon B, Woodworth PL (2008) Tide gauge datum continuity at Brest since 1711: France's longest sea-level record. Geophys Res Lett 35:L22605, doi:10.1029/2008GL035783

Young EF, Holt JT (2007) Prediction and analysis of long-term variability of temperature and salinity in the Irish Sea. J Geophys Res 112:C01008, doi:10.1029/2005JC003386